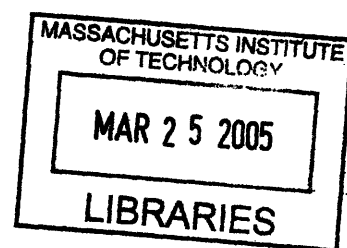# Quantitative Analysis of Carbon Fluxes
for Fat Biosynthesis
in Wild-type and IRS-1 Knockout Brown Adipocytes

By

Hyun-Tae Yoo

B.S. Chemistry
Seoul National University, 1998

Submitted to the Department of Chemistry
in Partial Fulfillment of the Requirements for the Degree of

Doctor of Philosophy in Biological Chemistry

at the

Massachusetts Institute of Technology

February 2005

Signature of Author ....
Department of Chemistry
December 15, 2004

Certified by ....
Gregory Stephanopoulos
Professor of Chemical Engineering
Thesis Supervisor

Accepted by ....
Robert W. Field
Chairman, Departmental Committee on Graduate Students

This doctoral thesis has been examined by a Committee of the Department of Chemistry as follows:

....
Daniel S. Kemp
Professor of Chemistry
Committee Chair

....
Gregory Stephanopoulos
Professor of Chemical Engineering
Thesis Supervisor

....
Alice Y. Ting
Assistant Professor of Chemistry

Quantitative Analysis of Carbon Fluxes
for Fat Biosynthesis
in Wild-type and IRS-1 Knockout Brown Adipocytes

By

Hyun-Tae Yoo

Submitted to Department of Chemistry in Partial Fulfillment of the
Requirements for the Degree of Doctor of Philosophy in Biological Chemistry

ABSTRACT

Excessive fat synthesis and the subsequent dysregulation of lipid metabolism constitute the major pathological factors of obesity and type 2 diabetes through triggering insulin resistance. Thus, controlling fat synthesis by identifying key sites for regulation of lipogenesis and modulating the lipogenic fluxes may provide novel approaches to intervention of the diseases. As a first step to quantitative investigation of lipogenic fluxes from various carbon sources as related to insulin signaling, relative contribution of glucose, glutamine, and acetoacetate to fat biosynthesis in wild-type (WT) and insulin receptor substrate-1 knockout (IRS-1 KO) brown adipocytes were analyzed by stable-isotope labeling, GC/MS, and flux estimation. Glutamine contributed more to fatty acid synthesis than glucose in WT cells while glucose's contribution was heavier in IRS-1 KO cells. Unlike the straightforward pathway for lipogenesis from glucose, two possibilities for glutamine's route to fatty acid synthesis have been proposed: glutaminolysis pathway through conventional tricarboxylic acid cycle and a pathway via reductive carboxylation of α-ketoglutarate to isocitrate. These pathways were integrated into a metabolic network model for quantitative estimation of individual lipogenic fluxes. Incubation of the cells with [U-^{13}C] glutamine for 6 hrs led to metabolic and isotopic steady state where individual fluxes of the model were estimated with 95% confidence by least-square fit method. Dose dependent repression of estimated net flux of reductive carboxylation by specific inhibition of NADP$^+$-dependent isocitrate dehydrogenase and the subsequent reduction in glutamine's contribution to fatty acid synthesis in WT cells strongly indicated that reductive carboxylation is an important site of regulating glutamine's lipogenic flux. Abolition of this net flux, reduction in glutamine's lipogenic contribution, and concurrent rise in glucose's lipogenic contribution in IRS-1 KO cells were consistent with the importance of reductive carboxylation. Differential effects of lack of insulin signaling on individual lipogenic fluxes suggested that there might be specific sites at which insulin signaling regulates lipogenic utilization of carbon sources. These results revealed the importance of other carbon sources such as glutamine in fat synthesis and the means by which the flux of these carbon sources to fat synthesis can be controlled.

Thesis Supervisor: Gregory Stephanopoulos
Title: Professor of Chemical Engineering

Acknowledgements

First, I would like to thank my thesis advisor, professor Gregory Stephanopoulos, for his consistent support for my research throughout good times and bad times. When I was looking for a project involving application of biochemistry to the systemic approach for cell biology, he kindly accepted me and provided me with an intriguing project geared towards novel approaches for obesity and diabetes. His thoughtful guidance kept me from losing sight of the research progress when I was sometimes obsessed with little obstacles. Professor Joanne Kelleher was such a great source of knowledge and ideas about details of mammalian physiology, and I cannot thank her enough for those times when many discussions with her saved me from a lot of trouble and kept me on track. I would like to also thank professors Daniel Kemp and Alice Ting for their support in completing the thesis. I am grateful to Matt for helping me with mammalian cell culturing and GC/MS technology in the beginning of my doctoral years. I was very lucky to have Maciek help me with using another GC/MS instrument and his Metran program. This program was essential in making the tremendous amount of GC/MS data into something meaningful. I cannot forget all the help and the fun that I enjoyed from talking to the rest of the previous and current members of the Metabolic Engineering and Bioinformatics group, including (previous members:) Angelo, Daehee, Gary (Gyoo-Yeol), Giovana, Ilias, Jatin, Javier, Juan Carlos, Kosuke, Manish, Maria, Saliya, (current members:) Adrian, Curt, Hal, Keith, Kohei, Kyle, Joel, Jose, Lily, Mark, Mike, Pete, Tina, and Yongsu. As senior Koreans in the group, Gary, Daehee, and Yongsu were always reliable on matters about both research and personal stuff.

I cannot even start to talk about my life at MIT without thinking of my wife Jeongyeon. As my soul mate, she gave me all the comfort and encouragement that I need to complete this thesis. Even when she was back in Korea, each moment when I shared with her (on the phone and in person) kept me excited about my research and my life at MIT. I hope that I have given her the same for her study at MIT and her work in Seoul. My son Ryan (Jisoo) have been such a sweet baby since he was born that the time I spent with him was always special and made me even happier. My parents and my parents-in-law believed in me and supported me throughout the five-and-a-half years at MIT. I deeply appreciate everything they have done for Jeongyeon, Jisoo, and me. My brother and brother-in-law were there for

4

me every time when I needed their help. I wish I could help them in whatever way that they need me in the future.

And, my special thanks go to my previous and current friends in Boston for the fun times that we shared, including Donghwan, Sangkyun, Sanghyuk, Taehong, Jiamin, Jangwoo, Jung-In, Jiehyun, Yunkyu, Seungjib, Hongmyung, and Hoi-Sung. They made my life in Boston more memorable and enjoyable. Last but not least, I would like to thank my advisors at Seoul National University, professors B. Moon Kim and Eun Lee. Their teachings were invaluable in getting to know how exciting and useful chemistry can be, and their support made it possible for me to start the great experience at MIT. In particular, I was so lucky to have my first experience of research in professor Kim's group with the help from many people including Soonmog and Jinseong.

Table of Contents

Chapter 4. Restoration of fat synthesis in IRS-1 KO cells by metabolite
supplementation

9

List of Figures and Tables

Abbreviations

AC	acetate
AC+	culture condition with addition of 2 mM acetate from day 2 to day 6
AcAc+	culture condition with addition of 10 mM acetoacetate from day 2 to day 6
AcCoA	acetyl-CoA
BTC	benzenetricarboxylate
D(x)	fractional contribution of labeled carbon source (x) to acetyl-CoA pool and palmitate synthesis in ISA model
Dex	dexamethasone
Dex-	culture condition with removal of dexamethasone from day 0 to day 2
DMEM	Dulbecco's Modified Eagle Medium
DOG	deoxyglucose
FAS	fatty acid synthase
g (time)	fractional synthesis of palmitate during time t (as a fraction of the total amount of palmitate) in ISA model
G3P	glycerol-3-phosphate
GC	Gas Chromatography
GC/MS	Gas Chromatography/Mass Spectrometry
Glc	glucose
Glc-	culture condition with removal of glucose from day 2 to day 6
Gln	glutamine
Gln-	culture condition with removal of glutamine from day 2 to day 6
GLUT1	glucose transporter-1
GLUT4	glucose transporter-4
IBMX	isobutylmethylxanthine
Indo	indomethacin
IR	insulin receptor
IRS-1	insulin receptor substrate-1
IRS-1 KO	insulin receptor substrate-1 knockout
IRS-2	insulin receptor substrate-2
ISA	isotopomer spectral analysis

M+x	isotopomer with m/z = M+x where M is the base mass
MTBSTFA	N-methyl-N-*tert*-butyldimethylsilyltrifluoroacetamide
NAD-ICDH	NAD^+-dependent isocitrate dehydrogenase
NADP-ICDH	$NADP^+$-dependent isocitrate dehydrogenase
OAA	oxaloacetate
PEP	phosphoenolpyruvate
PEPCK	phosphoenolpyruvate carboxykinase
PI3K	phosphatidylinositol 3-kinase
SEM	standard error of measurement
SIM	selected ion monitoring
SSRES	sum of square residuals
Std	standard: culture condition following standard protocol
TBDMS	*tert*-butyldimethylsilyl
TCA	tricarboxylic acid
U-^{13}C	uniformly ^{13}C-labeled
UCP1	uncoupling protein-1
WT	wild-type

Introduction

Obesity and Type 2 diabetes are among the most widespread and high-cost epidemics that have gained increasing attention for the last two decades due to their long-lasting socioeconomic impacts. Current estimate of 150 million people affected by diabetes worldwide are projected to reach 300 million people in 2025. Most cases of diabetes are type 2 diabetes, which is tightly linked to obesity (14). Despite the complexity of genetic and environmental factors that might cause obesity and type 2 diabetes, there are strong evidences that dysregulation of lipid metabolism is one of the major pathological factors. Thus, the common features of the diseases such as excessive fat synthesis, decreased responsiveness to insulin signaling (insulin resistance), and high blood glucose have been shown to have cause-and-effect relationship by various *in vitro* and *in vivo* studies led by Shulman and coworkers (Perseghin *et al.*(8) and references therein). Their hypothesis for cellular mechanism linking lipid metabolism to insulin resistance starts with increased intracellular fatty acid metabolites activating serine/threonine kinase cascade (Fig. 1). This leads to phosphorylation of serine/threonine of insulin receptor substrate proteins (IRS-1 and IRS-2), which inhibits activation of phosphatidylinositol 3-kinase (PI3K). Therefore, the signaling events downstream of PI3-kinase, including stimulation of glucose transport, are deactivated, which results in high concentration of glucose in blood.

The implications above have motivated this research, with the possibility that obesity and type 2 diabetes may be largely prevented or intervened by controlling fat synthesis either before or after the onset of the diseases. In order to synthesize fat, carbon sources from nutrition needs to be metabolized and transformed through a series of metabolic pathways into lipogenic building blocks such as glycerol-3-phosphate and acetyl-CoA. If the flow of
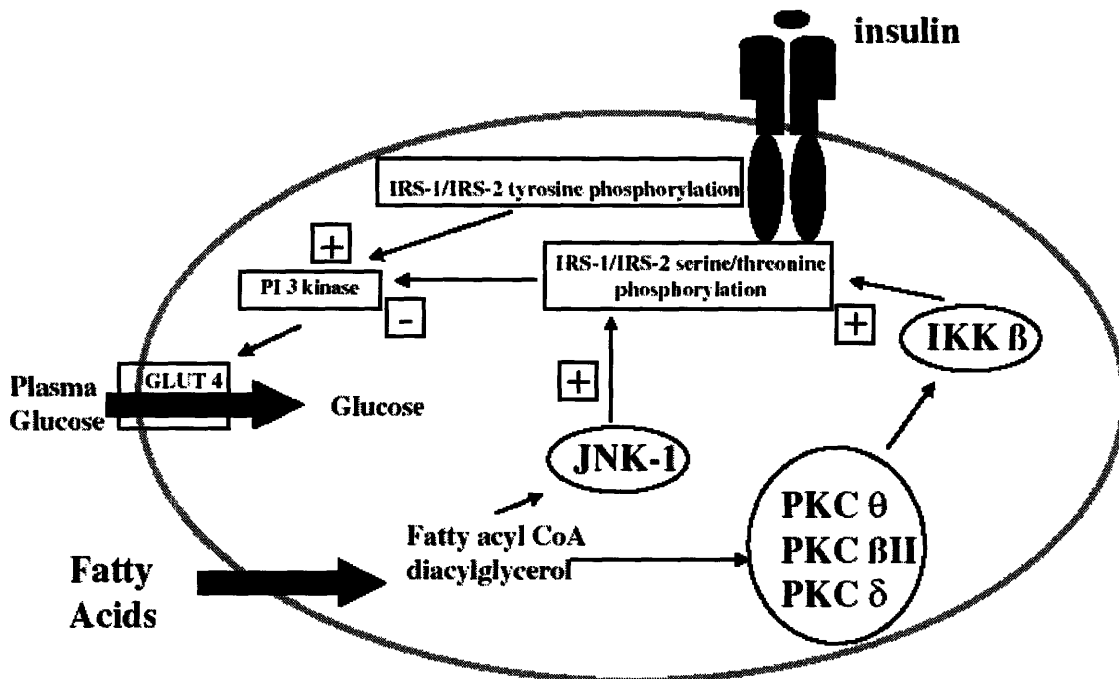
Fig. 1. Proposed mechanism for fatty acid-induced insulin resistance (8).

An increase in the delivery of fatty acids to muscle or a decrease in the intracellular metabolism of fatty acids leads to an increase in intracellular fatty acid metabolites, such as diacylglycerol, ceramides and fatty acyl CoA. These metabolites activate a serine/threonine kinase cascade possibly initiated by PKCθ, PKCβII, PKCδ or by IKK-β or JNK, leading to phosphorylation of serine/threonine sites of the insulin receptor substrates (IRS-1 and IRS-2), which in turn reduces the ability of IRSs to activate PI3-kinase. As a consequence, glucose transport activity and other events downstream of insulin receptor signaling are diminished.

carbons through these pathways can be efficiently modulated at specific sites, this could enable us to find insights both into better understanding of the pathogenesis of the diseases and into better means of intervention. Identification of these key sites for metabolic activities of lipogenesis would require quantitative understanding of the fluxes involved in the lipogenic process, which can be most easily achieved by methods of dynamic metabolomics. Conventional metabolomics approach is based on measurements of amounts of various metabolites, which need to be performed at many time-points of metabolic non-steady state in order to estimate the individual fluxes between metabolites (12). For dynamic metabolomics approach, researchers have taken advantage of highly dynamic nature of metabolism: stable-isotope label contained in input metabolites is quickly transferred to the downstream metabolites, whose labeling patterns depend on the individual fluxes between metabolites. Appropriate models of metabolic network can be constructed, and equations can be set up based on the individual fluxes as unknown and the labeling patterns of metabolites as variables. Then, a single experiment with stable-isotope labeling of input metabolites followed by analysis of labeling patterns of the metabolites in the network model could make it possible for the fluxes to be estimated by solving those equations. The solution can become straightforward if metabolic and isotopic steady-state can be assumed. The estimated fluxes can also be easily validated by an independent experiment with stable-isotope labeling of another input metabolite. Mathematical basis for estimation of fluxes throughout a metabolic network using dynamic metabolomics techniques have been rigorously examined together with the metabolic and isotopic steady-state assumption (4, 13).

Stable-isotope labeling coupled with mass spectrometry has been most useful in the measurement of complex metabolic fluxes for polymerization biosynthesis (e.g. fatty acid synthesis), DNA synthesis, protein synthesis, triglyceride turnover, and multiple phenotypes by using ^{13}C-labeled substrates or ^{2}H$_2$O (reviewed in (15)). In particular, the application to polymerization biosynthesis has been theoretically developed by Kelleher and Masterson (16) and demonstrated in flux analysis of fatty acid synthesis (17; see "Isotopomer Spectral Analysis" in Experimental Procedure of Chapter 1 for details). The application to flux analysis of a more complicated network of reactions has been extensively studied in *Corynebacterium glutamicum* by the researchers in this laboratory (18), and the basis of calculation of the metabolic fluxes has been delineated initially with such a simple model of metabolic network as is illustrated in Figure 2 (19). In the process of gluconeogenesis, [U-^{13}C] pyruvate is carboxylated to produce [1,2,3-^{13}C] oxaloacetate. If this flux relative to the TCA cycle flux is designated as y, the dilution of [1,2,3-^{13}C] oxaloacetate can be expressed as y / (1 + y), which is defined to be R. Reversible exchange reaction of oxaloacetate with malate and fumarate leads to a mixture of two positional isotopomers of mass M+3, i.e. [1,2,3-^{13}C] oxaloacetate and [2,3,4-^{13}C] oxaloacetate. When the fraction of each isotopomers is designated as A for [1,2,3-^{13}C] oxaloacetate and B for [2,3,4-^{13}C] oxaloacetate (A + B = 1), pyruvate directly converted from oxaloacetate will contain [1,2,3-^{13}C] pyruvate (mass = M+3) and [2,3-^{13}C] pyruvate (mass = M+2). Moreover, oxaloacetate can also go through one or more rounds of TCA cycle, which would yield other isotopomers shown in Figure 2 due to loss of ^{13}C as CO$_2$ through the decarboxylation reactions of the cycle. Then, the composition of differentially labeled isotopomers will be a function of two parameters: A for reversible reaction with malate and

Masses: M+1   M+1   M+2   M+3   M+2   M+1   M+1

```
    C       C       C       C       C       C       C
    C-OP    C-OP    C-OP    C-OP    C-OP    C-OP    C-OP
    C       C       C       C       C       C       C
         ↑                     ↗       ↖            ↑
    C       C       C                       C       C       C
    C=O     C=O     C=O                     C=O     C=O     C=O
    C       C       C                       C       C       C
    C       C       C                       C       C       C

       TCA    ↑                   /    \           ↑  TCA
       Cycle  |                  /      \          |  Cycle
                              FUM
    C   C   C=O   C   ◄──────────────►   C   C   C=O   C
                              MAL
                      ↖                 ↗
                        C   C   C=O   C

                              PC  ↑

                              C
                              C=O
                              C
```
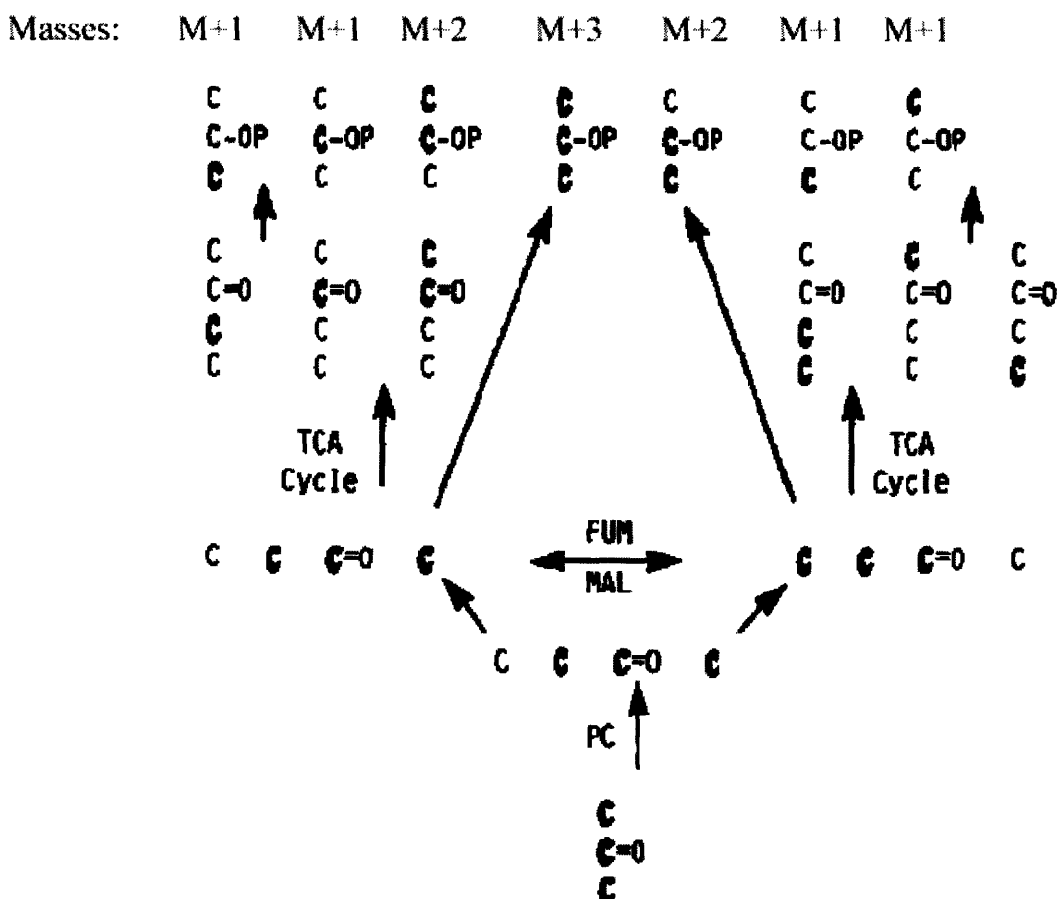
Fig. 2. Simple model of gluconeogenesis as an example of flux analysis by stable-isotope labeling and mass spectrometry

Carbons labeled with ^{13}C are represented in bold. [U-^{13}C] pyruvate is converted to various isotopomers of phosphoenolpyruvate via oxaloacetate. Dilution of [U-^{13}C] pyruvate and partial equilibration of oxaloacetate with malate (MAL) and fumarate (FUM) are represented with parameters R and A (see text for definition). PC stands for pyruvate carboxylase. Reactions of pyruvate dehydrogenase (pyruvate to acetyl-CoA) and pyruvate kinase (PEP to pyruvate) are ignored.

fumarate and R for the dilution of [U-^{13}C] pyruvate. The ratios of (M+1)/(M+3) and

(M+2)/(M+3) can be determined experimentally and related to the parameters A and R:

$$(M+1)/(M+3) = 0.5R(1 + R)/A(1 - 0.5R), (M+2)/(M+3) = (1 - A + 0.5R)/A$$

Thus, A and R can be calculated, which will also give y, the flux of pyruvate carboxylation

relative to the global flux through TCA cycle.

However, this kind of calculation with artificial parameters based on crude assumptions

may easily overlook some unexpected labeling of metabolites and the definition of those

parameters can be misleading. In order to include all possible labeling of metabolites in

setting up balanced equations systematically, a method with mathematical rigor has been

developed in our laboratory to calculate the fluxes from isotopomer distribution

measurements, which was the basis for the flux estimation in Chapters 2 and 3. Consider

the imaginary network of reactions in Figure 3. The network consists of 4 metabolites (all

with 2 carbon units), 3 extracellular fluxes, and 3 intracellular reactions, one of which is

reversible. The atomic transitions of the carbons in the reactions are defined to be as

follows:

reaction	carbon transitions
1. A → B	ab → ab
2. A + B → C + D	ab + AB → aA + bB
3. B ↔ D	ab ↔ ab

For the purpose of setting up equations, each reaction can be decomposed into a set of

reactions with specific isotopomers reacting. For example, for reaction 2, there are 16

possible combinations of isotopomers of metabolites A and B reacting. The labelings of

two carbon units are represented as 0 for ^{12}C and 1 for ^{13}C. Thus, A_{00} means metabolite A

with both carbons unlabeled (A: ^{12}C-^{12}C) while A_{01} means A: ^{12}C-^{13}C. Also, a_{00} denotes

the concentration of A_{00} as a fraction of total amount of metabolite A. Then, the relative
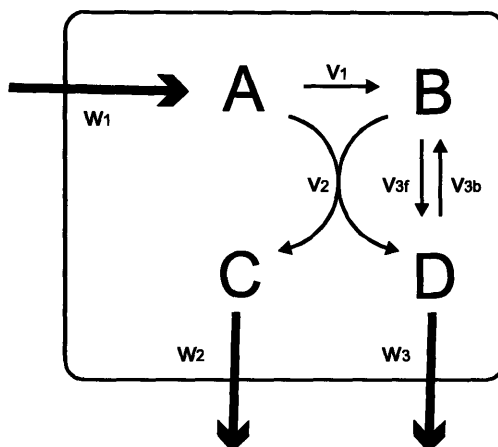
Fig. 3. Imaginary network under steady state as an example of flux estimation.

velocities for reaction 2 are defined as follows:

reaction	relative velocity
$A_{00} + B_{00} \rightarrow C_{00} + D_{00}$	$v_2 \cdot a_{00} \cdot b_{00}$
$A_{00} + B_{01} \rightarrow C_{00} + D_{01}$	$v_2 \cdot a_{00} \cdot b_{01}$
$A_{00} + B_{10} \rightarrow C_{01} + D_{00}$	$v_2 \cdot a_{00} \cdot b_{10}$
etc...	

Under metabolic and isotopic steady state, the balance equations can be set up for

isotopomers of metabolite D as follows:

$$0 = v_2 \cdot (a_{00} \cdot b_{00} + a_{00} \cdot b_{10} + a_{10} \cdot b_{00} + a_{10} \cdot b_{10}) + v_{3f} b_{00} - (v_{3b} + w_3) \cdot d_{00}$$
$$0 = v_2 \cdot (a_{00} \cdot b_{01} + a_{00} \cdot b_{11} + a_{10} \cdot b_{01} + a_{10} \cdot b_{11}) + v_{3f} b_{01} - (v_{3b} + w_3) \cdot d_{01}$$
etc...

If one can determine the uptake/export fluxes (w_1, w_2, and w_3) and fractional isotopomer

distribution of metabolites (e.g. $B_{M+0} = b_{00}$, $B_{M+1} = b_{01} + b_{10}$, and $B_{M+2} = b_{11}$), the fluxes

can be calculated by solving the nonlinear equations with the solvers in commercially

available programs like MATLAB.

Most studies on the metabolic activities of lipogenesis have been focused on the

pathways from glucose to fatty acid synthesis, such as glucose uptake, glycolysis, citrate

transport across mitochondrial membrane, and fatty acid synthesis from acetyl-CoA. Even though glutamine and ketone bodies have been recognized as lipogenic carbon sources (1, 6, 9), little has been done for quantitative understanding of their contribution relative to that of glucose.

Adipose tissues have attracted great attention in light of whole-body lipid metabolism and the two metabolic diseases, since it has been established that adipose tissues function not only as the sites for storage of body fat, but as the central sites of regulating whole-body lipid metabolism and energy balance through release of such hormones as adipsin, tumor necrosis factor (TNF)-α, leptin, and plasminogen activator inhibitor-1 (10). Brown adipose tissue is particularly interesting with regard to regulation of energy balance because of its unique capability of heat generation through uncoupling mitochondrial proton gradient and ATP synthesis by uncoupling protein-1 (UCP1) located in inner membrane of mitochondrion. Found as depots mostly in small mammals (rat, mouse, hamster) and newborns of large mammals (including human), brown adipocytes are distinguished from white adipocytes by multiple lipid droplets and many copies of mitochondria in the cell (11). These features enable brown adipocytes to readily produce heat from fatty acid oxidation upon norepinephrine signaling through β₃-adrenergic receptors. With a high number of high-affinity endogenous insulin receptor (IR) brown adipocytes are also very sensitive to insulin signaling (7), consistent with the roles in diet-induced thermogenesis and whole-body glucose clearance (11). A prominent role of brown adipocytes for insulin-stimulated whole-body glucose clearance has been demonstrated by studies on transgenic mouse whose insulin receptor was knocked out specifically in brown adipose tissue (3). Despite the relatively minor size of brown adipose tissue in this animal, fasting

hyperglycemia and impaired glucose tolerance was evident. In addition, Kahn and coworkers established preadipocyte cell lines from brown adipose tissue with specific knock-out of insulin signaling substrate (IRS) proteins (5), and only IRS-1 knockout (IRS-1 KO) cell line showed downregulation of insulin sensitivity and UCP expression, along with decreased expression of lipogenic transcription factors (C/EBPβ, PPARγ) and lipogenic enzymes like glucose transporter-4 and fatty acid synthase, leading to reduced fat synthesis (2). Thus, in this thesis wild-type (WT) brown adipocytes and the corresponding IRS-1 KO cells were selected as *in vitro* models for quantitative investigation of the effect of insulin signaling on utilization of lipogenic carbon sources.

Throughout the studies of this thesis, Gas Chromatography/Mass Spectrometry (GC/MS) instrument was mainly used for measurement of the amounts of metabolites and the fractional distribution of their isotopomers. The capillary column for Gas-Chromatography was DB-XLB (60 m x 0.25 mm id x 0.25 μm) from J&W scientific. Although the exact chemical composition of the column was not disclosed due to its proprietary status, the low-polarity column was amenable to separation of fatty acid methyl esters as well as silyl derivatives of organic acids and amino acids that are related to tricarboxylic acid (TCA) cycle. With the temperature profile between 100°C and 300°C, exceptionally reproducible retention times were achieved for all the analytes using this column.

Ionization of analytes by electron impact (EI) and mass analysis by quadrupole mass analyzer have provided reliable and reproducible measurement of peak intensity for the m/z range of 100 to 500, which was examined as follows: measured natural abundance of the metabolites was very close to theoretical natural abundance and triplicate measurement of ^{13}C-labeled metabolites produced relatively small errors for fractional isotopomer

distributions. Consistent mass resolution of 1 a.m.u. or below was appropriate for measuring intensities of mass isotopomers from ^{13}C-labeling.

With these knowledge and experimental techniques at hand, the following questions were first asked: (1) Is glucose the only significant carbon source for lipogenesis? (2) If other metabolites participate, what are their relative contributions? (3) Is insulin signaling indispensable for fat synthesis of adipocytes? Can we restore fat synthesis of IRS-1 KO cells by supplementing with other metabolites? Two perturbed conditions (removal of dexamethasone during the induction period and addition of acetoacetate during the differentiation period) were selected after screening various perturbations for elevated lipogenesis in IRS-1 KO cells (Chapter 4). These perturbations were compared with standard culture condition in the analysis of relative utilization of carbon sources (glucose, glutamine, and/or acetoacetate) in Chapter 1. When glutamine was found to contribute heavily as lipogenic carbon source in all three conditions, two possible pathways for glutamine's metabolic route to fatty acid synthesis were integrated into quantitative estimation of fluxes involved in lipogenesis from glucose and glutamine in WT cells under standard condition in Chapter 2. The robust results of flux estimation strongly suggested that a novel pathway involving reductive carboxylation of α-ketoglutarate to isocitrate could be a major pathway for glutamine's flux to fatty acid synthesis, also providing potential key sites for controlling lipogenic flux in adipocytes. In Chapter 3, a similar analysis was conducted using IRS-1 KO cells, which gave quantitative insights for the differential effects of insulin signaling on the regulation of carbon source utilization in lipogenesis. In conclusion, the four chapters were summarized and some future experiments were suggested in Chapter 5.

References

1. Cooney, G., R. Curi, A. Mitchelson, P. Newsholme, M. Simpson, and E.A. Newsholme. 1986. Activities of some key enzymes of carbohydrate, ketone body, adenosine and glutamine metabolism in liver, and brown and white adipose tissues of the rat. *Biochem Biophys Res Commun* **138**: 687-92.

2. Fasshauer, M., J. Klein, K.M. Kriauciunas, K. Ueki, M. Benito, and C.R. Kahn. 2001. Essential role of insulin receptor substrate 1 in differentiation of brown adipocytes. *Mol Cell Biol* **21**: 319-29.

3. Guerra, C., P. Navarro, A.M. Valverde, M. Arribas, J. Bruning, L.P. Kozak, C.R. Kahn, and M. Benito. 2001. Brown adipose tissue-specific insulin receptor knockout shows diabetic phenotype without insulin resistance. *J Clin Invest* **108**: 1205-13.

4. Isermann, N. and W. Wiechert. 2003. Metabolic isotopomer labeling systems. Part II: structural flux identifiability analysis. *Math Biosci* **183**: 175-214.

5. Klein, J., M. Fasshauer, H.H. Klein, M. Benito, and C.R. Kahn. 2002. Novel adipocyte lines from brown fat: a model system for the study of differentiation, energy metabolism, and insulin action. *Bioessays* **24**: 382-8.

6. Kowalchuk, J.M., R. Curi, and E.A. Newsholme. 1988. Glutamine metabolism in isolated incubated adipocytes of the rat. *Biochem J* **249**: 705-8.

7. Lorenzo, M., A.M. Valverde, T. Teruel, and M. Benito. 1993. IGF-I is a mitogen involved in differentiation-related gene expression in fetal rat brown adipocytes. *J Cell Biol* **123**: 1567-75.

8. Perseghin, G., K. Petersen, and G.I. Shulman. 2003. Cellular mechanism of insulin resistance: potential links with inflammation. *Int J Obes Relat Metab Disord* **27 Suppl 3**: S6-11.

9. Robinson, A.M. and D.H. Williamson. 1980. Physiological roles of ketone bodies as substrates and signals in mammalian tissues. *Physiol Rev* **60**: 143-87.

10. Rosen, E.D. and B.M. Spiegelman. 2000. Molecular regulation of adipogenesis. *Annu Rev Cell Dev Biol* **16**: 145-71.

11. Sell, H., Y. Deshaies, and D. Richard. 2004. The brown adipocyte: update on its metabolic role. *Int J Biochem Cell Biol* **36**: 2098-104.

12. Stitt, M. and A.R. Fernie. 2003. From measurements of metabolites to metabolomics: an 'on the fly' perspective illustrated by recent studies of carbon-nitrogen interactions. *Curr Opin Biotechnol* **14**: 136-44.

13. Wiechert, W. and M. Wurzel. 2001. Metabolic isotopomer labeling systems. Part I: global dynamic behavior. *Math Biosci* **169**: 173-205.

14. Zimmet, P., K.G. Alberti, and J. Shaw. 2001. Global and societal implications of the diabetes epidemic. *Nature* **414**: 782-7.

15. Hellerstein, M.K. 2004. New stable isotope-mass spectrometric techniques for measuring fluxes through intact metabolic pathways in mammalian systems: introduction of moving pictures into functional genomics and biochemical phenotyping. *Metab Eng* **6**: 85-100.

16. Kelleher, J.K. and T.M. Masterson. 1992. Model equations for condensation biosynthesis using stable isotopes and radioisotopes. *Am J Physiol* **262**: E118-25.

17. Kharroubi, A.T., T.M. Masterson, T.A. Aldaghlas, K.A. Kennedy, and J.K. Kelleher. 1992. Isotopomer spectral analysis of triglyceride fatty acid synthesis in 3T3-L1 cells. *Am J Physiol* **263**: E667-75.

18. Klapa, M.I., J.-C. Aon, and G. Stephanopoulos. 2003. Systematic quantification of complex metabolic flux networks using stable isotopes and mass spectrometry. *Eur J Biochem* **270**: 3525-3542.

19. Katz, J., W. Lee, P. Wals, and E. Bergner. 1989. Studies of glycogen synthesis and the Krebs cycle by mass isotopomer analysis with [U-13C]glucose in rats. *J. Biol. Chem.* 264: 12994-13004.

Chapter 1. Quantifying carbon sources for *de novo* lipogenesis in wild-type and IRS-1 knockout brown adipocytes

Introduction

The differentiation of brown adipocyte cells from a fibroblast-like precursor is evolutionarily related to pre-hibernation fat accumulation and thus linked to total body energy metabolism (1). Adipogenesis occurs under conditions of excess nutrients and accompanying hormones and involves changes in gene expression and cell signaling, leading to a substantial increase in *de novo* synthesis and storage of triglyceride. Cell surface receptors, especially for insulin and insulin-like growth factor-1 (IGF-1) provide a mechanism for hormonal response to nutrient abundance. Recent investigations of adipogenesis have focused on gene expression and cell signaling events associated with this conversion (2-4). The importance of the insulin receptor substrate-1 (IRS-1) signaling pathway for differentiation has been demonstrated by the finding that an IRS-1 knockout (IRS-1 KO) preadipocyte cell line is unable to differentiate under the standard condition where wild-type (WT) cells accumulate triglyceride and express adipocyte-specific genes including UCP-1 and fatty acid synthase (5). A consequence of the IRS-1 KO is that these cells are deficient in insulin-stimulated glucose uptake via insulin-sensitive glucose transporter, GLUT4. The studies of *in vitro* adipogenesis are normally conducted under constant nutrient conditions using cell culture media where glucose (25 mM) and glutamine (2-4 mM) provide the major carbon sources for cell metabolism. In the work presented here, the role of the nutrient and hormonal environment on the process of lipogenesis accompanying brown adipocyte differentiation was investigated.

Animal studies support the concept that glucose is a major carbon source for brown adipose lipogenesis. Lipid synthesis measured with ^3H_2O increases on glucose administration and is insulin-sensitive (6). However, ketone bodies may also supply carbon for brown adipose lipogenesis. Investigations using rats and slices of rat brown adipose tissue demonstrated that acetoacetate was utilized by brown adipose tissue both for oxidation and for *de novo* lipogenesis. In fasted animals, the incorporation ^{14}C-labeled β-hydroxybutyrate into lipids in brown adipose tissue was ten-fold greater on a weight basis than into liver or white adipose tissue (7). In addition, incorporation of β-hydroxybutyrate into fatty acid was increased in brown adipose tissue of cold-adapted rats (8). In concert with these fluxes, elevated levels of mitochondrial enzymes required for the conversions of acetoacetate to acetyl CoA, 3-oxoacid CoA-transferase and acetoacetyl-CoA thiolase, have been found in brown adipose tissue from suckling and weanling rats (9, 10). In addition to fatty acid synthesis, nutrients are required for the glycerol backbone of the triglyceride. In most cells, glucose supplies the glycerol-3-phosphate (G3P) precursor for the triglyceride backbone. Brown adipocytes may also utilize the glyceroneogenesis pathway involving glycerol-3-phosphate synthesis from three carbon compounds via phosphoenolpyruvate carboxykinase (PEPCK) (11). A third possible route for G3P formation in brown adipocyte cells is from glycerol via glycerokinase. A futile cycle involving glycerokinase and triglyceride hydrolysis has been suggested as an additional heat generating mechanism in brown adipocyte cells (12, 13).

A standard procedure for *in vitro* differentiation of brown preadipocytes has been adopted from the procedure used for white adipocyte differentiation (14). The procedure involves incubating confluent preadipocytes in dexamethasone, indomethacin, and

isobutylmethylxanthine (IBMX). Dexamethasone, in brown preadipocytes, appears to repress the expression of insulin-insensitive glucose transporter GLUT1 and stimulate the level of insulin-sensitive glucose transporter GLUT4 in a dose-dependent manner. In the absence of dexamethasone, brown preadipocytes may differentiate by transporting glucose primarily through GLUT1 (15, 16). Thus, both the nutrient environment and the hormonal conditions inducing differentiation may affect the intracellular metabolic environment that allows the cells to rapidly accumulate triglyceride during differentiation.

The studies presented here, focus on the role of nutrients in the synthesis of triglyceride during the brown adipocyte differentiation process using the WT and IRS-1 KO cell lines developed by Kahn and co-workers (5). This model provides the opportunity to compare the two cell types to assess their ability to accumulate lipid under a variety of nutrient conditions. In white adipose 3T3-L1 cells, the IRS-1 KO cells retain partial ability to differentiate (17). Thus, the hypothesis that alternations in nutrients could affect the lipogenic ability of the IRS-1 KO brown adipose cells was tested. ^{13}C-labeled metabolites were employed to investigate the carbon sources for lipogenesis and glycerol backbone. Labeling data were analyzed with Isotopomer Spectral Analysis (ISA) to estimate parameters associated with lipogenesis. This method has been used previously to assess the synthesis of triglyceride fatty acids in differentiating 3T3-L1 white adipocyte cells (18). These studies have provided insights into the role of nutrients in brown adipocyte differentiation to complement the extensive work on signaling and transcriptional changes underway in other laboratories (3, 5, 19).

Experimental Procedures

Materials

Biochemicals were obtained from Sigma Chemical Co., St. Louis, MO. ^{13}C-labeled chemicals were obtained from Cambridge Isotope Laboratories, Inc., Andover, MA. Tissue culture media were obtained from Invitrogen, Co., Carlsbad, CA.

Cell culture, adipocyte differentiation and lipid isolation

Brown preadipocyte cells were cultured essentially as described in Fasshauer *et al.* (20) and as outlined in Figure 1.1. All studies were conducted in 10-cm^2 (surface area) 6-well plates containing 4 mL media. WT and IRS-1 KO brown preadipocyte cells (kindly provided by Dr. C. R. Kahn, Joslin Diabetes Center, Boston) were cultured until confluence (day 0) in "Differentiation media" (Dulbecco's Modified Eagle Medium (DMEM) containing 25 mM glucose and 4 mM glutamine, supplemented with 10% fetal bovine serum, 20 nM insulin, and 1 nM thyroid hormone (T3)). On day 0, media were changed to "Induction media", which is Differentiation media supplemented with 0.125 mM indomethacin, 0.25 mM IBMX, and 5 μM dexamethasone (In some studies, dexamethasone was omitted from the Induction medium: "Dex-"). After 48 hours, media were changed back to Differentiation media (in some studies, 10 mM sodium acetoacetate or 2 mM sodium acetate was added to Differentiation media: "AcAc+" or "AC+"). For all ^{13}C-labeling experiments, glucose, glutamine, added acetoacetate, or added acetate in the medium was individually replaced with the corresponding [U-^{13}C] labeled carbon source, and DMEM was replaced with DMEM Base medium (from Sigma Chemical Co.) with no glucose or glutamine (buffered with 44 mM sodium bicarbonate at pH 7.2). Media were
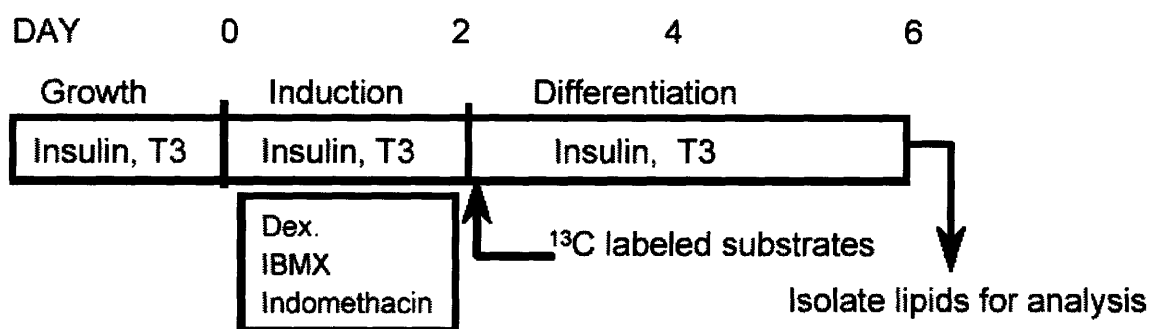
Fig. 1.1. Protocol for brown adipose cell differentiation.

Cells were seeded into a well of 10-cm^2 surface area with Differentiation medium and grown to confluence. On day 0, medium was changed to Induction medium containing the following induction chemicals: Dex, IBMX, and indomethacin. On day 2, cells were returned to Differentiation medium containing ^{13}C-labeled substrates. On day 6, lipids were extracted from the cells for analysis.

replaced on day 4 with the same differentiation media used on day 2.

On day 6, the experiment was terminated by removing the medium and adding 1.0 mL of 2% perchloric acid for 10 minutes at room temperature to each well (21). After removing the acidic solution, cellular lipid was isolated twice by adding 1.3 mL of hexane-isopropanol (3:2) mixture for 30 min at room temperature, when 20 μg of triheptadecanoin in 10 μL hexane-isopropanol (3:2) was added to the organic solvent for quantification of total fatty acids. Combined hexane-isopropanol solution was evaporated and redissolved in 400 μL of methane-benzene (2:1) mixture, 100 μL of which was mixed with 100 μL of fresh BF_3/MeOH. The mixture was vortexed in glass vial and incubated at 75 °C for 2 hours to derivatize the entire fatty acid moiety in lipids into the corresponding methyl esters. The reaction product was then purified by hexane extraction (3 x 0.3 mL) against 0.2 mL of saturated aqueous NaCl solution. Combined hexane solution was treated with 100 mg of sodium sulfate to remove residual water. The hexane solution was then diluted appropriately before injection into the GC/MS instrument.

For ISA analysis of the glycerol portion of the lipids, glycerol was derivatized with *tert*-butyldimethylsilyl (TBDMS) group and the mass isotopomer distribution determined by GC/MS as described by Flakoll *et al.* (22) Upon separation of organic phase after methylation of the fatty acid moiety of lipids, 0.2 mL of the aqueous solution was evaporated to dryness and dissolved in the mixture of 100 μL pyridine and 100 μL of N-Methyl-N-[*tert*-butyldimethylsilyl]trifluoroacetimide (MTBSTFA, from Pierce). The mixture was incubated at room temperature for 30 minutes prior to GC/MS analysis.

GC/MS for fatty acid quantification and ISA analysis

Samples with fatty acid methyl esters in 1 μL hexane were injected into a Hewlett-Packard model 6890A GC connected to JMS-GCmate II (JEOL, Peabody, MA) and equipped with DB-XLB (60 m x 0.25 mm id x 0.25 μm) capillary column (J&W Scientific, Folsom, CA). Helium flow was maintained at 1.0 mL per minute via electronic pressure control. The injection port temperature was 230°C. The temperature of the column was started at 100°C for 1 minute, increased to 250°C at 25°C/min, and held for 5 minutes. The temperature was then increased to 300°C at 25°C/min and held for 1 min. For general detection of fatty acid methyl ester, $m/z = 100$ to 330 was scanned and recorded with scan speed of 0.51 second and interscan delay of 0.2 second. Myristate ($m/z = 242$), palmitate ($m/z = 270$), palmitoleate ($m/z = 268$), oleate ($m/z = 296$), and stearate ($m/z = 298$) methyl esters were detected above detection limit, together with the internal standard, heptadecanoate methyl ester ($m/z = 284$). For quantification of total fatty acids, the intensities of M+0 peaks ("M+x" denotes the isotopomer with $m/z = M + x$ where M is the base mass) of fatty acid methyl esters were normalized by that of heptadecanoate methyl ester. Various known amounts of tripalmitin were derivatized and measured together with the samples to construct a standard curve for calculating the absolute amounts of the fatty acids. Protein amounts of the replicate cell culture samples were measured using protein assay kit (Sigma Diagnostics, St. Louis, MO) after extraction of protein from the cell cultures with 1% Triton X-100 (0.7 mL per well) for 20 minutes at 37 °C and centrifugation (18,000 × g for 2 min).

Because palmitate was the major fatty acid under all experimental conditions, the analysis of methyl palmitate was used for representative ISA analysis on fatty acid

synthesis in brown adipocytes. For detection of mass isotopomers of methyl palmitate in ^{13}C-labeling studies, relative intensities of the molecular ions and their isotopomers (M+0, M+1, M+2,... M+16 (m/z = 270 to 286)) were monitored by selected ion monitoring (SIM). For detection of mass isotopomers of TBDMS derivative of lipidic glycerol in ^{13}C-labeling studies, the same instrumental setup as for fatty acid methyl esters was used except for the following GC temperature profile: temperature held at 100 °C for 0.5 minute, increased to 300°C at 25°C/min, and held for 1.5 minute. Relative intensities of M–57 ions (M–*tert*-butyl) and their isotopomers (m/z = 377 to 384) were also monitored by SIM (22).

Assay on rates of glucose and glutamine uptake and lactate production

The concentration of glucose and lactate in media samples was measured by YSI 2300 STAT glucose/L-lactate analyzer (Yellow Springs Instruments, Yellow Springs, OH). Glutamine concentration was measured by TBDMS derivatization and GC/MS, and corrected for the spontaneous decomposition of glutamine at 37°C. The mixture of 100 μL of each medium sample plus 40 μL of 10 mM [U-^{13}C] glutamine was first acidified by adding 100 μL of 2% perchloric acid. Then, the mixture was loaded onto a column with 2 mL of Dowex 50Wx8-400 cation exchange resin. After washing the column with 1 mL of distilled water, glutamine was eluted by 3 mL of 6 M NH$_4$OH aqueous solution. The eluant was evaporated and dissolved into 50 μL of dimethylformamide by sonication, before mixing with 70 μL of MTBSTFA. The mixture was then incubated at 70°C for 30 minutes prior to injection into GC/MS instrument. Standard glutamine solutions of known concentration were used for construction of a standard curve. GC/MS setup was the same as in glycerol analysis above, except for the following GC temperature profile: temperature

34

held at 140°C for 2 minutes, increased to 200°C at 25 °C/min, and held for 1 minute; temperature increased again to 250°C at 3 °C/min and held for 7.9 minutes; temperature raised to 300°C at 5 °C/min and held for 5 minutes. Relative intensities of M – 57 (M – *tert*-butyl) ions from of natural glutamine (m/z = 431) and [U-^{13}C] glutamine (m/z = 436) were used for the calculation of glutamine concentrations of the media samples.

Isotopomer spectral analysis (ISA)

The flux of carbon sources to fatty acids was evaluated by ISA, a stable isotope method for estimating the fractional contribution and the fractional new synthesis of carbon sources to lipogenesis (18, 23). This method utilizes the mass isotopomer distribution of a polymer produced in part by *de novo* synthesis as illustrated in Figure 1.2. In this study, palmitate synthesized from ^{13}C-enriched precursors was analyzed. The ISA model produces estimated values for the two parameters controlling flux of ^{13}C to the sampled palmitate. D is the fractional contribution of a ^{13}C-labeled precursor to the lipogenic acetyl CoA, and g(time) is the fractional amount of newly synthesized palmitate in the sample. The parameter g(time) is equivalent to the fractional synthesis of the product at the specified time. The model used here assumes that the flux of the precursors to the lipogenic acetyl CoA pool is constant during the time course of ^{13}C incubation. ISA uses equations for the probability of appearance of each isotopomer based on test values for D and g(time). These probabilities are compared to the fractional abundance determined for each palmitate isotopomer to obtain the best-fit solution. The fit is obtained by weighted nonlinear regression with the weights proportional to the inverse of the standard deviation of the isotopomer measurement. In practice, the weighting insures that the parameter estimates
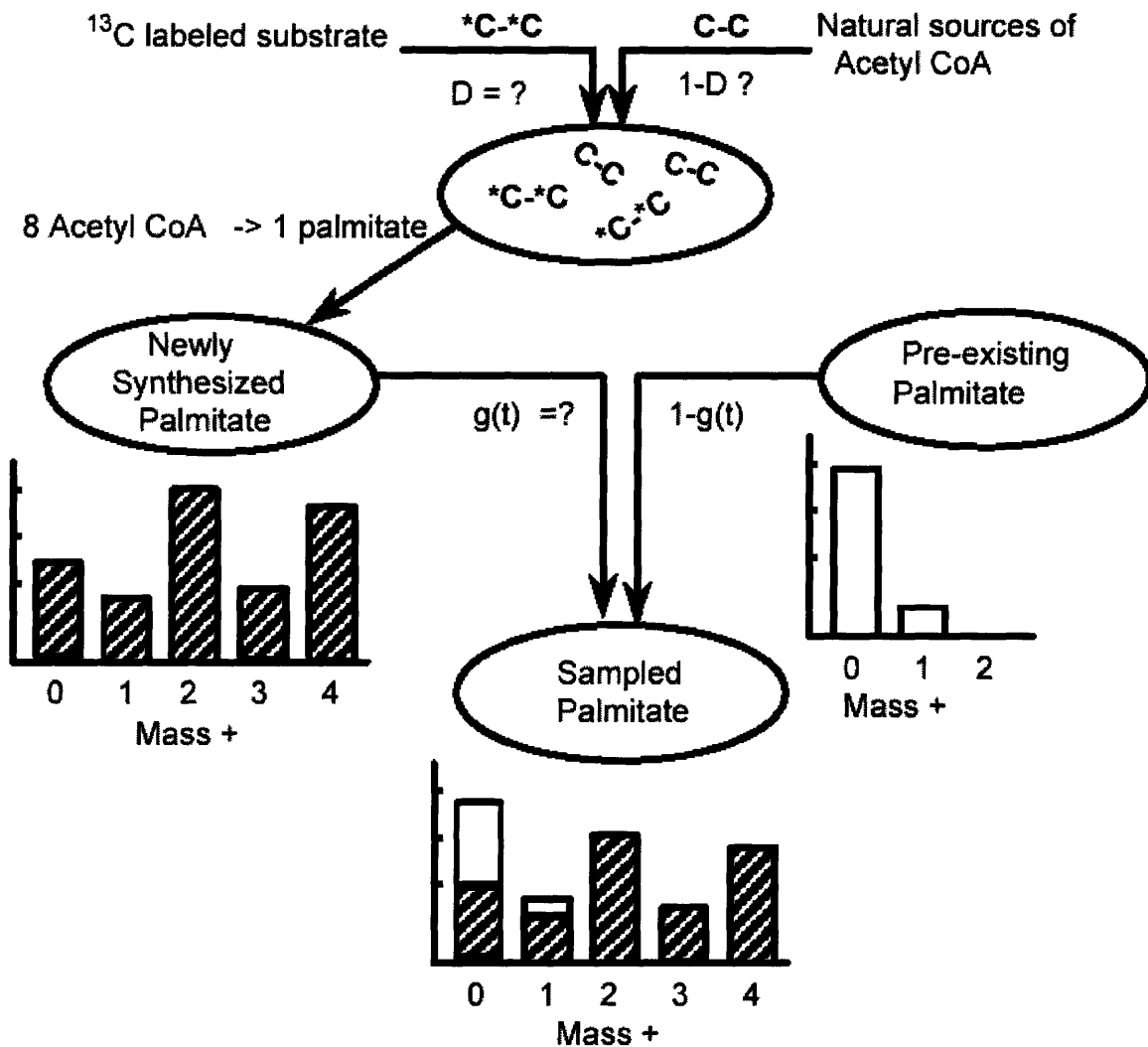
Fig. 1.2. Isotopomer spectral analysis (ISA) model for *de novo* biosynthesis of palmitate.

Substrate labeled with ^{13}C is converted to ^{13}C-labeled acetyl CoA, which is mixed with acetyl CoA derived from natural sources in intracellular pool of acetyl CoA at a constant ratio of D to 1-D. One molecule of palmitate is synthesized from eight molecules of acetyl CoA in the homogeneous pool. When total cellular palmitate is sampled at the end of the incubation after the time period "t", the fraction of palmitate resulting from *de novo* biosynthesis is g(t).

36

will not be strongly affected by the least reliable measurements.

Results and Discussion

Quantifying total fatty acid content of WT and IRS-1 KO brown adipocytes

Confluent WT and IRS-1 KO brown adipocytes were cultured under the standard (Std) condition or one of two modified conditions: AcAc+ or Dex- (see "Experimental Procedures" for details). Under Std condition, WT cells produced approximately three times as much total fatty acids per protein mass as IRS-1 KO cells by day 6 (Fig. 1.3). Under AcAc+ or Dex- conditions, WT and IRS-1 KO cells produced similar amounts of fatty acids as in Std condition. Removing any one of the induction chemicals (IBMX, dexamethasone, and indomethacin) from the induction medium for WT cells did not alter the total fatty acid amounts noticeably, but absence of two or more induction chemicals reduced fatty acid production of WT cells to that of IRS-1 KO cells under Std condition (Fig. 1.4). Previous studies comparing the amount of total fatty acids synthesized in WT and IRS-1 KO cells used Oil Red O staining to demonstrate qualitatively the decreased triglyceride accumulation in the KO cells (20). The data in Figure 1.3 quantify the total fatty acid amounts in both cell lines, allowing calculations of amounts of total fatty acids per mg of protein. The finding that the Dex- condition did not alter the total fatty acid accumulation suggests that any shift in the population of GLUT1 and GLUT4 does not affect total fatty acid synthesis (15, 16).
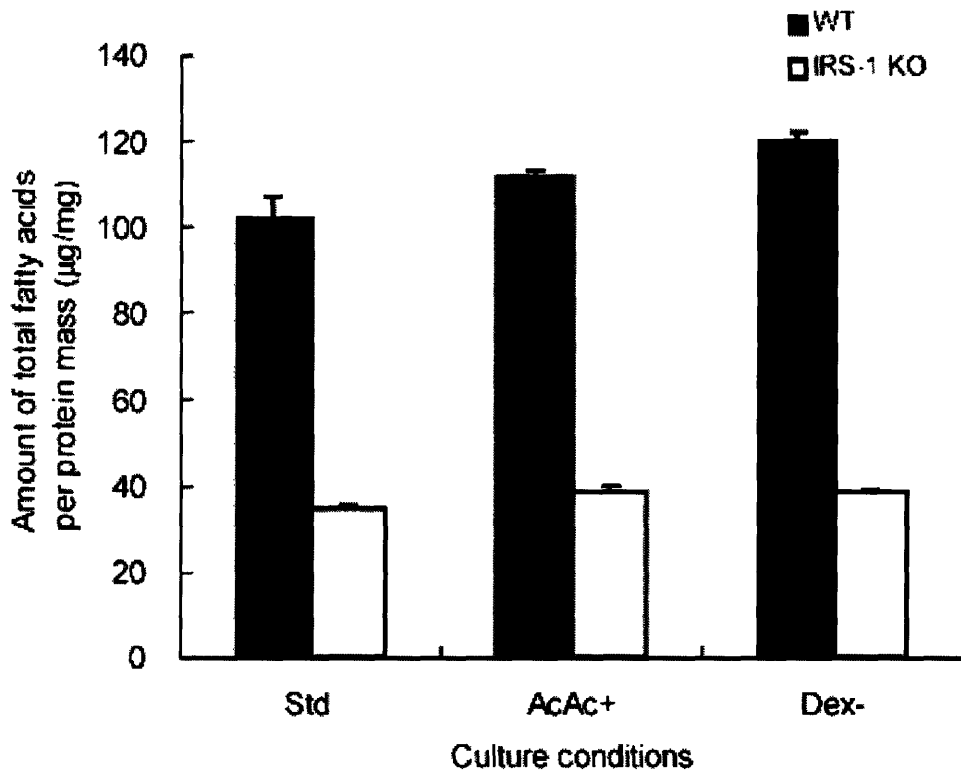
Fig. 1.3. Quantifying fatty acid synthesis in WT and IRS-1 KO cells.

Amounts of total fatty acids under three culture conditions on day 6 measured by GC/MS using triheptadecanoin as the internal standard (conditions as described in Methods and Fig. 1A). Std: Induction medium from day 0 to day 2, Differentiation medium from day 2 to day 6; AcAc+: addition of 10 mM acetoacetate from day 2 to day 6; Dex-: Induction medium without Dex from day 0 to day 2. Data shown are mean ± SEM (n = 3) in WT and IRS-1 KO brown adipocytes. No significant difference was found among the three conditions in either WT or IRS-1 KO cells.

Relative amounts of
total fatty acids per well

3.5
3.0
2.5
2.0
1.5
1.0
0.5
0.0
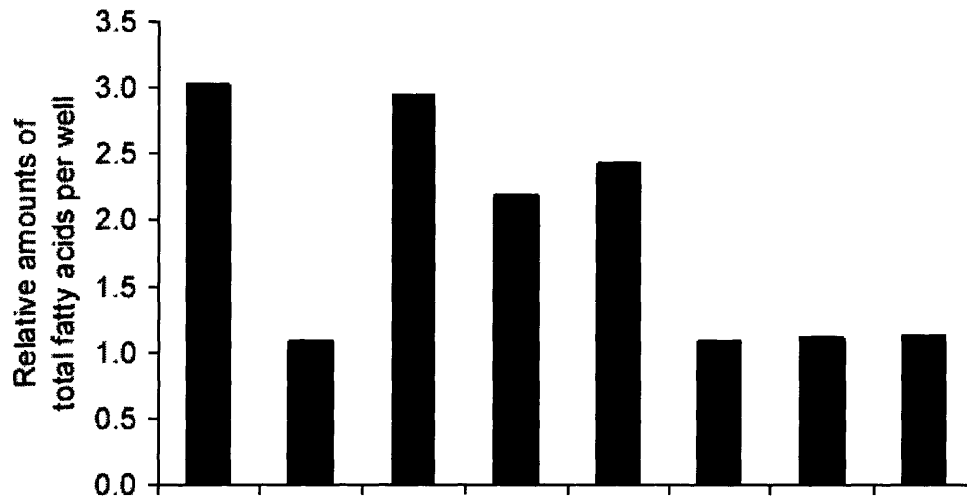
Induction chemicals	Dex	+	----	+	+	----	+	----	----
	IBMX	+	----	----	+	+	----	+	----
	Indo	+	----	+	----	+	----	----	+

Fig. 1.4. Effect of different combination of individual induction chemicals on fat production of WT brown adipocytes.

Relative amounts of total fatty acids per well were measured for WT brown adipocytes on day 6 of differentiation period under different induction conditions where the three induction chemicals (5 μM Dex; 0.25 mM IBMX; 0.125 mM Indo) were added in various combinations from day 0 to day 2. Amounts of total fatty acids per well are expressed as fold over the amount in IRS-1 KO cells under standard condition on day 6.

Lipogenesis under varied conditions for differentiation: adding acetoacetate and removing dexamethasone

To determine the flux of various carbon sources to lipogenesis, cells were incubated in ^{13}C-labeled substrates for the four-day differentiation period, from day 2 to day 6 (Fig. 1.1). For each of the three conditions, the fractional contribution and fractional new synthesis of glucose, glutamine, and acetoacetate when present, were estimated by the ISA parameters, D and g(4 day) (Fig. 1.2). A sample ISA experiment showing the mass isotopomer distribution and the fit of the model to the data demonstrates the key features of the analysis (Fig. 1.5).

The results of the ISA analysis indicate that brown adipocytes can utilize a variety of carbon sources for *de novo* lipogenesis (Fig. 1.6A). Glucose (25 mM) and glutamine (4 mM) are the major lipogenic carbon sources in the differentiation medium. ISA analysis indicated that both glucose and glutamine make substantial contributions of carbon for lipogenesis under all conditions examined. Acetoacetate (10 mM) was readily converted to lipid, indicating that these cell lines have a large capacity for acetoacetate utilization consistent with the results in animal studies (9, 10). The activity of acetoacetyl-CoA synthetase has been correlated with the incorporation of acetoacetate carbon into lipid, which was increased in the presence of glucose and insulin (9). Acetoacetate displaced glucose and glutamine as lipogenic carbon sources as indicated by the high $D_{(AcAc)}$ values and the decreases in the D values for these substrates in the presence of acetoacetate. When dexamethasone was removed from the induction medium (Dex- condition), the fractional contribution of glucose to lipogenesis increased in the WT cells, consistent with the finding that this condition increases the expression of GLUT1 (15, 16; see also Fig. 1.7).
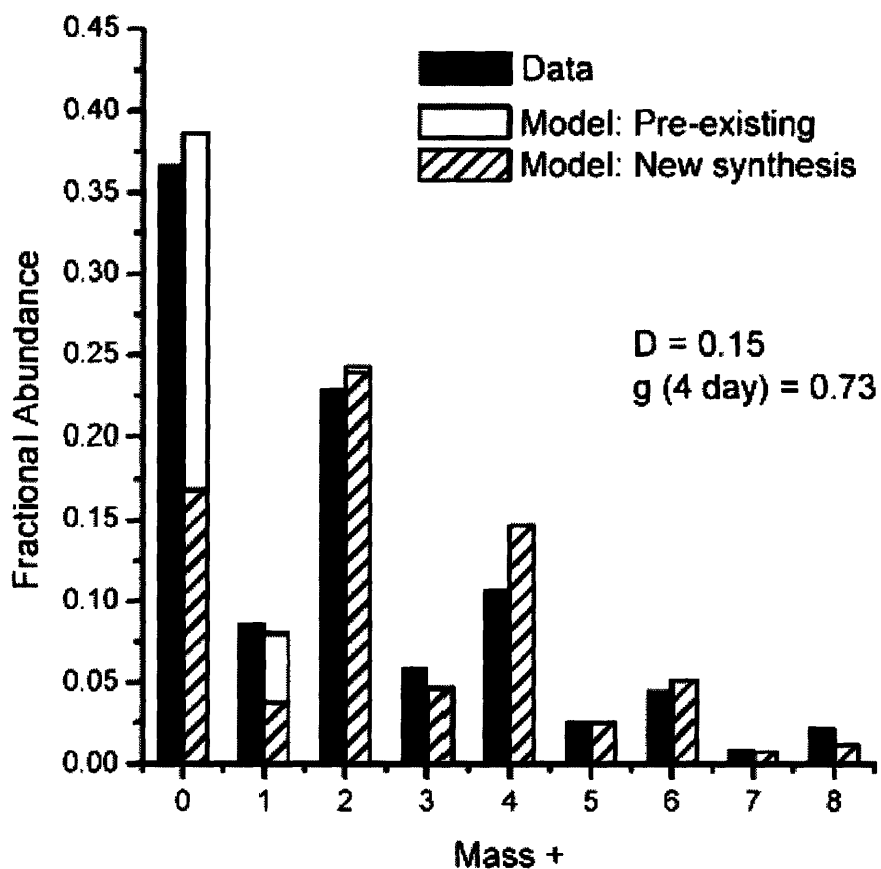
Fig. 1.5. ISA of palmitate synthesis in brown adipose cells.

Representative isotopomer distribution of methyl palmitate (sampled on day 6 from WT brown adipocytes under AcAc+ condition with [U-^{13}C] glutamine from day 2 to day 6) compared to its fit by ISA model with D = 0.15 and g(4 day) = 0.73.

A.

Culture conditions and ^{13}C-labeled precursors

B.

Culture conditions
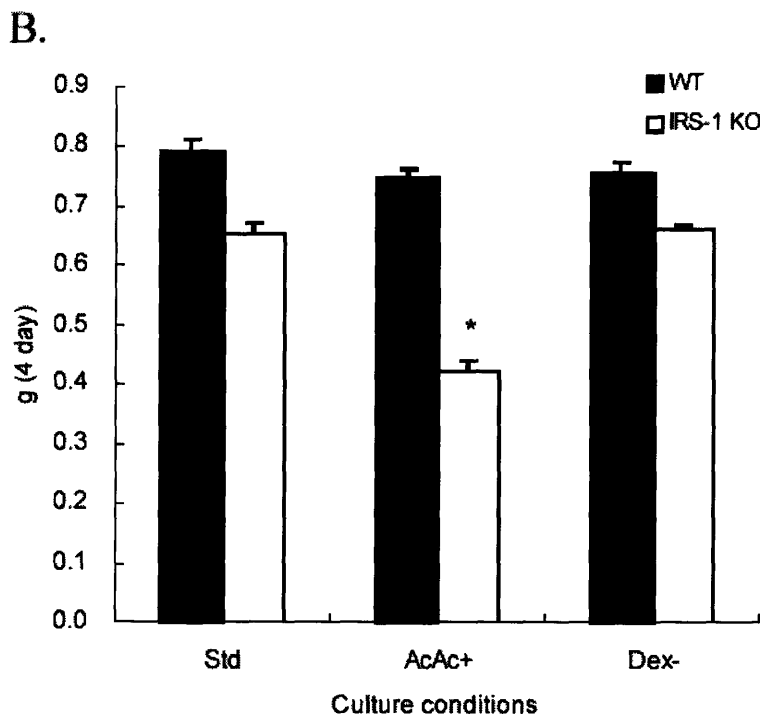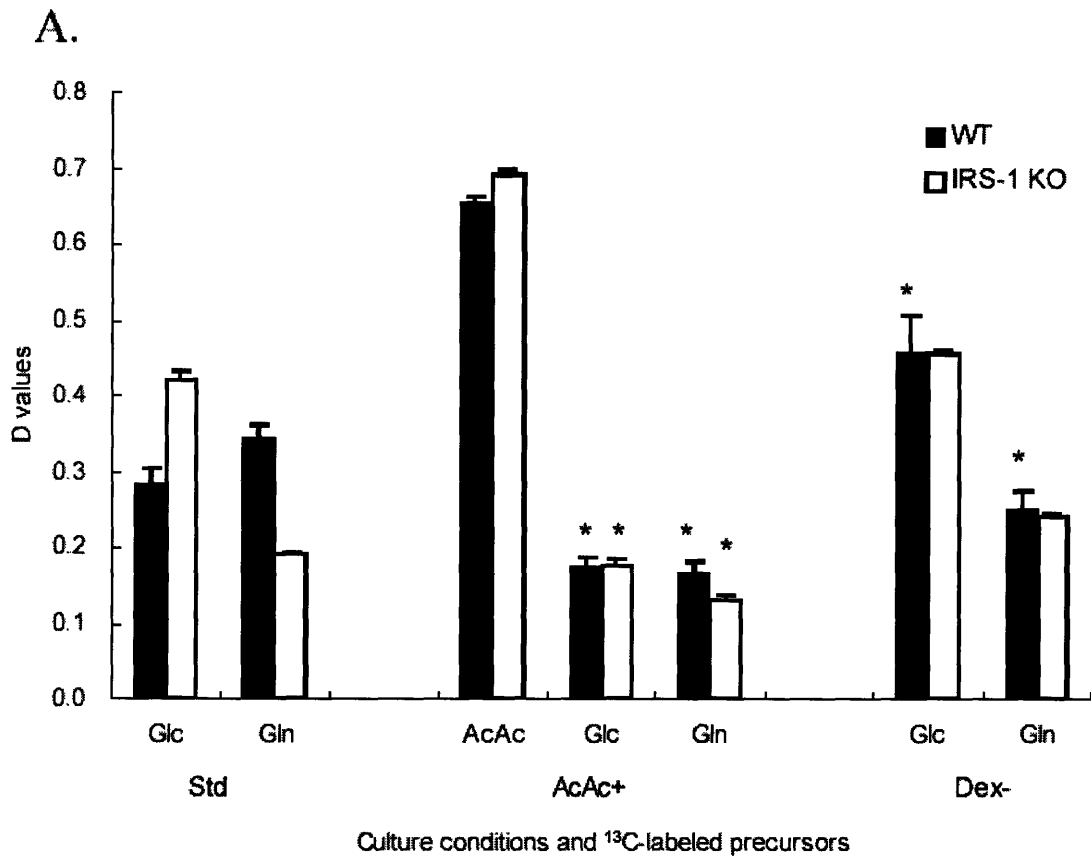
Fig. 1.6. Flux of carbon sources to lipids in brown adipose cells.
A: Fractional tracer contribution (D values) for palmitate synthesis from Glc, Gln, or AcAc in WT and IRS-1 KO brown adipocytes on day 6 (^{13}C-labeling from day 2 to day 6) under Std, AcAc+, or Dex- conditions.
B: Fractional synthesis (g(4 day) values) for the same conditions as above. Data shown are mean ± SEM (n = 6). Asterisk (*) indicates significant difference between the standard condition and each of the modified conditions with the same ^{13}C-labeled precursors at P ≤ 0.01.

42

D values estimate the fractional contribution of a substrate to the lipogenic acetyl CoA pool. To examine the total flux of a substrate to fatty acids, it is necessary to consider the fraction of total fatty acids that was newly synthesized during the isotope incubation period. The ISA term for this variable, g(4 day) (Fig. 1.2), was estimated as shown in Figure 1.6B. Except for IRS-1 KO cells in the presence of acetoacetate, 60 to 80% of the total fatty acids in WT and IRS-1 KO cells was synthesized during the differentiation period (from day 2 to day 6). The total flux to fatty acids per mg protein was determined by multiplying g(4 day) with the total content of fatty acids (Fig. 1.7). This calculation assumes that there is little turnover of the newly synthesized fatty acids during the four-day experiment. The isotopic flux of each substrate to fatty acids may be calculated as: (flux of substrate per mg protein) = $D_{(substrate)}$ × g(4 day) × (total amount of fatty acids / mg protein). In Figure 1.7, the total flux is partitioned among the ^{13}C labeled substrates and other carbon sources. For each of the three conditions, the D values for all carbon sources are expected to sum to 1 according to the ISA model (Fig. 1.2). Sources of carbon for lipogenic acetyl CoA other than the compounds investigated as ^{13}C substrates are grouped together and labeled "Other". This term includes metabolites in the medium as well as intracellular metabolites. Although the fractional contribution from glucose and glutamine for IRS-1 KO cells are comparable to that in WT cells (Fig. 1.6A), the absolute fluxes of the carbon sources in IRS-1 KO cells are much lower than in WT cells under all three conditions as shown in Figure 1.7. Thus, despite the changes in substrate use, the IRS-1 KO cells were not able to overcome the defect in total lipogenesis (20).

To further explore the quantitative use of glucose and glutamine for lipid synthesis, the changes in concentration in the medium of WT cells under Std condition were measured

120

100

(Amount of total fatty acid per protein mass) x g (4 day) (ug/mg)

80

60

40

20

0

■ WT

□ IRS-1 KO

Other

Gln

Glc

Other

Glc

Gln

AcAc

Gln

Glc

AcAc

*

Gln
Glc

Other

Gln

Glc

Other

Glc

Gln

Std   AcAc+   Dex-

Culture Conditions
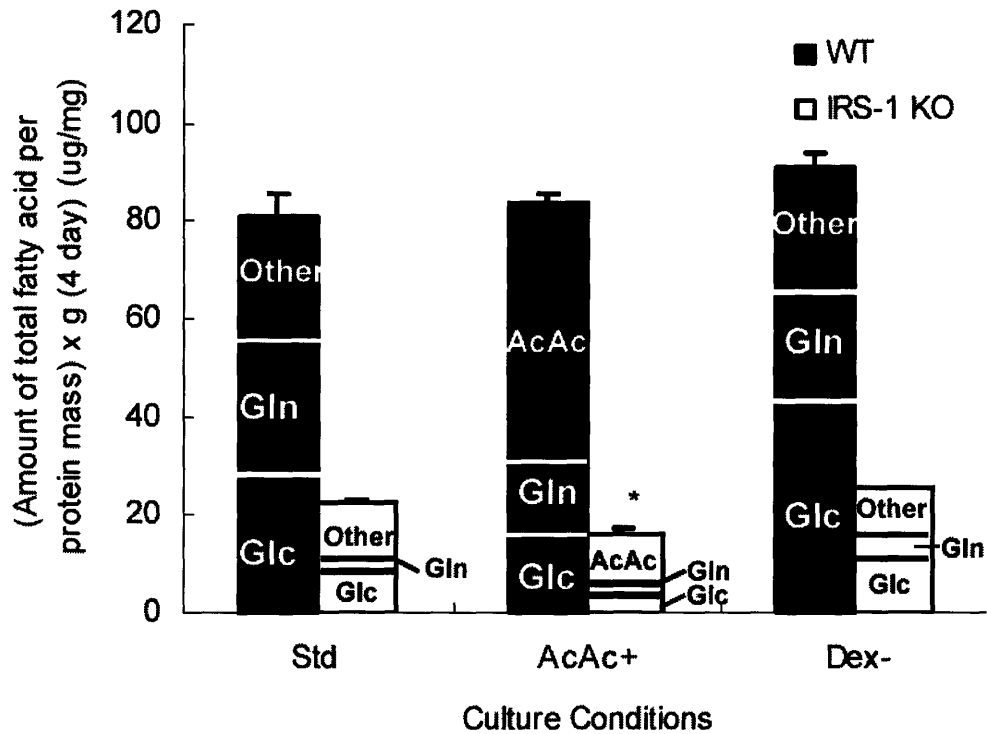
Fig. 1.7. Partitioning of fatty acid synthesis among substrates.

The products of g(4 day) × the amount of total fatty acids per protein mass (μg/mg) were partitioned for the corresponding D values. Data shown are mean ± SEM (n = 6). Asterisk (*) indicates significant difference between the standard condition and each of the modified conditions with the same ^{13}C-labeled precursors at P ≤ 0.01.

during the period of the most active lipogenesis, from day 4 to day 6 (Fig. 1.8). Glutamine

consumption of WT cells from the medium amounted to 4.1 μmol per well over 48 hrs. In

order to calculate the amount of glutamine used for fatty acid synthesis during the last 2

days of differentiation, it was assumed that one molecule of glutamine provides a two-

carbon unit of acetyl CoA for fatty acid synthesis and that palmitate is the representative

fatty acid. Also, from Figure 1.7, it was calculated that 0.3 μmol of fatty acid was

synthesized from glutamine over 4-day period in a well (2.8 mg of protein per well).

Together with the measurement that 83% of the newly synthesized fatty acids during the 4-

day differentiation period is produced from day 4 to day 6, glutamine usage for fatty acid

synthesis was estimated to be 2.0 μmol. These results indicate that an isotopic flux of 49%

of the glutamine consumed from medium was used for synthesis of fatty acids during the

48-hr period. In parallel with the result from glutamine analysis, 63 μmol of glucose was

consumed and 77 μmol of lactate was produced per well over the 48-hr period (Fig. 1.8),

consistent with glucose's contribution to lipogenesis (Fig. 1.7 and Fig. 1.10).

Under Std and Dex- conditions where glucose and glutamine were the major carbon

sources in the medium, the sum of $D_{(Glc)}$ and $D_{(Gln)}$ was considerably less than 1, indicating

that other carbon sources supplied nearly 40% of the acetyl units used for *de novo* fatty acid

synthesis. On the other hand, addition of 10 mM acetoacetate made the sum of $D_{(AcAc)}$,

$D_{(Glc)}$, and $D_{(Gln)}$ equal to 1.00 in both WT and IRS-1 KO cells. Acetoacetate was able to

entirely displace the contribution of the "Other" sources and reduced the contribution of

both glucose and glutamine. This finding suggests that both WT and IRS-1 KO cells have

a high capacity to metabolize acetoacetate to acetyl CoA without affecting total fatty acid

synthesis (Fig. 1.3).
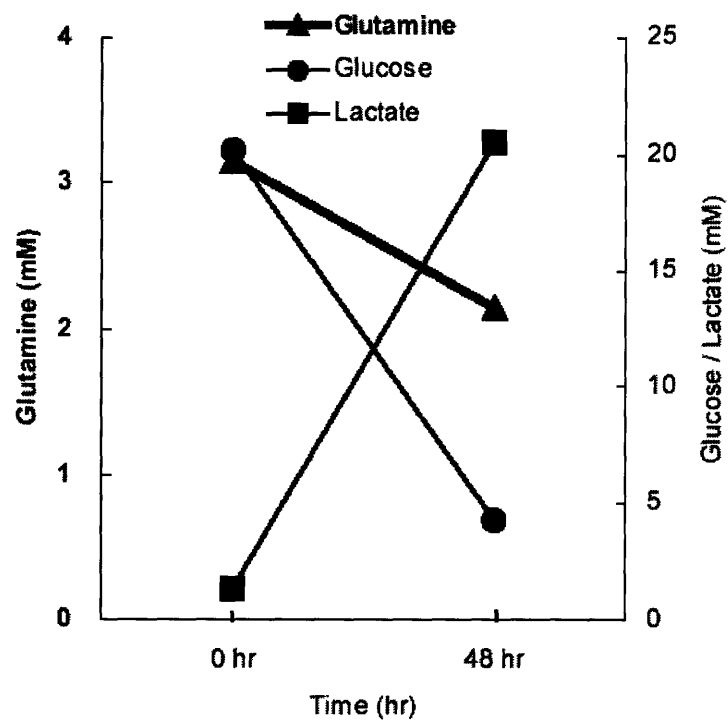
Fig. 1.8. Consumption of glutamine and glucose from the medium and production of lactate by WT brown adipocytes.

The changes in concentration of glucose, glutamine, and lactate in the medium over 48 hrs (from day 4 to day 6) were measured for WT brown adipocytes under standard condition. See "Experimental Procedures" for details.

Lipogenesis in the absence of glucose or glutamine

The studies presented in Figures 1.6-1.8 demonstrate substantial flux of both glucose and glutamine to the lipogenic acetyl CoA during differentiation of WT brown adipocytes. To further explore this issue, we removed either glutamine (Gln-) or glucose (Glc-) from the standard medium from day 2 to day 6 and examined the flux of ^{13}C labeled glucose and glutamine to lipogenic acetyl CoA. The results of this ISA analysis are summarized in Figure 1.9. When glutamine was removed, the fractional contribution of glucose was almost doubled ($D_{(Glc)} = 0.51 \pm 0.03$) from that in WT cells with 25 mM glucose and 4 mM glutamine ($D_{(Glc)} = 0.28 \pm 0.02$) and amounted to 81% of the sum of the two D values ($D_{(Glc)} + D_{(Gln)} = 0.63 \pm 0.03$). In parallel with these findings, total fatty acid production in WT cells under Gln- condition was similar to that in WT cells under Std condition (Fig. 1.9B). Thus, glucose's flux to lipogenic acetyl CoA can largely compensate for the absence of glutamine in WT cells. In contrast, when glucose was removed from the medium (Glc-), glutamine provided only 24 ± 1 % of the carbon sources for fatty acid synthesis. This D value was lower than $D_{(Gln)}$ (0.34 ± 0.02) in WT cells under Std condition. With glucose removed from the medium, total fatty acid production in WT cells was reduced to the level as low as that in IRS-1 KO cells under Std condition, which was not restored even after addition of acetoacetate (Fig. 1.9B). These results indicate that glucose is required to support triglyceride synthesis from glutamine during differentiation of brown adipocytes.

Carbon sources for glycerol backbone of triglyceride

The studies removing glucose or glutamine from the medium during differentiation raise

47

A.
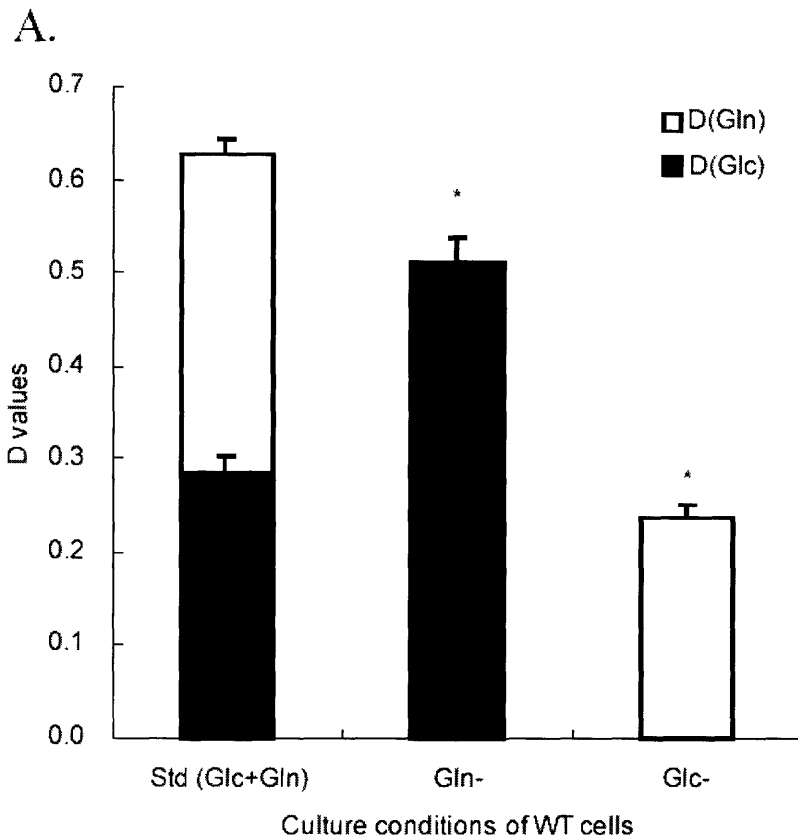
Fig. 1.9. Effect of absence of glucose or glutamine on flux of carbon sources to fatty acids.

A: D values for palmitate synthesis from either Glc or Gln in WT brown adipocytes under Std, Gln-, and Glc- conditions on day 6 (^{13}C-labeling of Glc or Gln from day 2 to day 6). Data shown are mean ± SEM (n ≥ 4). Asterisk (*) indicates significant difference between the conditions with the same ^{13}C-labeled precursors at P ≤ 0.01.
B: Relative amounts of total fatty acids per protein mass in WT cells - effect of the absence of glucose. Conditions were the same as in 1.9A except for Glc-AcAc+: the addition of 10 mM acetoacetate and the absence of glucose from day 2 to day 6.
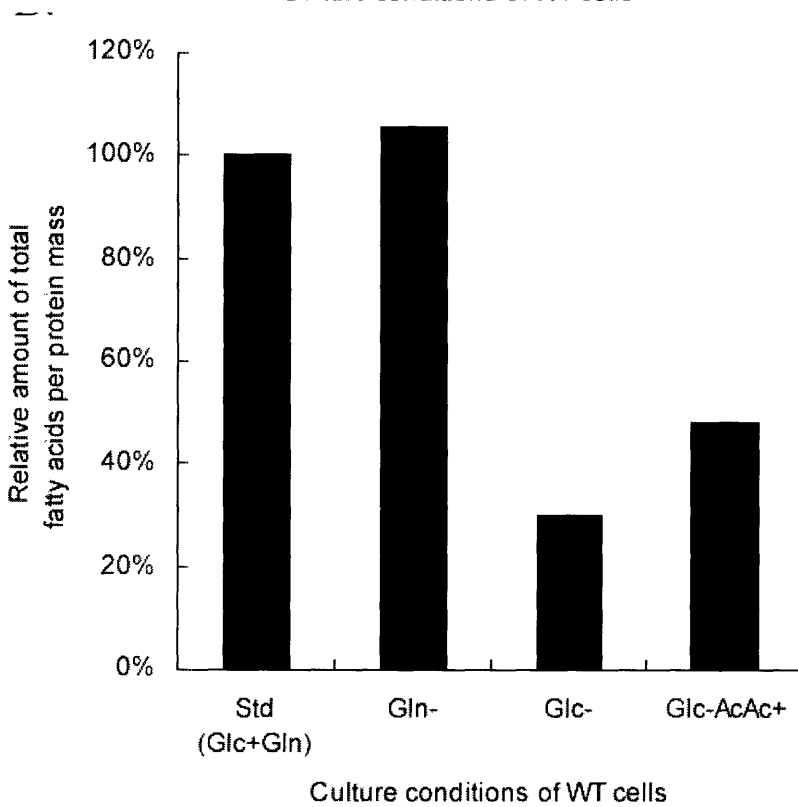
the issue of the carbon sources for the glycerol backbone of the newly synthesized lipids as an explanation for the limited lipogenic ability of WT cells under Glc- condition. Two hypotheses were considered for the failure of the WT cells under Glc- condition to produce normal amounts of fatty acids. First, glucose may be required for adequate production of acetyl CoA such that lipogenesis will not proceed unless the acetyl units provided by glucose are available to supplement those from glutamine and other sources. Second, glucose may be required for providing the glycerol backbone to the synthesis of lipids. To evaluate these hypotheses, the labeling of the glycerol moiety of the lipids were examined under Std condition or under AcAc+ condition in the presence of 25 mM [U-^{13}C] glucose for WT cells (Fig. 1.10). Carbon from neither glutamine nor acetoacetate under the two conditions contributed to lipidic glycerol (Figs. 1.10A and 1.10B). The isotopomer distribution of TBDMS-derivatized glycerol indicated that ^{13}C-labeled glucose provided 79% of the glycerol backbone for WT cells calculated as (M+3) / {(M+0) + (M+3)} after correction for natural abundance (Fig. 1.10A). The percentage agrees well with the g(4 day) value of 0.79 for WT cells under Std condition, indicating that 79% of the lipids was newly synthesized. This result also agrees with the finding that the amount of total fatty acids increased approximately four-fold over the 4-day differentiation period. Thus, glucose from the medium appears to be the sole carbon source for glycerol used for *de novo* lipogenesis of WT cells under the Std condition.

Several routes for the synthesis of glycerol-3-phosphate (G3P), the immediate precursor for glycerol backbone of lipids, have been proposed in brown adipose tissue. As the previous data indicate, carbon of G3P can be derived from glucose. A second route, glyceroneogenesis (glycerol synthesis from non-glucose sources) has been reported to be
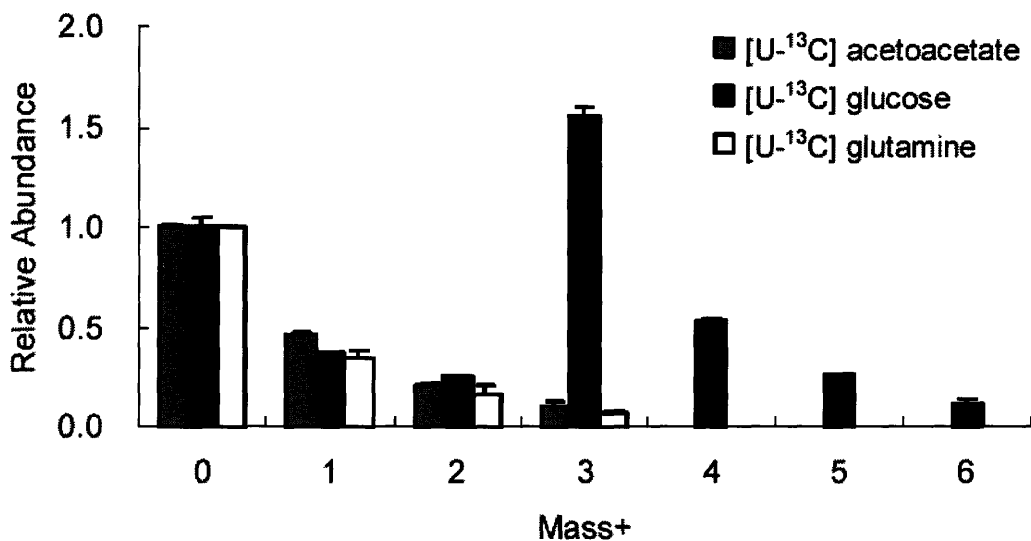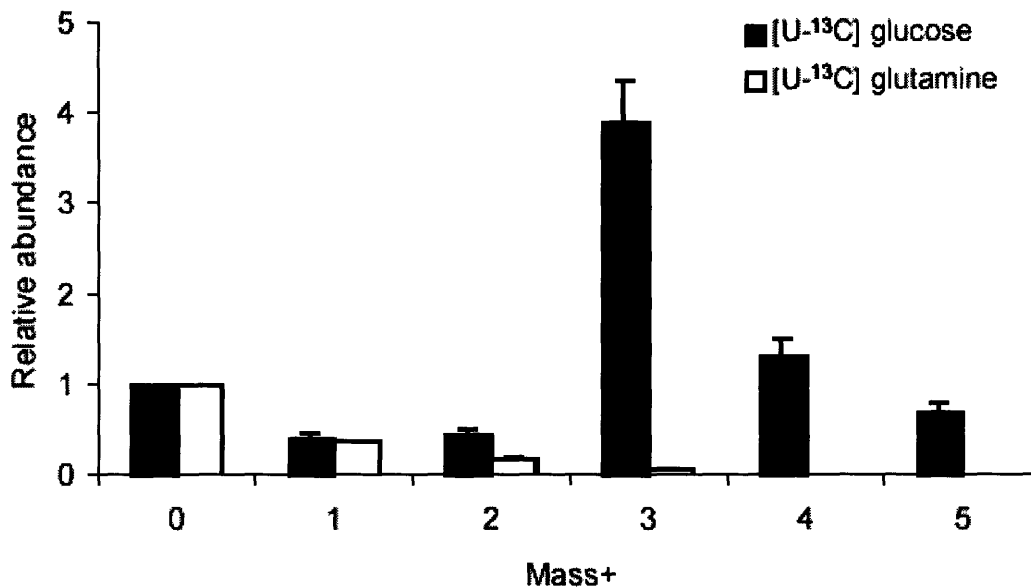
Fig. 1.10. Carbon sources for glycerol backbone of lipids.

Isotopomer distribution of TBDMS derivative of glycerol from lipids of WT cells following four-day labeling with either $[U-{}^{13}C]$ glucose or $[U-{}^{13}C]$ glutamine on day 6 under Std condition (A) or with unlabeled glucose and glutamine plus $[U-{}^{13}C]$ acetoacetate (B). Large M+3 value indicates that glucose, and neither glutamine or acetoacetate, supplies carbon for glycerol. Data shown are the averages of two independent determinations with error bars indicating the ranges.

active in brown adipose tissue (11), but its quantitative significance has not been investigated. A third possibility is the recycling of glycerol via glycerokinase (25). Whether glyceroneogenesis and/or glycerol cycling could replace the role of glucose in supplying G3P for lipidic glycerol was tested as following. WT cells were incubated from day 2 to day 6of differentiation in the absence of glucose but in glutamine (4 mM) supplemented with one of the following; pyruvate (5 mM); lactate (5 mM) plus pyruvate (0.5 mM); glycerol (10 mM). None of these conditions increased the synthesis of total fatty acids over those found for Glc- condition. In addition, the possibility that glutamine could form glycerol via glyceroneogenesis was investigated in the Glc- condition using [U-^{13}C] glutamine. GC/MS analysis of lipidic glycerol was unable to detect flux of glutamine to glycerol in the Glc- condition. Thus, no evidence was found that alternative carbon sources could compensate for the role of glucose to stimulate *de novo* lipogenesis in the presence of glutamine.

Lipogenesis in the presence of added acetate

Acetate is a commonly used substrate for lipogenesis and has been used previously with ISA to quantify the contribution in lipogenesis of 3T3-L1 cells (18). To evaluate the contribution of acetate to the lipogenic acetyl CoA pool, 2 mM acetate was added to the differentiation medium from day 2 to day 6 for WT and IRS-1 KO brown adipocytes. For ISA analysis, acetate, glucose, or glutamine in the medium was replaced in individual wells with [U-^{13}C] acetate, [U-^{13}C] glucose, or [U-^{13}C] glutamine, respectively. The isotopomer distribution of methyl palmitate was evaluated by ISA to determine the D and g(4 day) values (Fig. 1.11). The data demonstrate that acetate is an effective carbon source for

lipogenic acetyl CoA in both WT and IRS-1 KO brown adipocytes. Comparing the D

values from Figures 1.11A and 1.6A indicates that acetate added to the medium displaced

some of the contribution of glutamine to lipogenic acetyl CoA in WT cells. This result was

obtained by noting that the sum of D values of added carbon sources for WT cells in the

presence of acetate, $D_{(AC)} + D_{(Glc)} + D_{(Gln)} = 0.67 \pm 0.01$, was not different from that of WT

cells under Std condition, $D_{(Glc)} + D_{(Gln)} = 0.63 \pm 0.03$. $D_{(Glc)}$ remained similar between the

two condition (Std: $D_{(Glc)} = 0.28 \pm 0.02$, AC+: $D_{(Glc)} = 0.26 \pm 0.01$) while $D_{(Gln)}$ was

reduced (from 0.34 ± 0.02 to 0.20 ± 0.00) mainly due to the contribution from acetate

$(D_{(AC)} = 0.20 \pm 0.00)$.

A different result was found for IRS-1 KO cells (Fig. 1.11; see also Fig. 1.6). The sum

of D values of added carbon sources in IRS-1 KO cells under AC+ condition (0.75 ± 0.02)

was increased from those in IRS-1 KO cells under Std condition (0.61 ± 0.01) by the same

amount as $D_{(AC)}$ (0.14 ± 0.00). $D_{(Glc)}$ (Std: $D_{(Glc)} = 0.42 \pm 0.01$, AC+: $D_{(Glc)} = 0.45 \pm 0.01$)

and $D_{(Gln)}$ (Std: $D_{(Gln)} = 0.19 \pm 0.00$, AC+: $D_{(Gln)} = 0.16 \pm 0.01$) remained similar. These

results indicate that acetate replaced "Other" carbon sources in fatty acid synthesis of the

IRS-1 KO cells. When acetate was added to the medium, the g(4 day) value for WT cells

was 0.79, identical to that found for the Std condition (Figs. 1.6B and 1.11B). Likewise,

for IRS-1 KO cells, the g(4 day) value was not affected by adding acetate. These results

indicate that addition of 2 mM acetate altered the fluxes of carbon to lipogenic acetyl CoA

but did not affect fractional synthesis of total fatty acids.
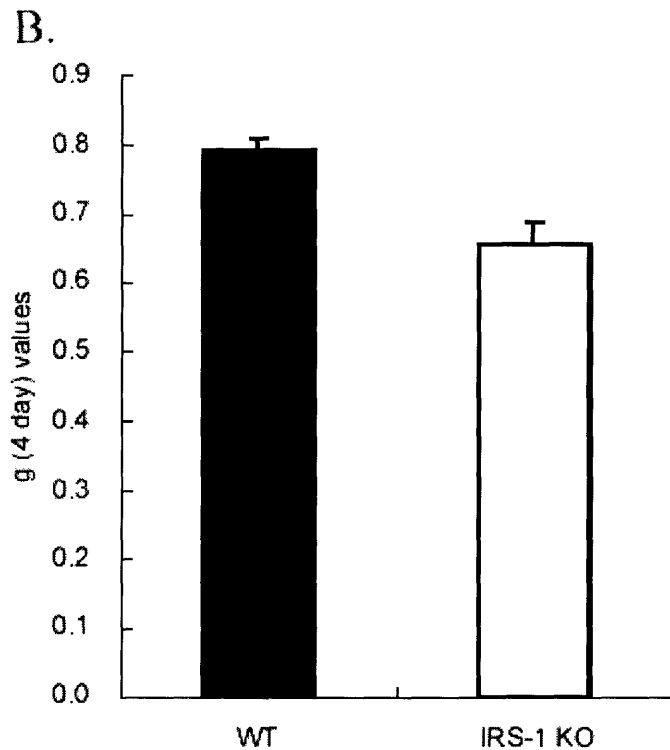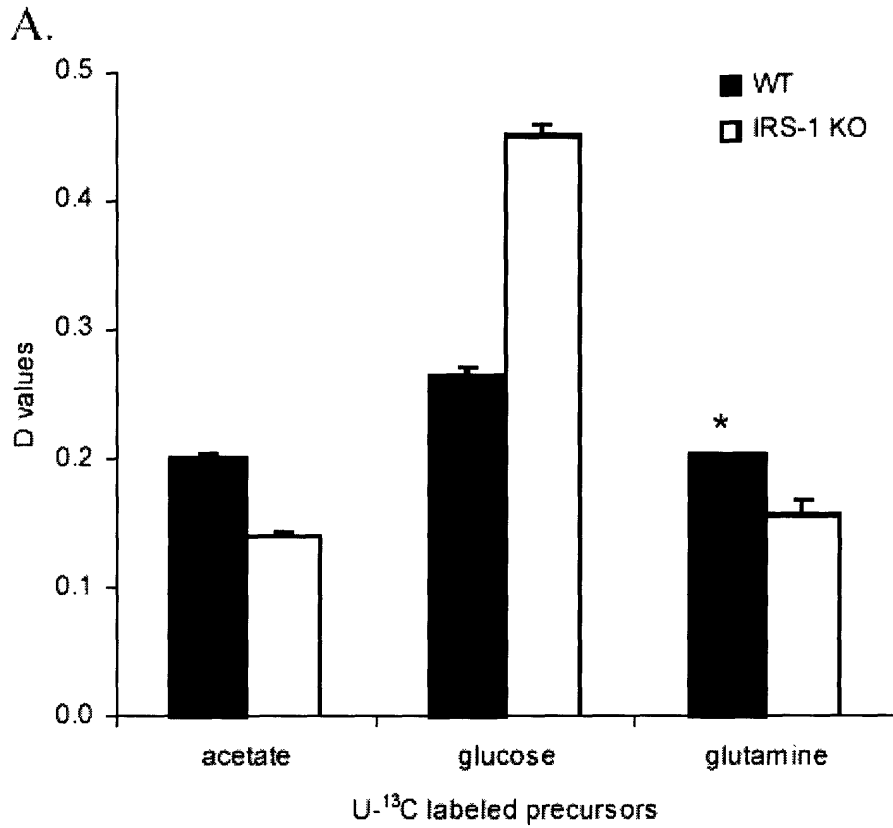
Fig. 1.11. Effect of acetate on flux of carbon sources to fatty acids.

A: Fractional tracer contribution, D values, for palmitate synthesis from Glc, Gln, or AC in WT and IRS-1 KO BF cells under standard + acetate condition (AC+) on day 6 (^{13}C-labeling from day 2 to day 6). Data shown are mean ± SEM (n ≥ 3). Asterisk (*) indicates significant difference between the standard condition (Fig. 1.6A) and the AC+ condition with the same ^{13}C-labeled precursors at P ≤ 0.01. B: Fractional synthesis, g (4 day) values, for the same conditions as in 1.11A.

Physiology of lipogenesis in brown adipocytes

Taken together, the results of this study demonstrate the utilization of a number of carbon sources for *de novo* lipogenesis in brown IRS-1 KO preadipocytes and differentiating WT adipocytes. The finding that the contribution of glutamine to lipogenic acetyl CoA was nearly equal to that of glucose was novel, as glutamine has not been noted as a lipogenic carbon source in adipocytes. Low rates of glutamine flux to triglyceride have previously been reported for white adipose tissue (26). Two routes are known for flux of glutamine to acetyl CoA. Glutaminolysis flux described by Newsholme and colleagues (27) involves TCA cycle metabolism to α-ketoglutarate followed by flux of malate or oxaloacetate to pyruvate via malic enzyme or PEPCK and pyruvate kinase. Alternatively, the reductive carboxylation pathway metabolizes α-ketoglutarate to citrate by reversal of the NADPH coupled isocitrate dehydrogenase (28). The studies performed here do not distinguish between these pathways. However, isotopic methods can be used to determine the relative flux by each pathway (29) and this technique may be useful to clarify the role of glutamine as a carbon source for lipogenesis. Although glutamine was an important carbon source for lipogenesis, neither glutamine, nor glutamine plus acetoacetate, could compensate for removal of glucose from the medium (Fig. 1.9B).

In the absence of glucose, the amount of triglyceride fatty acids in WT cells was low, similar to that of the IRS-1 KO cells under standard condition. These findings indicate a distinct role for glucose in lipid synthesis during differentiation. A distinct metabolic action of glucose is as the source for G3P for the glycerol backbone of triglyceride and for NADPH generation in the pentose phosphate pathway. In this study, no evidence was found for alternatives to glucose for G3P synthesis despite the ample evidence for

glyceroneogenesis and glycerokinase flux in brown adipose tissue (30). Thus, G3P

synthesis remains a candidate for a pathway not duplicated by other substrates investigated

here. A second candidate for a distinct metabolic role of glucose is the production of

lipogenic NADPH through the pentose phosphate pathway. However, NADPH may be

produced both via glucose-6-phosphate dehydrogenase (G6PDH) in the pentose phosphate

pathway and via malic enzyme. Brown adipocyte differentiation induces increases in both

of these enzymes and thus both may play a role in generating NADPH for lipogenesis (31,

32). As shown here, isotopic tools, including ISA, may be applied to further explore and

quantify lipogenic fluxes in brown adipose cells.

References

1. Lowell, B. B. and J. S. Flier. 1997. Brown adipose tissue, beta 3-adrenergic receptors, and obesity. *Annu.Rev.Med.* **48**: 307-316.

2. Spiegelman, B. M., P. Puigserver, and Z. Wu. 2000. Regulation of adipogenesis and energy balance by PPARgamma and PGC-1. *Int.J.Obes.Relat Metab Disord.* **24 Suppl 4**: S8-10.

3. Linhart, H. G., K. Ishimura-Oka, F. DeMayo, T. Kibe, D. Repka, B. Poindexter, R. J. Bick, and G. J. Darlington. 2001. C/EBPalpha is required for differentiation of white, but not brown, adipose tissue. *Proc.Natl.Acad.Sci.U.S.A* **98**: 12532-12537.

4. Boeuf, S., M. Klingenspor, N. L. van Hal, T. Schneider, J. Keijer, and S. Klaus. 2001. Differential gene expression in white and brown preadipocytes. *Physiol Genomics* **7**: 15-25.

5. Klein, J., M. Fasshauer, H. H. Klein, M. Benito, and C. R. Kahn. 2002. Novel adipocyte lines from brown fat: A model system for the study of differentiation, energy metabolism, and insulin action. *Bioessays* **24**: 382-388.

6. McCormack, J. G. and R. M. Denton. 1977. Evidence that fatty acid synthesis in the interscapular brown adipose tissue of cold-adapted rats is increased in vivo by insulin by mechanisms involving parallel activation of pyruvate dehydrogenase and acetyl-coenzyme A carboxylase. *Biochem.J.* **166**: 627-630.

7. Agius, L. and D. H. Williamson. 1981. The utilization of ketone bodies by the interscapular brown adipose tissue of the rat. *Biochemica Biophysica Acta* **666**: 127-132.

8. Wright, J. and L. Agius. 1983. Fatty acid synthesis and ketone body utilization by brown adipose tissue of the rat. Response to cold or nutritional state? *Biochemica Biophysica Acta* **753**: 244-248.

9. Williamson, D. H. and V. Ilic. 1985. Activities of enzymes of acetoacetate metabolism in rat brown adipose tissue during development. *Biochem.J.* **231**: 773-775.

10. Cooney, G., R. Curi, A. Mitchelson, P. Newsholme, M. Simpson, and E. A. Newsholme. 1986. Activities of some key enzymes of carbohydrate, ketone body, adenosine and glutamine metabolism in liver, and brown and white adipose tissues of the rat. *Biochem Biophys Res Commun* **138**: 687-92.

11. Brito, M. N., N. A. Brito, S. R. Brito, M. A. Moura, N. H. Kawashita, I. C. Kettelhut, and R. H. Migliorini. 1999. Brown adipose tissue triacylglycerol synthesis in rats adapted to a high-protein, carbohydrate-free diet. *Am.J.Physiol* **276**: R1003-R1009.

12. Kawashita, N. H., W. T. Festuccia, M. N. Brito, M. A. Moura, S. R. Brito, M. A. Garofalo, I. C. Kettelhut, and R. H. Migliorini. 2002. Glycerokinase activity in brown adipose tissue: a sympathetic regulation? *Am.J.Physiol Regul.Integr.Comp Physiol* **282**: R1185-R1190.

13. Tagliaferro, A. R., S. Dobbin, R. Curi, B. Leighton, L. D. Meeker, and E. A. Newsholme. 1990. Effects of diet and exercise on the in vivo rates of the triglyceride-fatty acid cycle in adipose tissue and muscle of the rat. *Int.J.Obes.* **14**: 957-971.

14. Bernlohr, D. A., C. W. Angus, M. D. Lane, M. A. Bolanowski, and T. J. Kelly. 1984. Exprssion of specific mRNAs during adipose differentiation: identification of an mRNA encoding a homologue of mylin P2 protein. *Proc.Natl.Acad.Sci.U.S.A.* **81**: 5468-5472.

15. Shimizu, Y., D. Kielar, H. Masuno, Y. Minokoshi, and T. Shimazu. 1994. Dexamethasone induces the GLUT4 glucose transporter, and responses of glucose transport to norepinephrine and insulin in primary cultures of brown adipocytes. *J.Biochem.(Tokyo)* **115**: 1069-1074.

16. Shima, A., Y. Shinohara, K. Doi, and H. Terada. 1994. Normal differentiation of rat brown adipocytes in primary culture judged by their expressions of uncoupling

protein and the physiological isoform of glucose transporter. *Biochemica Biophysica Acta* **1223**: 1-8.

17. Miki, H., T. Yamauchi, R. Suzuki, K. Komeda, A. Tsuchida, N. Kubota, Y. Terauchi, J. Kamon, Y. Kaburagi, J. Matsui, Y. Akanuma, R. Nagai, S. Kimura, K. Tobe, and T. Kadowaki. 2001. Essential role of insulin receptor substrate 1 (IRS-1) and IRS-2 in adipocyte differentiation. *Mol.Cell Biol.* **21**: 2521-2532.

18. Kharroubi, A. T., T. M. Masterson, T. A. Aldaghlas, K. A. Kennedy, and J. K. Kelleher. 1992. Isotopomer spectral analysis of triglyceride fatty acid synthesis in 3T3-L1 cells. *Am J Physiol* **263**: E667-E675.

19. Rosen, E. D. and B. M. Spiegelman. 2000. Molecular regulation of adipogenesis. *Annu.Rev.Cell Dev.Biol.* **16**: 145-171.

20. Fasshauer, M., J. Klein, K. M. Kriauciunas, K. Ueki, M. Benito, and C. R. Kahn. 2001. Essential role of insulin receptor substrate 1 in differentiation of brown adipocytes. *Mol.Cell Biol.* **21**: 319-329.

21. Hara, A. and N. S. Radin. 1978. Lipid extraction of tissues with a low-toxicity solvent. *Anal.Biochem.* **90**: 420-426.

22. Flakoll, P. J., M. Zheng, S. Vaughan, and M. J. Borel. 2000. Determination of stable isotopic enrichment and concentration of glycerol in plasma via gas chromatography-mass spectrometry for the estimation of lipolysis in vivo. *J.Chromatogr.B Biomed.Sci.Appl.* **744**: 47-54.

23. Kelleher, J. K. and T. M. Masterson. 1992. Model equations for condensation biosynthesis using stable isotopes and radioisotopes. *Am J Physiol* **262**: E118-E125.

24. Darlington, G. J., S. E. Ross, and O. A. MacDougald. 1998. The role of C/EBP genes in adipocyte differentiation. *J.Biol.Chem.* **273**: 30057-30060.

25. Chakrabarty, K., B. Chaudhuri, and H. Jeffay. 1983. Glycerokinase activity in human brown adipose tissue. *J.Lipid Res.* **24**: 381-390.

26. Kowalchuk, J. M., R. Curi, and E. A. Newsholme. 1988. Glutamine metabolism in isolated incubated adipocytes of the rat. *Biochem.J.* **249**: 705-708.

27. Newsholme, E. A. and A. L. Carrie. 1994. Quantitative aspects of glucose and glutamine metabolism by intestinal cells. *Gut.* **35**: S13-S17.

28. D'Adamo, A. F. and D. E. Haft. 1989. An alternative pathway of alpha-ketoglutarate catabolism in the isolated, perfused rat liver. *J.Biol.Chem.* **240**: 613-617.

29. Holleran, A. L., D. A. Briscoe, G. Fiskum, and J. K. Kelleher. 1995. Glutamine metabolism in AS-30D hepatoma cells. Evidence for its conversion into lipids via reductive carboxylation. *Mol Cell Biochem* **152**: 95-101.

30. Festuccia, W. T., N. H. Kawashita, M. A. Garofalo, M. A. Moura, S. R. Brito, I. C. Kettelhut, and R. H. Migliorini. 2003. Control of glyceroneogenic activity in rat brown adipose tissue. *Am.J.Physiol Regul.Integr.Comp Physiol* **285**: R177-R182.

31. Valverde, A. M., M. Benito, and M. Lorenzo. 1992. Hormonal regulation of malic enzyme and glucose-6-phosphate-dehydrogenase expression in fetal brown-adipocyte primary cultures under non-proliferative conditions. *Eur.J.Biochem.* **203**: 313-319.

32. Garcia-Jimenez, C., A. Hernandez, M. J. Obregon, and P. Santisteban. 1993. Malic enzyme gene expression in differentiating brown adipocytes: regulation by insulin and triiodothyronine. *Endocrinology* **132**: 1537-1543.

Chapter 2. Quantitative analysis of individual carbon fluxes from glutamine to fatty acid synthesis in wild-type brown adipocytes

Introduction

Glutamine's role as a carbon source for fat synthesis has been suggested for a variety of mammalian tissues, including adipocytes (18) and fibroblasts (24) as well as hepatoma cells (14), by radioactivity measurement of fat derived from ^{14}C-labeled glutamine. For uptake of glutamine into the cells, the first step of glutamine utilization, ASCT2 transporter has been identified as the transporter of glutamine with insulin-mediated stimulation in adipocytes (26). Then, incorporation of glutamine carbon into the synthesis of fatty acids begins with conversion of glutamine to glutamate and to α-ketoglutarate, which is the point of entry into tricarboxylic acid (TCA) cycle. The conventional pathway of α-ketoglutarate to succinate, fumarate, and malate, followed by malate's oxidation to pyruvate and further decarboxylation to acetyl-CoA has been accepted as the major metabolic route for glutamine to contribute to fatty acid synthesis (glutaminolysis) (1, 21)(Fig. 2.1A). However, an alternative pathway involving reductive carboxylation of α-ketoglutarate to isocitrate and cleavage of citrate to directly supply acetyl-CoA (Fig. 2.1B) has also been supported by studies with [5-^{14}C] glutamine, glutamate, or α-ketoglutarate in adipocytes (19,20), hepatocytes (5), and hepatoma cells (14,27).

Using the experimental results with [5-^{14}C] glutamine and other ^{14}C-labeled metabolites, it was possible to estimate the ratio between the relative contributions of the two pathways. More detailed information for the carbon fluxes involved in the two pathways was derived
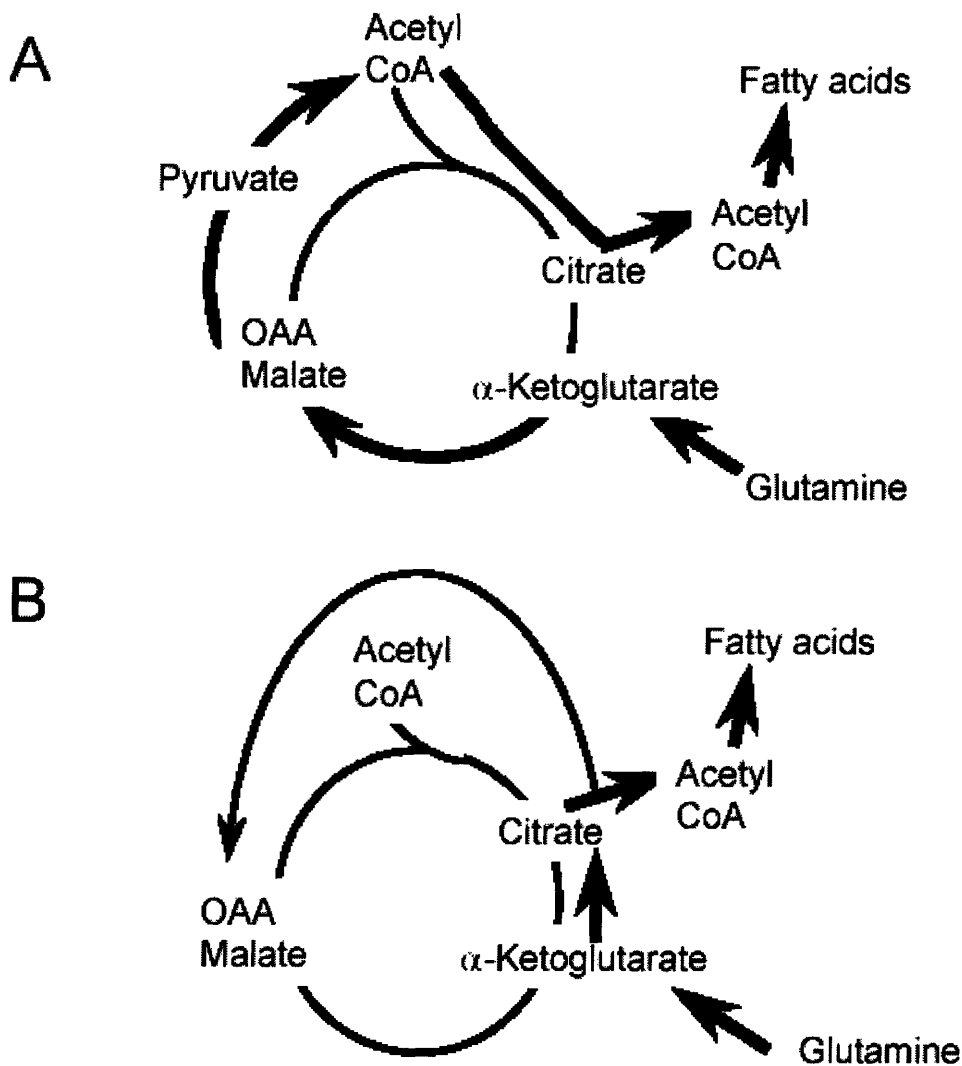
Fig. 2.1. Two pathways for glutamine's metabolic route to fatty acid synthesis.

A. Glutaminolysis pathway. Glutamine enters TCA cycle at α-ketoglutarate and converted to succinate, fumarate, and malate, whose further conversion to pyruvate and acetyl-CoA leads to fatty acid synthesis.

B. Reductive carboxylation pathway. Glutamine enters TCA cycle at α-ketoglutarate, which is directly converted to isocitrate and citrate via reductive carboxylation and cleaved to supply acetyl-CoA for fatty acid synthesis.

from analyzing ^{13}C-labeling patterns of some intermediate metabolites in studies with perfused rat organs with [U-^{13}C] glutamate or [U-^{13}C] glutamine (4,8). However, the estimated flux of reductive carboxylation of α-ketoglutarate in these studies was not directly correlated with their contribution to fatty acid synthesis.

The key enzyme in reductive carboxylation pathway is mitochondrial isocitrate dehydrogenase. In conventional pathway of TCA cycle, oxidative decarboxylation of isocitrate to α-ketoglutarate can be catalyzed by NAD$^+$-dependent isocitrate dehydrogenase (NAD-ICDH), whose kinetic properties are consistent with the enzyme's unidirectionality (11). On the other hand, the reversible reaction between isocitrate and α-ketoglutarate catalyzed by NADP$^+$-dependent isocitrate dehydrogenase (NADP-ICDH) has been found to favor the reductive carboxylation of α-ketoglutarate to isocitrate *in vivo*. The enzyme's Km for CO_2 (1.6 mM) is very close to physiological CO_2 concentration (1.5 mM) (6) and the enzyme's affinity for NADPH is approximately 100-fold higher than for NADP$^+$ (25).

Substantial contribution of glutamine to the synthesis of palmitate in wild-type brown adipocytes from mouse has been demonstrated in Chapter 1 (34). In addition, glutaminase, catalyzing the first reaction of glutamine to glutamate in glutamine's route to fatty acid synthesis, was reported to have high activity for brown adipocytes *in vitro* (18) and *in vivo* (7). Also, *in vivo* activity of NADP-ICDH in brown adipose tissue was shown to be significantly higher than in white adipose tissue (17). Thus, in this chapter, the importance of reductive carboxylation pathway in glutamine's route to fatty acid synthesis has been examined by an initial experiment with [5-^{13}C] glutamine and a follow-up experiment with specific inhibition of NADP-ICDH. Then, the carbon fluxes involved in fatty acid synthesis from glucose and glutamine were individually estimated by analysis of a

metabolic network model, using ^{13}C-labeling and GC/MS. The results provided compelling evidences for the significance of reductive carboxylation pathway in glutamine's route to fatty acid synthesis and showed how the flux through this pathway can be controlled by modulating the activity of NADP-ICDH.

Experimental Procedures

Materials

Biochemicals were obtained from Sigma Chemical Co., St. Louis, MO. ^{13}C-labeled

chemicals were obtained from Cambridge Isotope Laboratories, Inc., Andover, MA. Tissue

culture media were obtained from Invitrogen, Co., Carlsbad, CA.

Cell culture and adipocyte differentiation

Brown adipocyte cells were cultured with the same procedure as in Chapter 1 (34).

Briefly, WT brown preadipocytes were grown in 6-well plates (surface area = 10 cm^2) to

confluence in differentiation media containing 25 mM glucose, 4 mM glutamine, 20 nM

insulin, 1 nM T3, and 10 % fetal bovine serum as well as 44 mM $NaHCO_3$ (day 0). The

media were then replaced with fresh induction media, which were differentiation media

with added induction compounds: 0.125 mM indomethacin, 0.25 mM IBMX, and 5 μM

dexamethasone. On day 2 and day 4, the media were replaced with fresh differentiation

media to reach day 6. In [5-^{13}C] glutamine experiment, the media from day 2 to day 6

contained 4 mM [5-^{13}C] glutamine and 25 mM unlabeled glucose. In studies for the

determination of carbon flux from glucose or glutamine to fatty acid synthesis through

tricarboxylic acid (TCA) cycle, on day 4 the media were changed to differentiation media

without glucose or glutamine at 42 hrs after day 2. The differentiation media were

supplemented with selected concentration of oxalomalate or 2-methylisocitrate and

incubated at 37°C for 10 min, followed by addition of glucose and glutamine with specified

[13]C-labeling. Stock solution of 2-methylisocitrate was prepared from 2-methylisocitrate

lactone (for synthesis, see (2)) according to Dr. Wolfgang Buckel (Philipps-Universitaet,

Marburg, Germany) as follows: threo-diastereoisomer of 2-methylisocitrate lactone (1:1 mixture of natural (2R,3S) and unnatural (2S,3R) diastereomers, gift from Dr. Buckel) in 1 M potassium hydroxide solution was incubated at 80°C for 20 min and then neutralized to pH 7 with HCl. After 6-hr incubation at 37°C, the media were removed and cells were extracted for organic/amino acids or lipids.

Isolation and derivatization of organic/amino acids and lipids

For isolation of organic/amino acids, the procedure described in Fiehn *et al.* (10) was modified as follows. 0.7 mL methanol and 25 µL water was added to each well of 6-well plate immediately after removal of the media. In 15 min after incubation at room temperature, methanol extract was mixed with 0.7 mL water and 0.37 mL chloroform in 15 mL tube. Vigorous vortexing was followed by centrifugation at 3000 x g for 3 min. The chloroform layer was carefully removed and the methanol/water layer was centrifuged again at 3000 x g for 3 min. Clear solution of methanol/water layer (separated from white precipitate) was then transferred to a glass vial and evaporated. The residue was dissolved in 70 µL of methoxyamine hydrochloride (20 mg/mL in pyridine) and vortexed. Treatment with methoxyamine protects α-keto carboxylic acids against decarboxylation by converting α-keto moiety to methoxyimino moiety (10). This pretreatment was beneficial for detecting pyruvate and α-ketoglutarate in this study. After 90 min incubation at 37°C, organic/amino acids were derivatized with 70 µL of N-methyl-N-*tert*-butyldimethylsilyltrifluoroacetamide (MTBSTFA) at 70°C for 30 min. The reaction mixture was then directly injected into GC/MS instrument for analysis of the isotopomer

distribution of organic/amino acids. Isolation of lipids and derivatization of palmitate moiety into methyl ester were performed as described previously (34).

GC/MS for isotopomer distribution measurement

Samples from [5-^{13}C] glutamine experiment were analyzed for palmitate isotopomer distribution with the same instrumental setup as previously reported (34). The samples from the rest of the experiments were analyzed with another GC/MS instrument described below. Isotopomer distributions of fatty acid methyl esters measured with the second GC/MS instrument with scan mode were essentially identical to those measured with the first GC/MS with selected ion monitoring (SIM) mode.

Samples were injected into a Hewlett-Packard model 5890 series II Gas Chromatograph connected to HP5971 series Mass Selective Detector and equipped with DB-XLB (60 m x 0.25 mm id x 0.25 μm) capillary column (J&W Scientific, Folsom, CA). Helium flow with 10 psi inlet pressure was maintained by electronic control. The temperatures of the injector and the detector were kept at 230°C and 300°C, respectively. For isotopomer distribution analysis of methyl palmitate and its isotopomers (M+0 to M+16 (m/z = 270 to 286)), GC column temperature was started at 100°C and held for 1 min. The temperature was then increased to 250°C at 10°C/min, and held for 5 min. It was increased to 300°C at 25°C/min and held for 2 min. Mass range of 100 to 350 was recorded at 2.7 scans per second. For isotopomer distribution analysis of TBDMS derivatives of organic and amino acids, GC temperature was started at 100°C and held for 5 min. The temperature was then increased to 300°C at 10°C/min, and held for 5 min. Mass range of 50 to 550 was recorded at 1.5 scans per second. The most abundant fragments (M−57 = M−*tert*-butyl) of the following

acid derivatives (*tert*-butyldimethylsilyl; TBDMS) were analyzed for their isotopomer

distributions: pyruvate (m/z=174-178), lactate (m/z=261-265), fumarate (m/z=287-293), α-

ketoglutarate (m/z=346-354), malate (m/z=419-423), aspartate (m/z=418-424), glutamate

(m/z=432-440), and citrate (m/z=459-468).

Measurement of uptake fluxes for glucose and glutamine

Uptake fluxes for glucose and glutamine into WT cells were calculated from the rates of

consumption of glucose and glutamine from medium as reported in Chapter 1 (34).

Data analysis

Fractional contribution of ^{13}C-labeled carbon sources to fatty acid synthesis (D value)

and fractional new synthesis of fatty acids during time t (g(t) value) were estimated with the

isotopomer distribution measurements of palmitate based on the model of isotopomer

spectral analysis (ISA) as reported previously (34). For estimation of fluxes in the

metabolic network model (Fig. 2.9) by integrating the isotopomer distributions of palmitate,

pyruvate, lactate, fumarate, α-ketoglutarate, malate, aspartate, glutamate, and citrate, a

MATLAB program was used. Given a metabolic network consisting of a set of reactions

with specific atomic transitions between defined metabolites, mass balance,

metabolic/isotopic steady state, and unknown fluxes, the program can set up equations for

all possible isotopomers for all metabolites. The exhaustive technique like this makes the

equations non-linear so that the solution can be best derived computationally by least-

square fit method. The program can then estimate fluxes for reactions in the metabolic

network model that fit the inputs of the metabolic network and measurements of

isotopomer distributions of some metabolites. Using measurement errors for the isotopomer distribution data, the program can also calculate how good the fit for each metabolite's measurement is and the uncertainty of each estimated flux.

Glucose and glutamine taken up from medium and preexisting palmitate were defined as substrates, and production of lactate (exported into medium), palmitate, and protein synthesis from aspartate were treated as sink. The rest of the metabolites were regarded as balanced except for CO_2, which was allowed to be unbalanced.

The equations for the whole metabolic network were set up with 32 variables (fluxes). The number of independent measurements for solving the equations was 50, the sum of "the number of isotopomers – 1" for nine metabolites. Each measurement of isotopomer distribution was corrected for natural abundance by the program before estimating fluxes.

For each set of flux estimation results, statistical evaluation of how good the fit was for each metabolite's isotopomer distribution was calculated in terms of sum of square residuals (SSRES) based on measurement errors. SSRES was defined as Σ (difference between data and fit / measurement error)^2. Overall goodness of fit was calculated by summing up SSRES values for all nine metabolites, which was compared with the range of SSRES values for 95% confidence calculated by the program.

Results

[5-^{13}C] Glutamine's contribution to palmitate synthesis

Glutamine carbon's substantial contribution to fatty acid synthesis in brown adipocytes

has been established by applying the measurements of palmitate isotopomer distribution

under 4-day incubation with [U-^{13}C] glutamine to ISA model in Chapter 1 (34). Two

pathways that have been suggested for glutamine's metabolic route to fatty acid synthesis

(Fig. 2.1) can be distinguished by stable-isotope labeling experiment with [5-^{13}C] glutamine

in brown adipocyte differentiation (Fig. 2.2). The label at C-5 of glutamine would be lost

before reaching fatty acid synthesis in glutaminolysis pathway, while the label would be

transferred to the carboxyl carbon of acetyl-CoA and be incorporated into fatty acid

synthesis in reductive carboxylation pathway. When WT brown adipocyte cells were

incubated from day 2 to day 6 of the differentiation procedure in medium containing 25

mM unlabeled glucose and 4 mM [5-^{13}C] glutamine, ^{13}C-labeled C-5 of glutamine provided

substantial proportion of precursors for synthesis of palmitate in WT cells (Fig. 2.3). The

distribution data of palmitate isotopomers were analyzed for quantitative estimation of

fractional contribution of [5-^{13}C] glutamine using ISA model as in Chapter 1: [5-^{13}C]

glutamine contributed 34.1 ± 0.6 % to palmitate synthesis in WT cells.

[U-^{13}C] glutamine's contribution to palmitate synthesis affected by specific inhibition of NADP-isocitrate dehydrogenase

As an independent experiment to distinguish the two pathways for glutamine's metabolic

route to fatty acid synthesis, an enzyme that affects one pathway to a much greater extent

than the other pathway was specifically inhibited. Oxalomalate has been known to inhibit
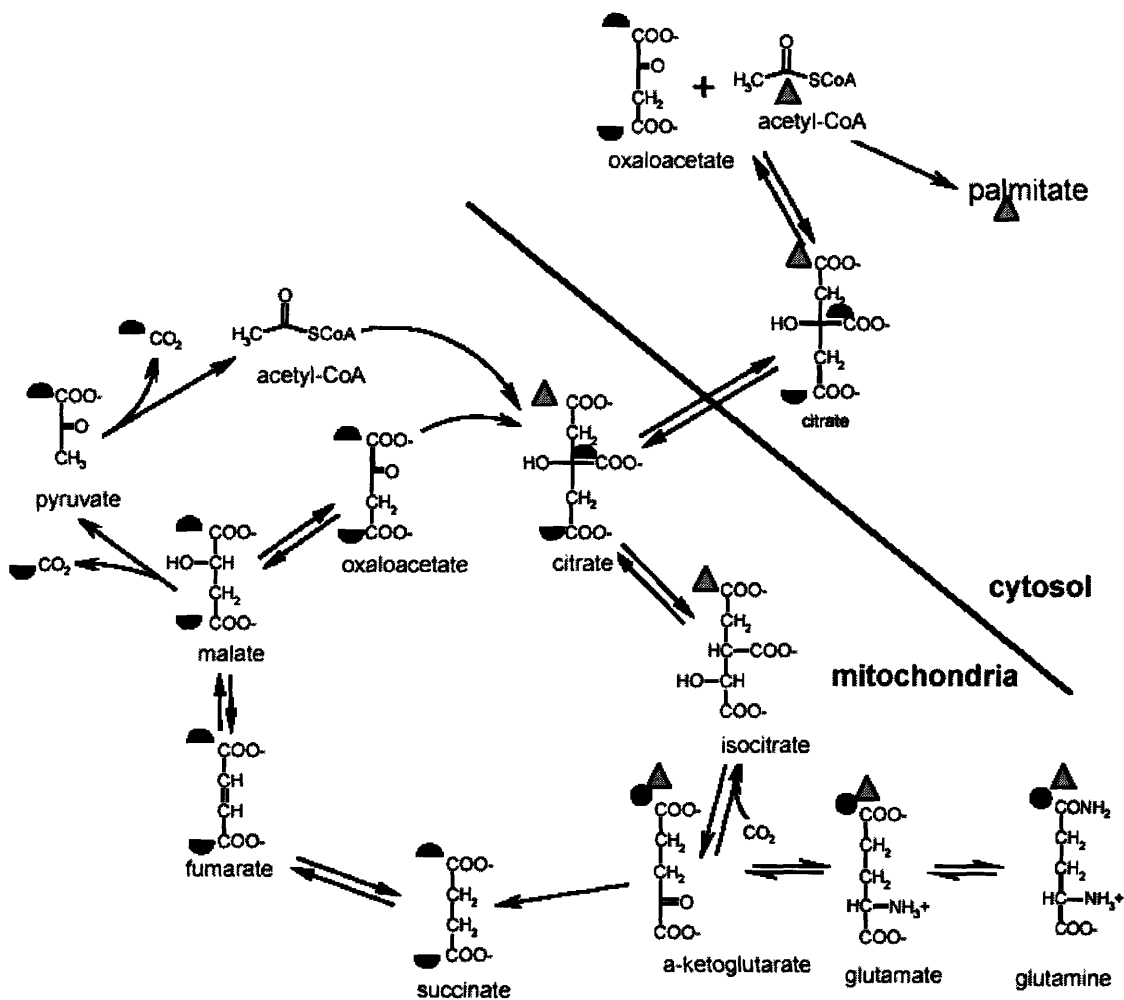
Fig. 2.2. Metabolic network scheme to distinguish the two pathways for glutamine's route to fatty acid synthesis, using [5-^{13}C] glutamine.

If glutamine follows glutaminolysis pathway, ^{13}C-label at C-5 of glutamine (black circle) will be found in either of the two terminal carbons of succinate because of its symmetry. Both ^{13}C-labels will then be lost as CO_2 when malate is converted to pyruvate and acetyl-CoA. ^{13}C-labels on the two terminal carbons of oxaloacetate will not be transferred to acetyl-CoA when citrate is cleaved back to oxaloacetate plus acetyl-CoA, because of the stereospecificity of ATP-citrate lyase.

If glutamine follows reductive carboxylation pathway, ^{13}C-label at C-5 of glutamine (grey triangle) will be maintained at acetyl-CoA side of the terminal carbon of citrate. When citrate is cleaved by ATP-citrate lyase, ^{13}C-label is transferred to acetyl-CoA and incorporated into fatty acid synthesis.

70
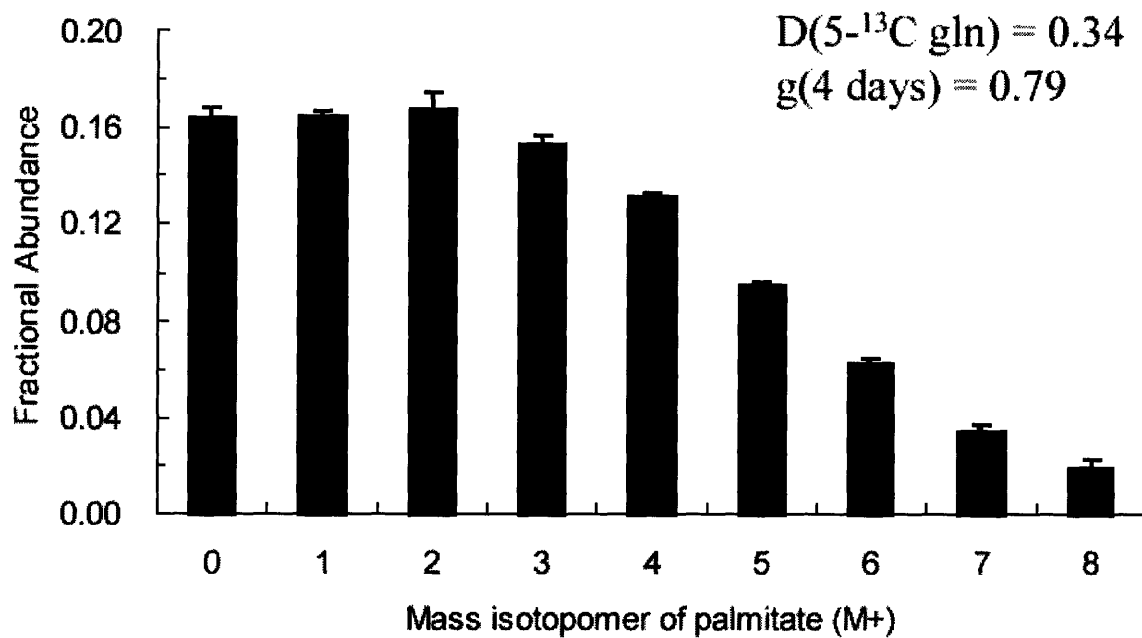
Fig. 2.3. Contribution of $[5\text{-}^{13}C]$ glutamine to palmitate synthesis.

Isotopomer distribution of palmitate isolated from WT brown adipocytes under incubation in media containing 4 mM $[5\text{-}^{13}C]$ glutamine from day 2 to day 6. Data shown are mean ± SEM (n = 3).

NADP-ICDH (responsible for reduction of α-ketoglutarate to isocitrate) specifically, and not affect the activity of NAD-ICDH (responsible for oxidation of isocitrate to α-ketoglutarate) (15). In order to investigate the effect of oxalomalate on fatty acid synthesis of WT cells from glutamine carbon, on day 4 of standard differentiation procedure WT cells were incubated in the presence of 4 mM [U-^{13}C] glutamine, 25 mM unlabeled glucose, and 0, 5, or 10 mM oxalomalate for 6 hrs before extraction. The isotopomer distributions of palmitate under the three conditions are shown in Figure 2.4A. The extent of palmitate labeling was lowered as the concentration of oxalomalate was increased. The isotopomer distribution measurements were analyzed for estimation of fractional contribution from [U-^{13}C] glutamine (D value) and fractional new synthesis during 6 hrs (g (6hr) value) according to ISA model (Fig. 2.5). Systematic decrease in D value upon incubation of WT cells under higher concentration of oxalomalate was evident whereas g (6hr) values from conditions with three different concentrations of oxalomalate did not change significantly.

Specific inhibition of NADP-ICDH by 2-methylisocitrate has been also well known (23). The effect of 2-methylisocitrate on glutamine's contribution to fatty acid synthesis in WT cells was investigated under the same condition as above in the presence of 0, 2, or 4 mM 2-methylisocitrate instead of 0, 5, 10 mM oxalomalate. The isotopomer distributions of palmitate under the three conditions (Fig. 2.4B) manifested analogous patterns as in Figure 2.4A.

In order to examine the possibility of non-specific effects of the specific inhibitors on palmitate isotopomer distribution, the same experimental procedure was performed in the presence of 5 or 10 mM citrate instead of the inhibitors. Little change was observed in D values and g (6 hr) values (Fig. 2.6).

Fig. 2.4. Effect of specific inhibitors of NADP-ICDH on palmitate synthesis from [U-^{13}C] glutamine.

Isotopomer distribution of palmitate from WT brown adipocytes on day 4 under 6-hr incubation in media containing 4 mM [U-^{13}C] glutamine and 0, 5, or 10 mM oxalomalate (A) or 0, 2, 4 mM 2-methylisocitrate (B). Data shown are mean ± SEM (n = 3).
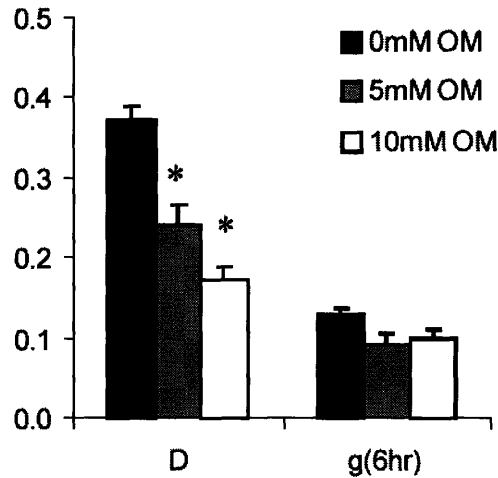
Fig. 2.5. Effect of increasing inhibition of NADP-ICDH by oxalomalate on D and g (6 hr) values of palmitate synthesis from [U-^{13}C] glutamine.

Fractional contribution of [U-^{13}C] glutamine to fatty acid synthesis (D value) and fractional new synthesis of palmitate during 6 hrs (g (6hr)) estimated from the data in Figure 2.4A by Isotopomer Spectral Analysis (ISA). Data shown are mean ± SEM (n = 3). Asterisk (*) indicates significant difference between the control condition and each of the oxalomalate-incubation conditions at P ≤ 0.01.
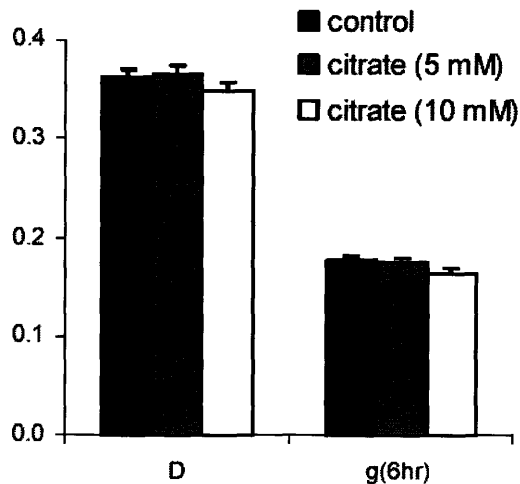
Fig. 2.6. Effect of increasing concentration of citrate in medium on D and g (6 hr) values of palmitate synthesis from [U-^{13}C] glutamine.

Fractional contribution of [U-^{13}C] glutamine to fatty acid synthesis (D value) and fractional new synthesis of palmitate during 6 hrs (g (6hr)) estimated by ISA. See text for experimental details. Data shown are mean ± SEM (n = 3).

[U-^{13}C] glucose's contribution to palmitate synthesis unchanged by specific inhibition of NADP-isocitrate dehydrogenase

As a control for [U-^{13}C] glutamine experiment, the same experiment for specific

inhibition by oxalomalate as above was performed with 25 mM [U-^{13}C] glucose and 4 mM

unlabeled glutamine. Because glucose carbon's metabolic route to fatty acid synthesis

(glucose → pyruvate → acetyl-CoA → citrate → acetyl-CoA → fatty acid) does not

directly involve reductive carboxylation of α-ketoglutarate to isocitrate in TCA cycle, the

extent of incorporating glucose carbon to palmitate synthesis was not expected to change

upon specific inhibition of NADP-ICDH. The palmitate isotopomer distribution under [U-

^{13}C] glucose did not change significantly when the concentration of oxalomalate was

increased from 0 mM to 5 or 10 mM (Fig. 2.7).

Isotopomer distribution of other metabolites related to fatty acid synthesis

The effect of oxalomalate and 2-methylisocitrate on glutamine's contribution to fatty

acid synthesis was further investigated by measuring the isotopomer distributions of other

metabolites that are metabolically related to glutamine's route to fatty acid synthesis. The

data for isotopomer distribution measurements of fumarate, malate, aspartate, pyruvate, and

lactate from the same condition as above in the presence of 0, 5, or 10 mM oxalomalate are

summarized in Appendix A. The effect of 5 or 10 mM oxalomalate was most pronounced

in isotopomer distributions of glutamate, α-ketoglutarate, and citrate, all of which are

intermediates for glutamine's route to fatty acid synthesis via reductive carboxylation

pathway (Fig. 2.8). M+5 isotopomers of glutamate and α-ketoglutarate were in parallel

with each other in that their fractional abundance increased upon treatment with higher
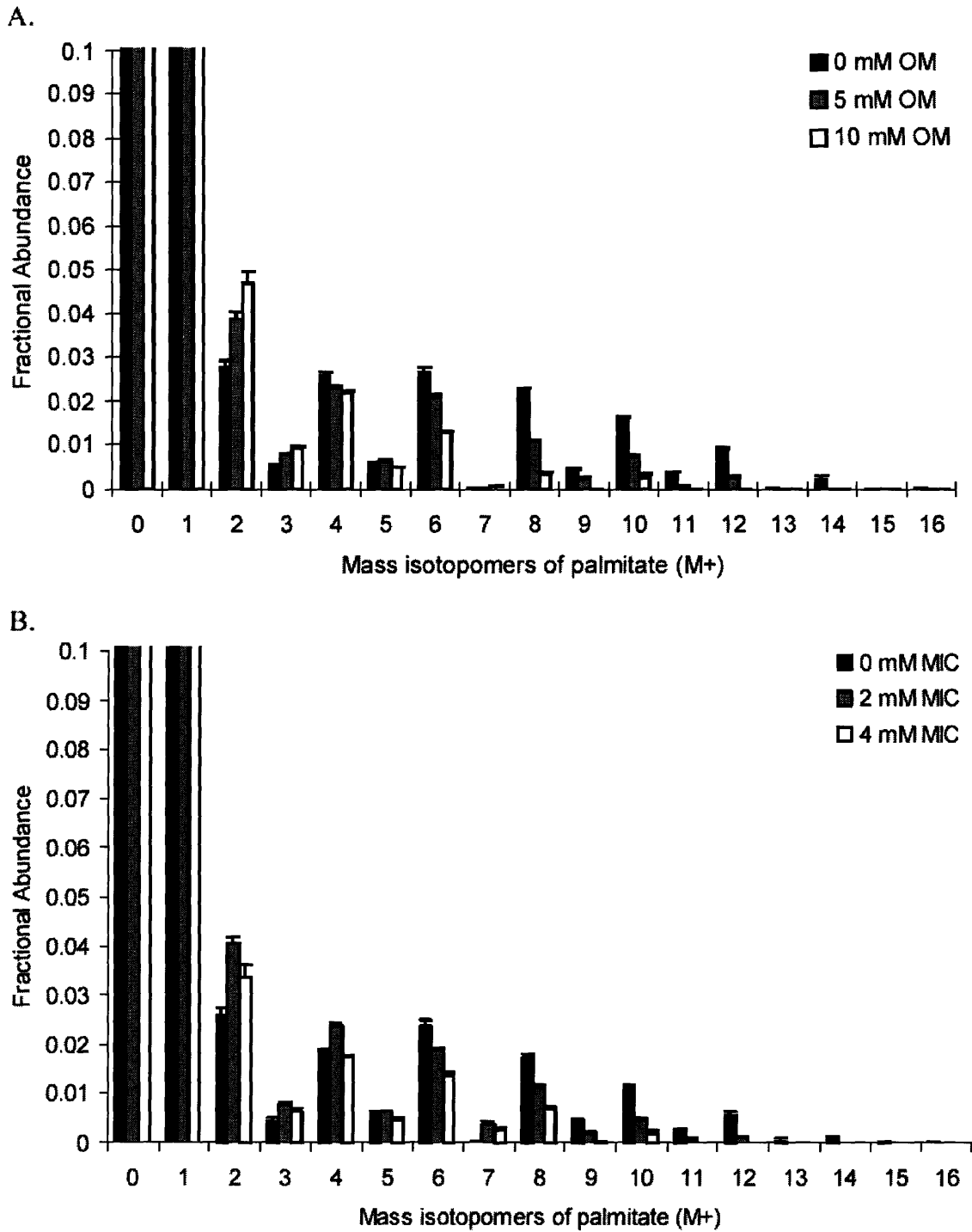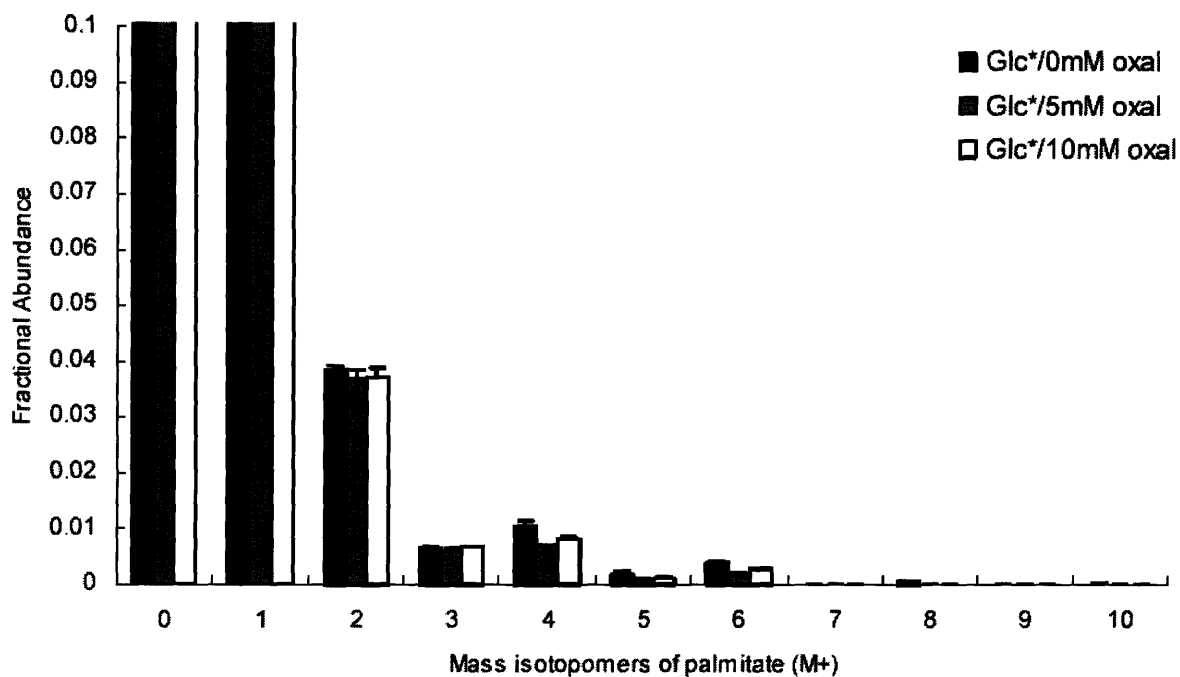
Fig. 2.7. Effect of specific inhibitors of NADP-ICDH on palmitate synthesis from [U-^{13}C] glucose.

Isotopomer distribution of palmitate from WT brown adipocytes on day 4 under 6-hr incubation in media containing 25 mM [U-^{13}C] glucose and 0, 5, or 10 mM oxalomalate. Data shown are mean ± SEM (n = 3).
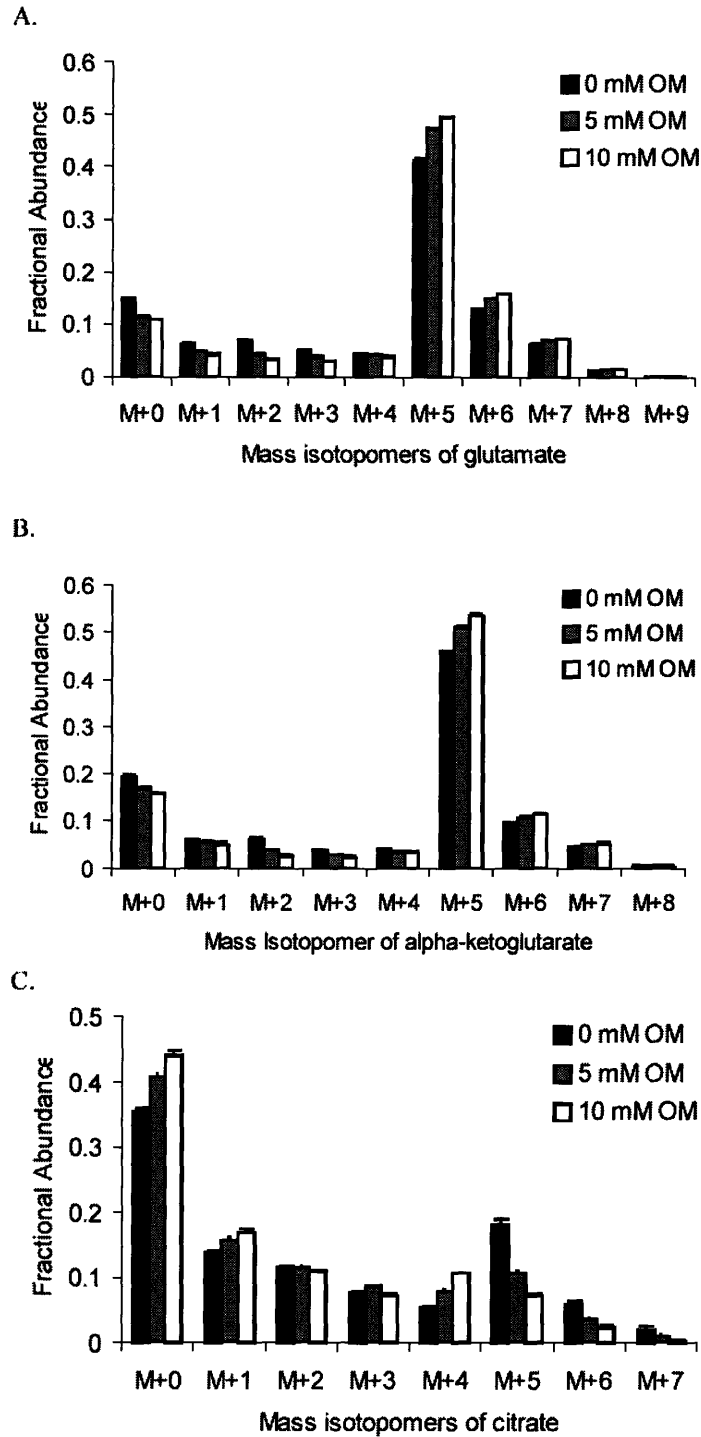
Fig. 2.8. Effect of increasing inhibition of NADP-ICDH by oxalomalate on isotopomer distribution of glutamate, α-ketoglutarate, and citrate.

Isotopomer distribution of glutamate (A), α-ketoglutarate (B), and citrate (C) from WT brown adipocytes on day 4 under 6-hr incubation in media containing 4 mM [U-^{13}C] glutamine and 0, 5, or 10 mM oxalomalate. Data shown are mean ± SEM (n = 3).

77

concentration of oxalomalate (Figs. 2.8A and 2.8B). On the other hand, the fractional

abundance of M+5 isotopomer of citrate, which can only originate from M+5 isotopomer of

α-ketoglutarate via reductive carboxylation, decreased systematically upon increase in

oxalomalate concentration from 0 to 5 and 10 mM (Fig. 2.8C).

Complete metabolic network model: steady-state assumption confirmed

The metabolic flux of glutamine carbon to fatty acid synthesis was examined in further

detail, with basic metabolic network model constructed from metabolic reactions of

glycolysis, fatty acid synthesis, and TCA cycle with addition of reversible reactions

between glutamine, glutamate, and α-ketoglutarate (Fig. 2.9). In order to test whether

reductive carboxylation of α-ketoglutarate to isocitrate/citrate happens mainly in cytosol or

in mitochondria, the dependence of the glutamine → palmitate flux on citrate transport

across mitochondrial membrane was examined by adding 5 mM of benzenetricarboxylate

(BTC: specific inhibitor of tricarboxylic acid transporter) to wild-type brown adipocytes for

6 hrs on day 4. Fractional contribution of glutamine to lipogenic acetyl-CoA (D value)

was reduced from 0.36 ± 0.01 to 0.28 ± 0.02. Fractional new synthesis during 6 hrs (g (6

hr) value) was also decreased from 0.18 ± 0.01 to 0.09 ± 0.01.

The fluxes in the metabolic network can be estimated by solving the equations set up for

each reaction with the input of the measured isotopomer distributions of metabolites. If the

steady-state assumption can be fulfilled, setting up the equations and solving them becomes

straightforward. In order to assess whether brown adipocytes on day 4 have reached

metabolic/isotopic steady state within 6 hrs of incubation in 4 mM [U-^{13}C] glutamine and

25 mM unlabeled glucose, the isotopomer distribution of eight metabolites were measured
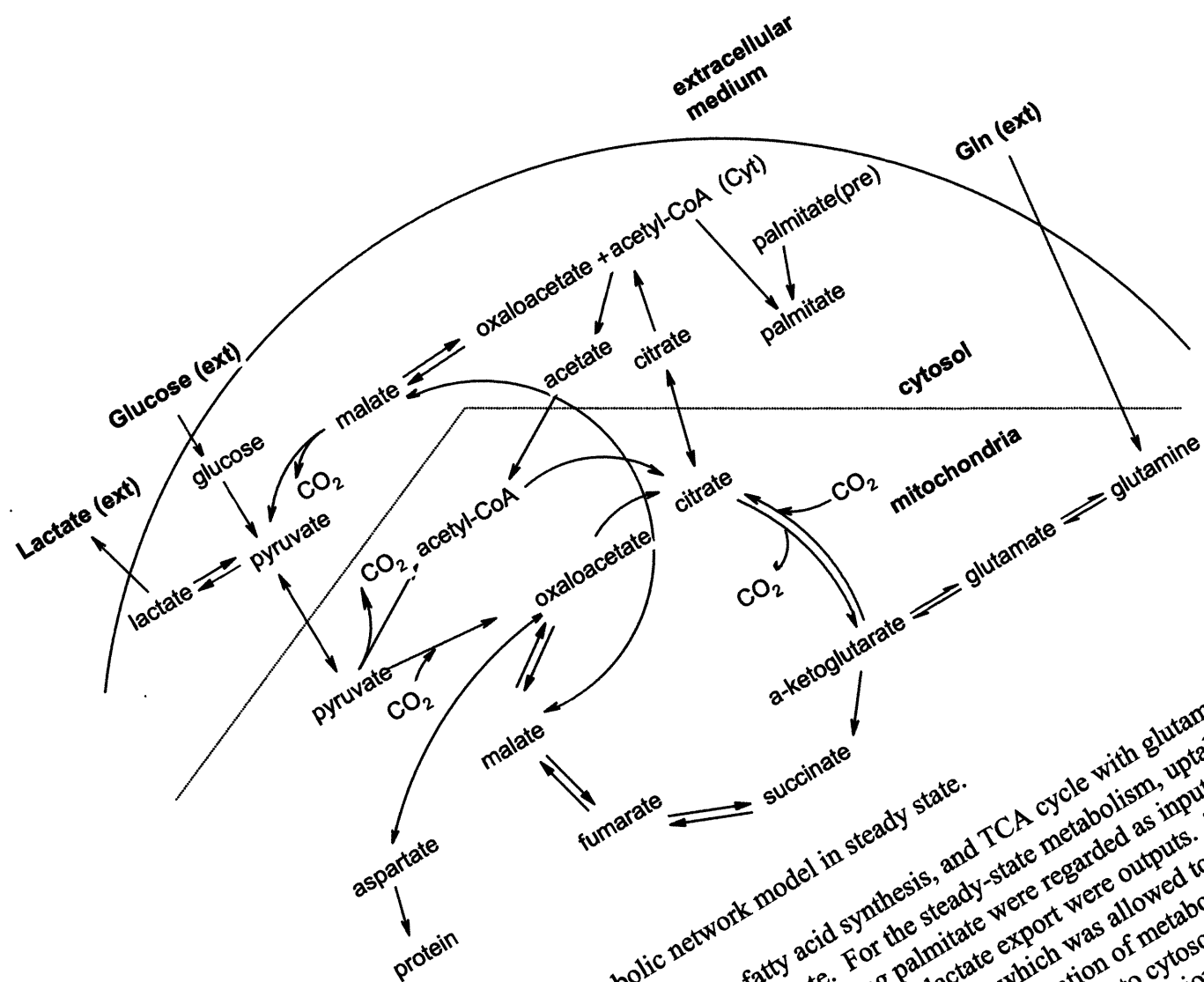
Fig. 2.9. Complete metabolic network model in steady state.
The model consists of glycolysis, fatty acid synthesis, and TCA cycle with glutamine entering at α-ketoglutarate via glutamate. For the steady-state metabolism, uptake of glucose and glutamine as well as pre-existing palmitate were regarded as inputs. Total palmitate, protein synthesis from aspartate, and lactate export were outputs. The rest of the metabolites were treated as balanced except for CO_2, which was allowed to be unbalanced. The model was constructed from the known compartmentation of metabolic reactions into cytosol or mitochondria, but only acetyl-CoA was separated into cytosolic ("acetyl-CoA(Cyt)") and mitochondrial ("acetyl-CoA") pools in the calculation of flux estimation. Except for palmitate ("palmitate(pre)" = pre-existing palmitate; "palmitate" = total palmitate), all other intracellular metabolites were assumed to be in a single pool.

79

at 2 hrs, 4 hrs, and 6 hrs after incubation of WT cells in medium with [U-^{13}C] glutamine.

Labeling patterns of two key metabolites – citrate and malate – stayed relatively constant at

three different time frames (Fig. 2.10) as well as those of the other six metabolites

(Appendix B).

Assessment of goodness of fit and flux estimation

In order to estimate the individual fluxes in the metabolic network of WT cells on day 4

under 4 mM [U-^{13}C] glutamine and 25 mM unlabeled glucose, the data for isotopomer

distribution of nine metabolites (including palmitate) from WT cells on day 4 under 0, 5, 10

mM oxalomalate for 6 hrs were plugged into the non-linear equations derived from the

metabolic network, using a MATLAB program designed for solving the equations with the

measurements by least-square fit method (see "Experimental Procedures" for details).

Evaluation of how good the overall fit was in terms of SSRES values for the three

conditions is summarized in Table 1. All three SSRES values fell within the 95%

confidence range.

Estimated fluxes for selected reactions in WT cells with 4 mM [U-^{13}C] glutamine under

0, 5, and 10 mM oxalomalate for 6 hrs are represented in graphs (Fig. 2.11). When the

uptake fluxes of glutamine and glucose were measured and set relatively to be 100 and

1550 respectively, the glutamine flux of 100 was sustained until α-ketoglutarate, where it

was divided into a net flux of 63 going to citrate via reductive carboxylation and 37 going

to succinate, under 0 mM oxalomalate condition. The net flux for reductive carboxylation

was linearly reduced to 32 and 5 under incubation with 5 mM and 10 mM oxalomalate,

consistent with specific inhibition of NADP-ICDH in a dose-dependent manner.
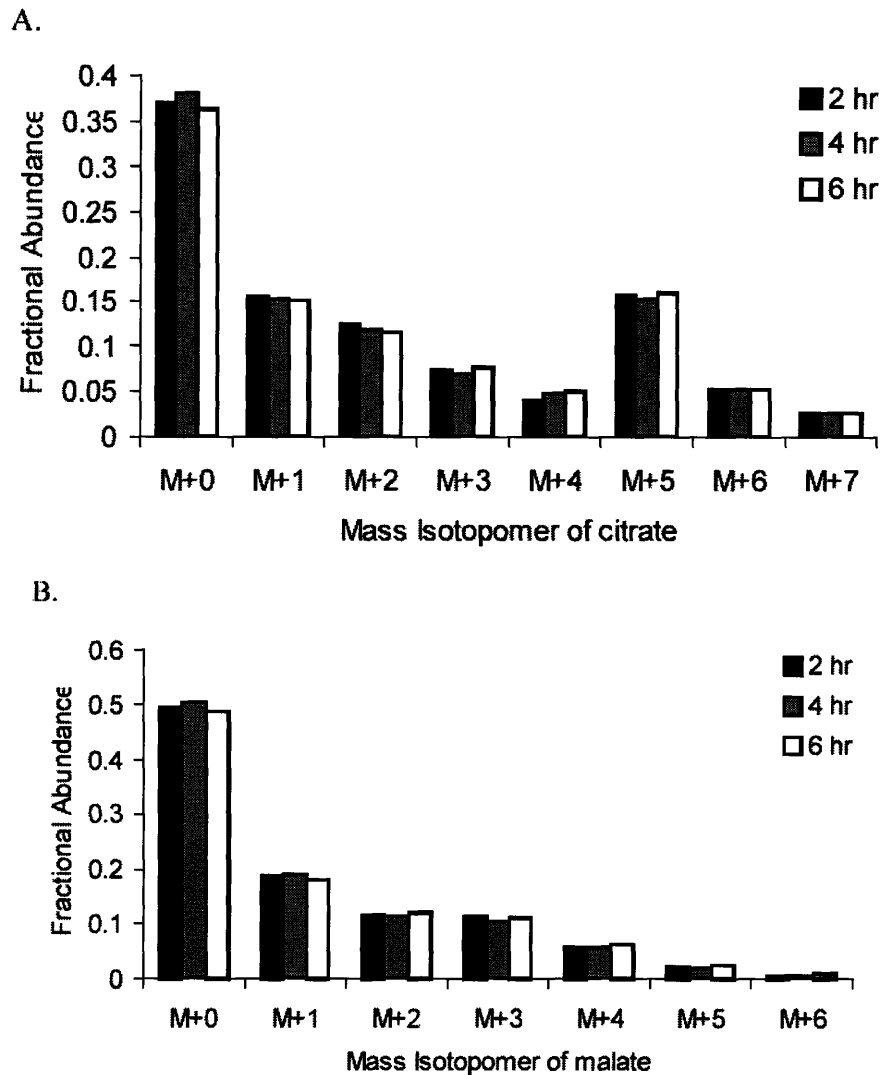
Fig. 2.10. Confirmation of steady-state assumption by time-course ^{13}C-labeling experiment.

Isotopomer distribution of citrate (A) and malate (B) from WT brown adipocytes measured at 2 hr, 4 hr, and 6 hr after incubation with 4 mM [U-^{13}C] glutamine on day 4.

Table 1. Overall goodness of fit for flux estimation in WT brown adipocytes.

From the experiments with WT brown adipocytes on day 4 under 6-hr incubation in media containing 25 mM unlabeled glucose, 4 mM [U-^{13}C] glutamine, and specific inhibitors of NADP-ICDH (oxalomalate (A) or 2-methylisocitrate (B)), the isotopomer distribution data of nine metabolites were obtained and integrated into the metabolic network model (Fig. 2.9). With steady-state assumption fulfilled, fluxes for the metabolic reactions in the metabolic network were estimated by solving balanced equations from the network. For each set of flux estimation, 95% confidence range of SSRES was calculated and compared with SSRES from measured data.

A.

Experimental conditions	95% confidence range of SSRES (calculated)	Measured SSRES
0 mM oxalomalate	25.999 – 61.777	59.688
5 mM oxalomalate	25.999 – 61.777	60.370
10 mM oxalomalate	25.999 – 61.777	58.330

B.

Experimental conditions	95% confidence range of SSRES (calculated)	Measured SSRES
0 mM 2-methylisocitrate	25.999 – 61.777	59.050
2 mM 2-methylisocitrate	25.999 – 61.777	48.173
4 mM 2-methylisocitrate	27.575 – 64.201	60.294
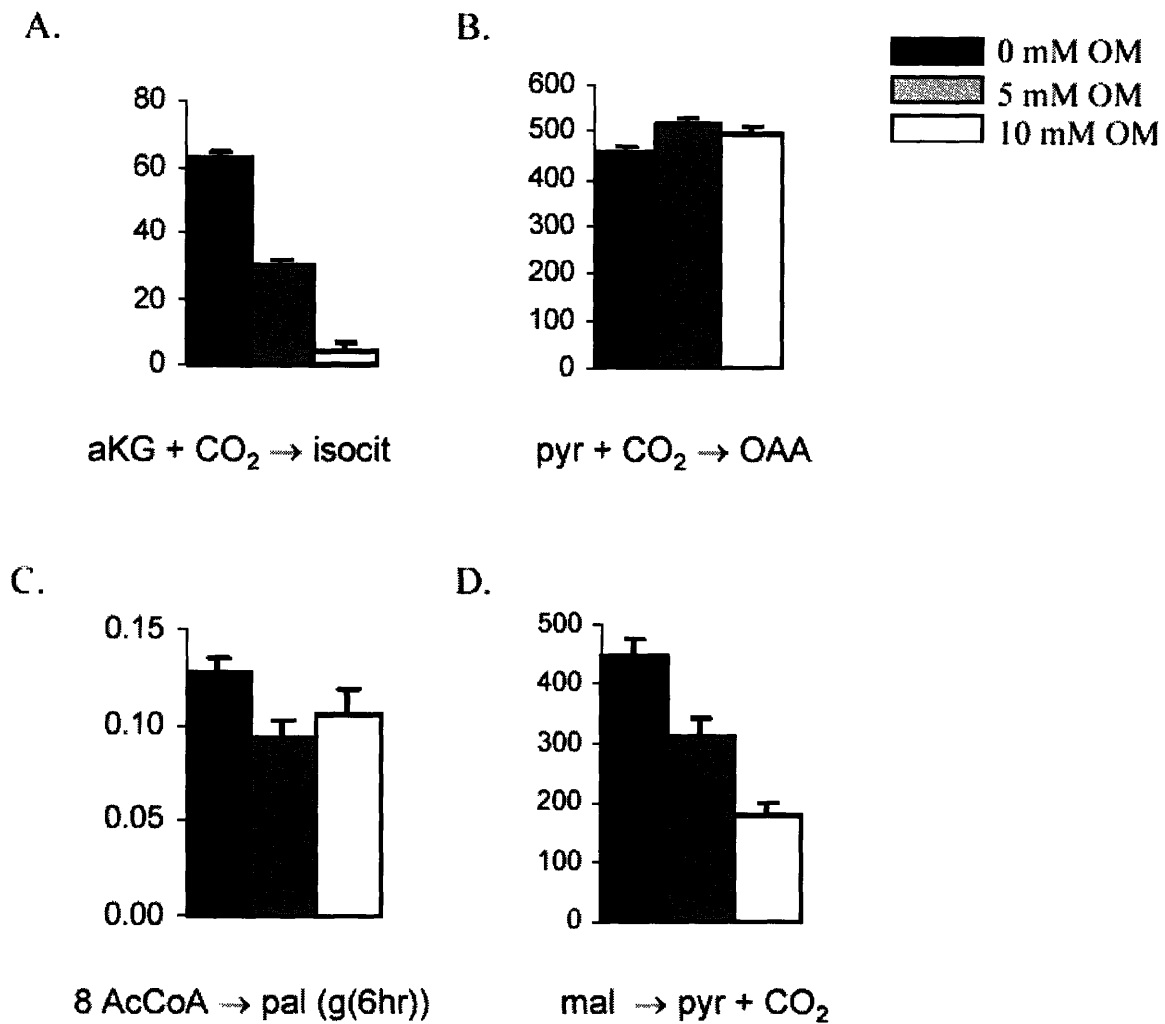
Fig. 2.11. Estimated fluxes for selected metabolic reactions in WT brown adipocytes under specific inhibition of NADP-ICDH by oxalomalate.

Estimated fluxes for α-ketoglutarate to citrate (represented in net flux), pyruvate to oxaloacetate, acetyl-CoA to palmitate (represented as g(6 hr) value), and malate to pyruvate in WT brown adipocytes under incubation with 4 mM [U-^{13}C] glutamine and 0, 5, or 10 mM oxalomalate. Data shown are mean ± SEM (n = 3).

Concurrently, the flux for α-ketoglutarate to succinate was increased to 68 and 95. In addition, the flux of converting malate to pyruvate (catalyzed by malic enzyme) was linearly decreased from 438 to 303 and 195 upon increasing the inhibition of NADP-ICDH by oxalomalate. The effect of specific NADP-ICDH inhibition was not as distinct on other fluxes such as those from pyruvate to acetyl-CoA and to oxaloacetate. Moreover, specific inhibition of NADP-ICDH did not change the fractional new synthesis of fatty acids (g (6hr) values) significantly, consistent with Figure 2.5.

Treatment of WT cells with 0, 2, or 4 mM 2-methylisocitrate gave rise to parallel patterns for the fluxes of α-ketoglutarate to citrate and to succinate (Fig. 2.12) as in the experiments with oxalomalate. However, the profile of estimated fluxes for malate to pyruvate under increasing concentrations of 2-methylisocitrate showed no significant difference. Comprehensive data sets for estimated fluxes in the presence of either 0, 5, 10 mM oxalomalate or 0, 2, 4 mM 2-methylisocitrate are summarized in Appendix C.

Estimation of key fluxes justified by experiments with [U-^{13}C] glucose or [U-^{13}C] aspartate

In order to justify some fluxes estimated above, a parallel experiment with 25 mM [U-^{13}C] glucose and 4 mM unlabeled glutamine was performed for 6 hrs on day 4. Isotopomer distribution of pyruvate and lactate (Fig. 2.13A) as well as fumarate, malate, and aspartate (Fig. 2.13B) showed conspicuous peaks of M+3 isotopomers, consistent with large glycolytic flux and high level of pyruvate's carboxylation to oxaloacetate as estimated in experiments with [U-^{13}C] glutamine (see above). On the other hand, low level of ^{13}C-enrichment in succinate (Fig. 2.13C) was in accordance with estimated net reaction of

A.

80
60
40
20
0

aKG + CO$_2$ → cit

B.

700
600
500
400
300
200
100
0

pyr + CO$_2$ → OAA

0 mM MIC
2 mM MIC
4 mM MIC

C.

0.12
0.10
0.08
0.06
0.04
0.02
0.00

8 AcCoA → pal (g(6hr))

D.

600
500
400
300
200
100
0

mal → pyr + CO$_2$
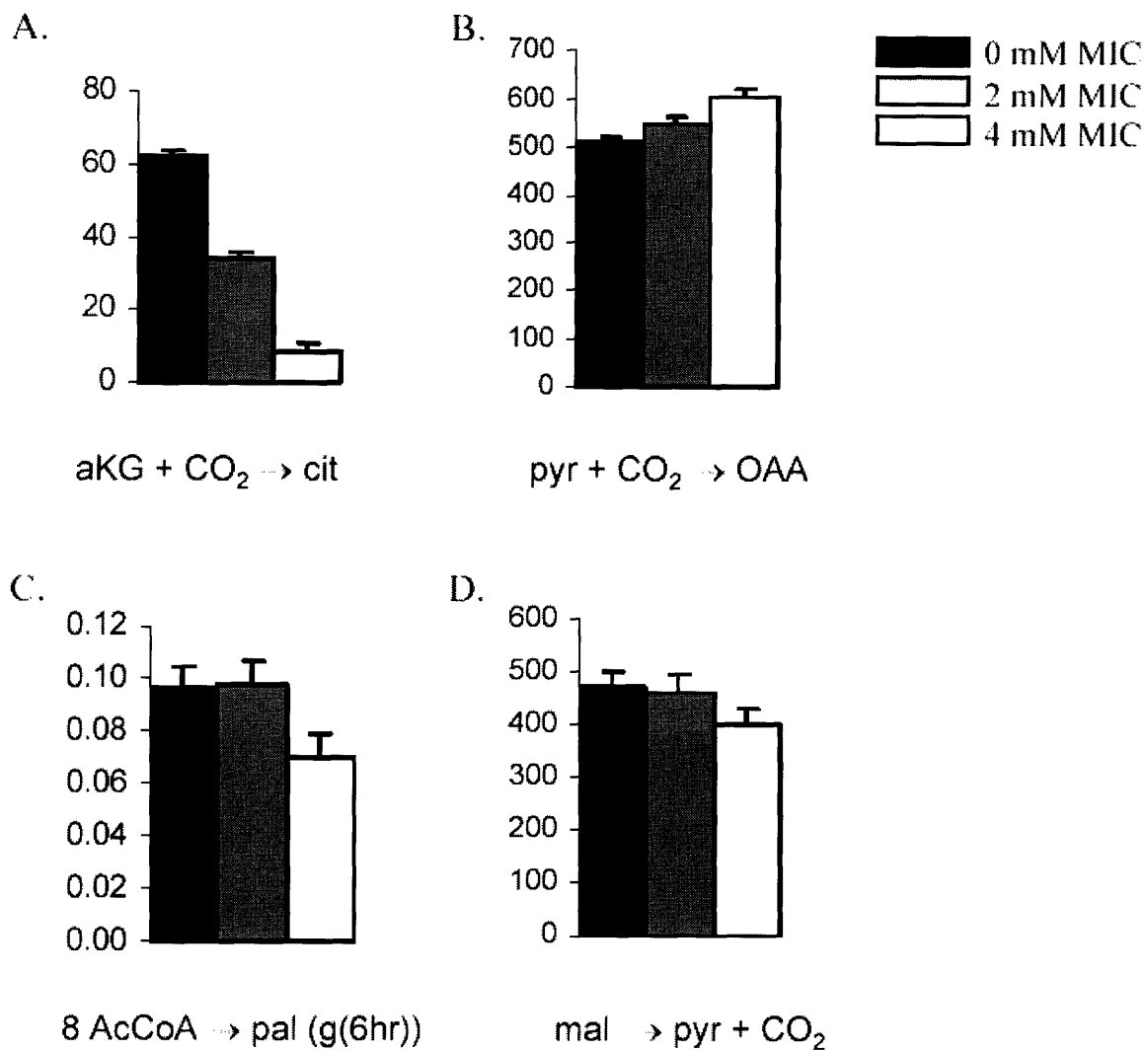
Fig. 2.12. Estimated fluxes for selected metabolic reactions in WT brown adipocytes under specific inhibition of NADP-ICDH by 2-methylisocitrate.

Estimated fluxes for α-ketoglutarate to citrate (represented in net flux), pyruvate to oxaloacetate, acetyl-CoA to palmitate (represented as g(6 hr) value), and malate to pyruvate in WT brown adipocytes under incubation with 4 mM [U-^{13}C] glutamine and 0, 2, or 4 mM 2-methylisocitrate. Data shown are mean ± SEM (n = 3).

85
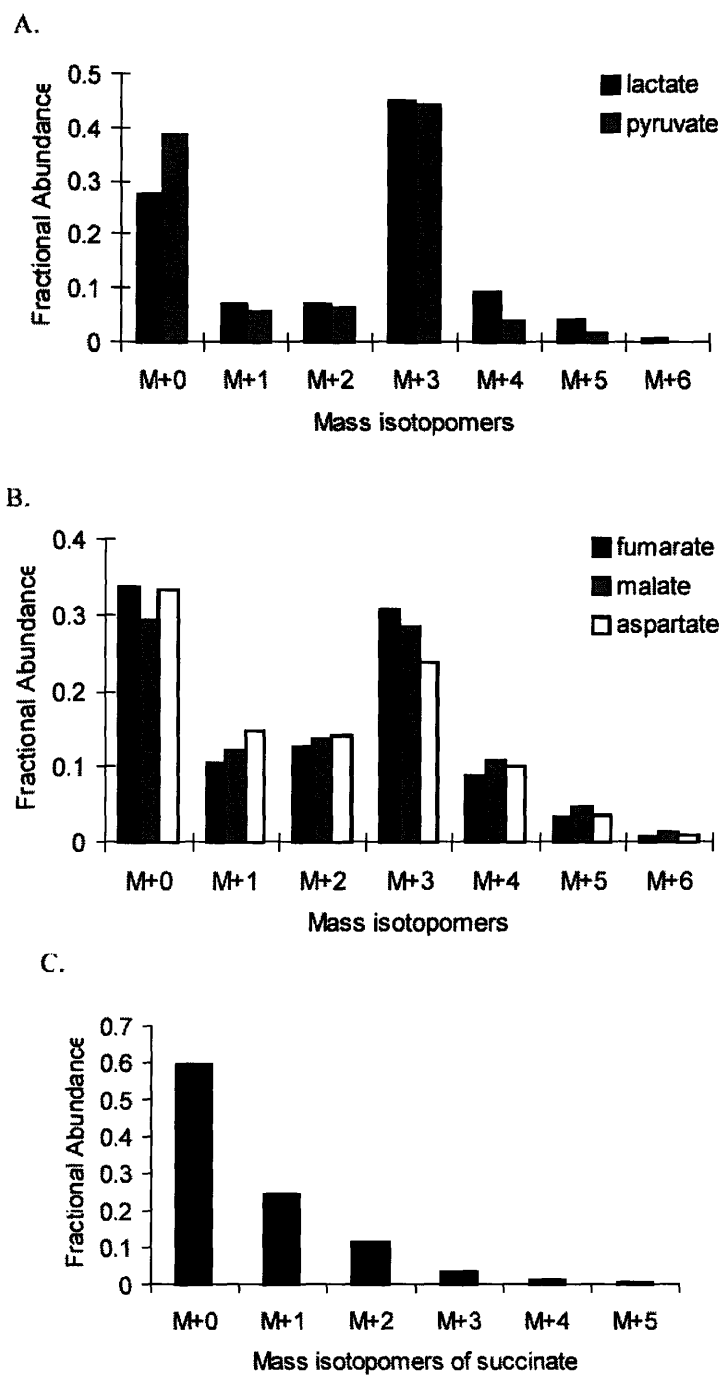
Fig. 2.13. Flux from [U-^{13}C] glucose to key intermediates of TCA cycle.

Isotopomer distributions of lactate and pyruvate (A), fumarate, malate and aspartate (B), and succinate (C) from WT brown adipocytes on day 4 under 6-hr incubation in media containing 25 mM [U-^{13}C] glucose and 4 mM unlabeled glutamine were measured.

succinate to fumarate with little reverse flux. The significant flux from malate to pyruvate (Fig. 2.11D and Fig. 2.12D) was verified with an independent labeling experiment, where WT cells were incubated with 4 mM unlabeled glutamine, 25 mM unlabeled glucose and 3 mM [U-^{13}C] aspartate for 6 hrs on day 4. Added [U-^{13}C] aspartate is expected to enter the TCA cycle by exchange reaction with oxaloacetate, and label other TCA cycle metabolites including malate. Then, generation of M+3 pyruvate from M+4 isotopomer of malate would be expected if there were a significant flux from malate to pyruvate. Thus, the isotopomer distributions of malate and pyruvate were measured and compared with those in WT cells under no stable-isotope labeling (Fig. 2.14). As expected, M+4 isotopomer of malate and M+3 isotopomer of pyruvate were detected, although at relatively small fractional abundances.
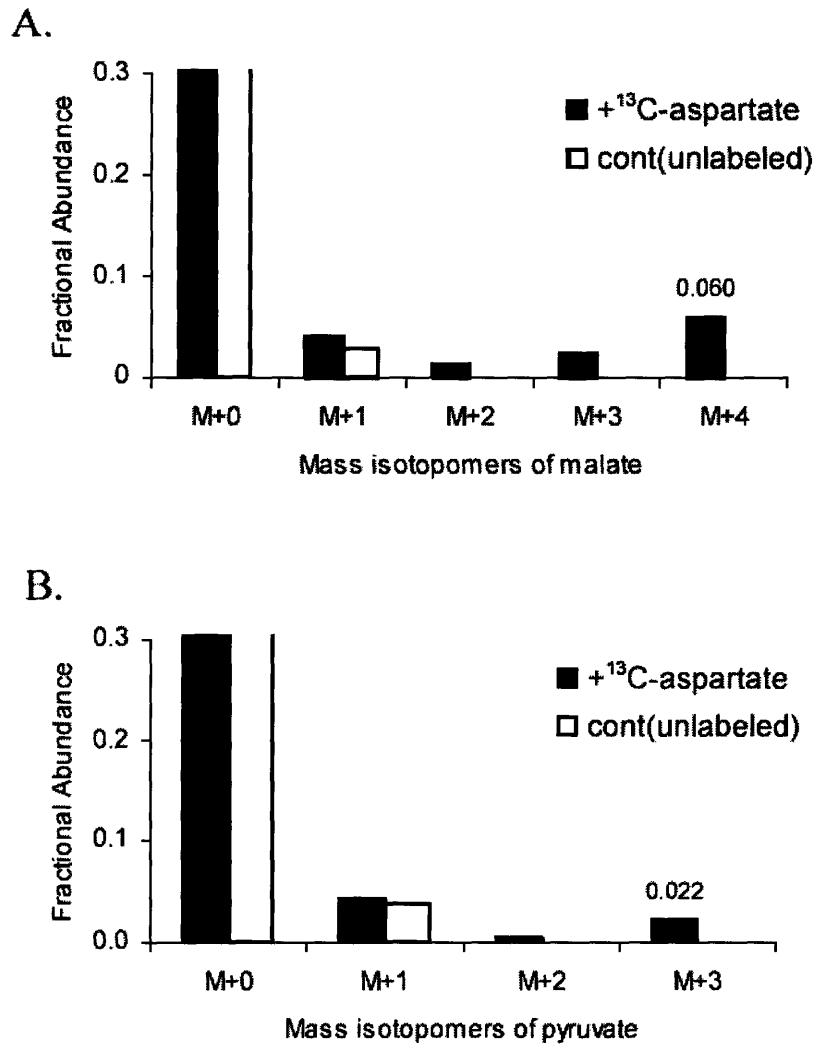
Fig. 2.14. Flux from malate to pyruvate in WT cells verified by ^{13}C-aspartate experiment.

Isotopomer distributions of malate (A) and pyruvate (B) from WT brown adipocytes on day 4 under 6-hr incubation in media containing 25 mM unlabeled glucose, 4 mM unlabeled glutamine and 3 mM [U-^{13}C] aspartate were measured (solid bars) and compared with those of malate and pyruvate from WT cells under no stable-isotope labeling (white bars). The isotopomer distributions presented here have been corrected for natural abundance.

Discussion

In Chapter 1, it was shown that wild-type brown adipocytes utilize glutamine more actively than glucose as carbon source for synthesis of fatty acids (34). Glutamine has attracted less attention as carbon source for fatty acid synthesis than glucose or acetate, and its entrance into TCA cycle via glutaminase has been mainly viewed as an oxidative pathway for energy production by generating NADPH through subsequent activity of malic enzyme, also known as glutaminolysis (21). The end product of glutaminolysis was thought to be pyruvate, which could be either converted to lactate and exported or converted to acetyl-CoA for utilization in fatty acid synthesis. Newsholme and coworkers have observed that glutamine can provide carbon sources to triacylglycerol synthesis in rat adipocytes (18). An alternative pathway of glutamine utilization via reductive carboxylation of α-ketoglutarate has been suggested (29), and the importance of this pathway relative to glutaminolysis pathway in glutamine's route to fatty acid synthesis has been supported by experiments using radioactive labeling at C-5 of glutamate (5; see also Fig. 2.2).

In order to examine the significance of glutamine's route to fatty acid synthesis through reductive carboxylation in brown adipocytes, the cells were grown in the presence of [5-^{13}C] glutamine for 4 days of differentiation. ISA analysis of the incorporation of ^{13}C-label into palmitate synthesis (16) yielded 34% contribution of [5-^{13}C] glutamine to lipogenic acetyl-CoA (Fig. 2.3). This result suggested that brown adipocytes could utilize substantial amount of glutamine for fatty acid synthesis through reductive carboxylation pathway, consistent with the results from radioactive labeling experiments using [5-^{14}C] glutamine in rat epididymal fat pads (19,20).

An independent experiment was performed to examine the activity of reductive

carboxylation in brown adipocytes, using specific inhibitors of NADP-ICDH. There have

been strong evidences that, in mitochondria, the oxidation of isocitrate to α-ketoglutarate in

TCA cycle is mainly catalyzed by NAD-ICDH, whereas NADP-ICDH is responsible for

the reduction of α-ketoglutarate to isocitrate (28). If these different roles of NAD-ICDH

and NADP-ICDH hold true in brown adipocytes, specific inhibition of NADP-ICDH would

lower the contribution of glutamine to fatty acid synthesis in reductive carboxylation

pathway. In contrast, the inhibition would have little effect on that in glutaminolysis

pathway.

In support of the above hypothesis, strong activity of NADP-ICDH in brown adipocytes

has been reported previously (17). Moreover, oxalomalate (15) and 2-methylisocitrate (23)

have been known to specifically inhibit the activity of NADP-ICDH, not that of NAD-

ICDH. Also, contribution of [U-^{13}C] glutamine to palmitate synthesis during 6 hr

incubation with wild-type brown adipocytes was manifested by D value (fractional

contribution to lipogenic acetyl-CoA) of 0.37 ± 0.02 and g (6hr) value (fractional new

synthesis during 6 hrs) of 0.13 ± 0.01. If there were significant carbon flux in reductive

carboxylation pathway, inhibition of NADP-ICDH would repress the incorporation of ^{13}C

from glutamine to lipogenic acetyl-CoA pool, affecting D value more than g (6hr) value

because the reaction catalyzed by NADP-ICDH lies on glutamine's pathway to acetyl-CoA

pool. Upon specific inhibition of NADP-ICDH by 5 or 10 mM oxalomalate, decrease in D

value was almost linear while little change in g (6hr) value was observed (Fig. 2.5). The

effect of specific inhibition of NADP-ICDH on glutamine's flux to palmitate synthesis was

further confirmed by similar yet independent experiment with 2 or 4 mM 2-methylisocitrate (Fig. 2.4B).

Additional evidences to elucidate the quantitative mechanism of glutamine's flux to fatty acid synthesis were provided by analysis of isotopomer distribution of other metabolites that are closely related to the metabolic route. M+5 isotopomer of citrate can be only derived from M+5 α-ketoglutarate through reductive carboxylation, while intensity of M+4 isotopomer is indicative of the glutaminolysis flux involving loss of one carbon unit as CO_2 at succinate. Upon treatment with oxalomalate, fractional abundance of M+5 isotopomer was reduced and that of M+4 isotopomer was elevated (Fig. 2.8C), consistent with the significance of reductive carboxylation pathway.

In order to integrate the isotopomer measurements of nine metabolites into estimation of individual lipogenic fluxes, a simplified metabolic network maintaining steady-state was constructed (Fig. 2.9) from pathways of glycolysis, fatty acid synthesis, and TCA cycle with glutamine entering at α-ketoglutarate through glutamate. In order to fit the measured data well under steady-state assumption, it was necessary to incorporate two additional pathways. The first one was the import of cytosolic acetyl-CoA into mitochondria via acetate cycle (Fig. 2.15). The process would start with conversion of acetyl-CoA to acetate by cytosolic acetyl-CoA hydrolase, followed by uptake of acetate into mitochondria and the synthesis of acetyl-CoA by mitochondrial acetyl-CoA synthetase. Both cytosolic activity of acetyl-CoA hydrolase and mitochondrial activity of acetyl-CoA synthetase have been observed before in mammalian cells (35-37). The second additional pathway was either the malic-enzyme catalyzed reaction of malate to pyruvate or the phosphoenolpyruvate (PEP)-mediated shuttle of oxaloacetate to pyruvate (PEP shuttle (9)). The PEP shuttle pathway
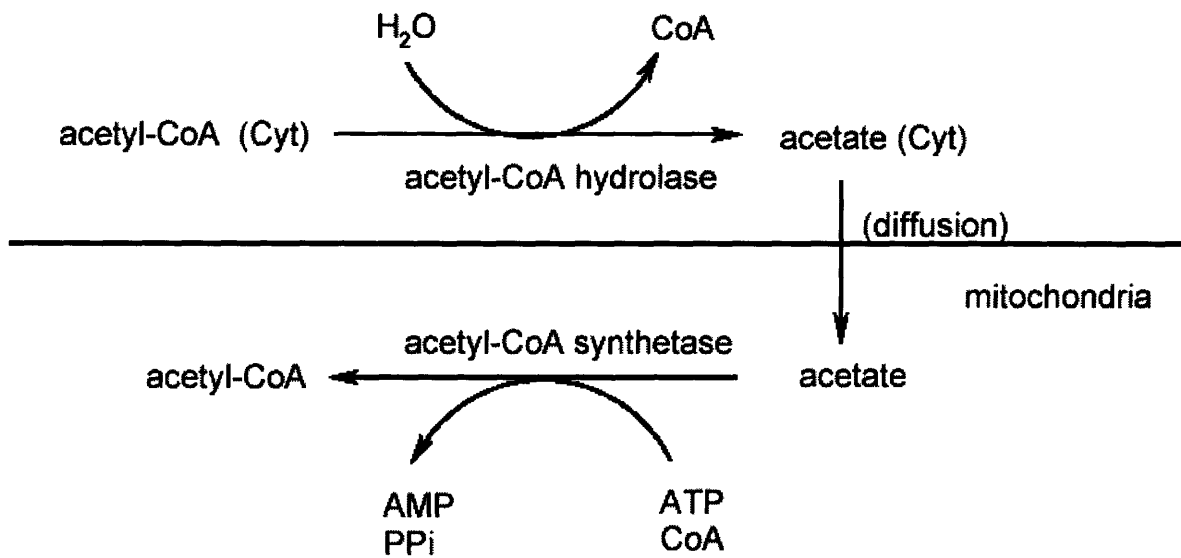
Fig. 2.15. Transport of acetyl-CoA from cytosol to mitochondria.

Acetyl-CoA in cytosol is converted to acetate by acetyl-CoA hydrolase, then acetate is imported into mitochondria by diffusion. Mitochondrial acetate can be combined with CoA to produce acetyl-CoA by acetyl-CoA synthetase at the expense of hydrolysis of ATP to AMP and diphosphate.
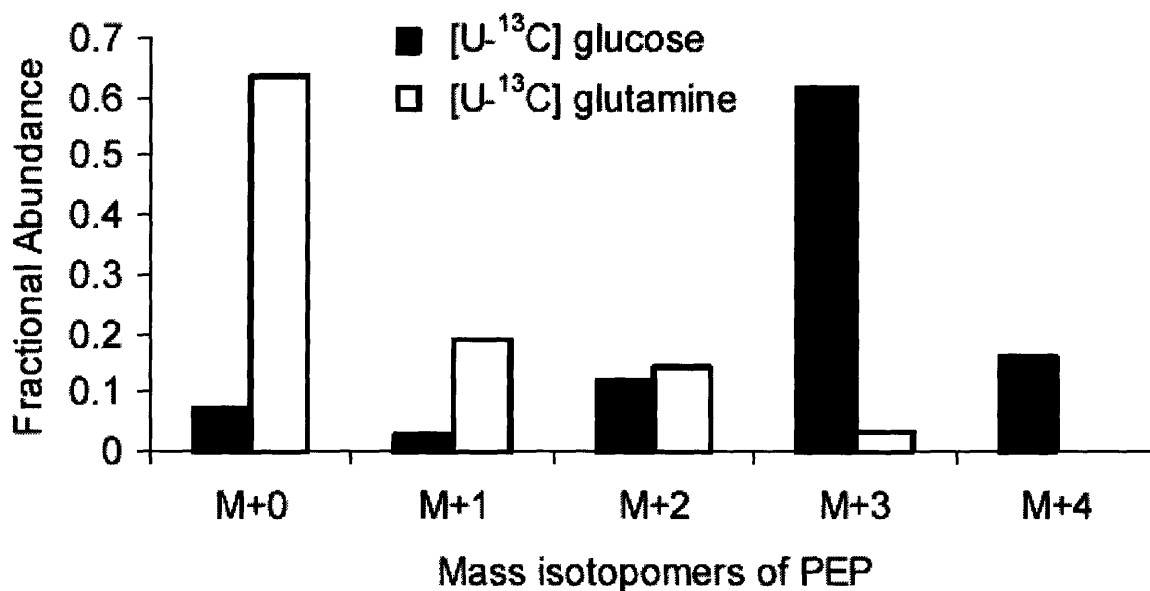
Fig. 2.16. Minimal incorporation of ^{13}C from [U-^{13}C] glutamine to phosphoenolpyruvate.

Isotopomer distribution of phosphoenolpyruvate (PEP) from WT brown adipocyte measured on day 6 under 6-hr incubation with [U-^{13}C] labeling of either 25 mM glucose or 4 mM glutamine. Incorporation of ^{13}C label from glucose into PEP confirms the normal activity of glycolysis in brown adipocytes, whereas minimal incorporation of ^{13}C label from glutamine on PEP excludes the involvement of PEP shuttle in the metabolic network for glutamine utilization in brown adipocytes.

was rejected because there was no significant enrichment of PEP from [U-^{13}C] glutamine in a preliminary experiment (Fig. 2.16).

It has been suggested that in adipose tissue reductive carboxylation can proceed in both cytoplasm and mitochondria (19). The dependence of glutamine's flux to fatty acid synthesis on the transport of tricarboxylic acids (including citrate) across mitochondrial membrane, shown by inhibition of glutamine's fractional contribution to palmitate synthesis (D value) upon treatment with BTC, is more consistent with major flux going through reductive carboxylation in mitochondria. However, the cytosolic flux cannot be excluded because ISA analysis also showed concomitant reduction of fractional new synthesis (g (6hr) value), which may be caused by the inhibition of cytosolic flux of reductive carboxylation by BTC. Also, indirect effects of inhibiting citrate transport on the cytosolic flux may exist.

Results from time-course labeling experiments with [U-^{13}C] glutamine for 2 hrs, 4 hrs, and 6 hrs indicated that brown adipocytes have reached the steady state within 2 hrs, which was maintained up to 6 hrs after incubation in 4 mM [U-^{13}C] glutamine (Fig. 2.10 and Appendix B), confirming the assumption of metabolic and isotopic steady-state.

Two sets of estimated fluxes involved in fatty acid synthesis of brown adipocytes under increasing concentration of two independent NADP-ICDH specific inhibitors were very similar, especially for reductive carboxylation of α-ketoglutarate to isocitrate (Figs. 2.11 and 2.12; see also Appendix C). Dose-dependent decrease of the flux from α-ketoglutarate to citrate upon oxalomalate treatment was reproduced for the experiments with 2-methyisocitrate. Little effect of the inhibitors on other key fluxes such as fatty acid

synthesis from acetyl-CoA or pyruvate's carboxylation to oxaloacetate demonstrates the specificity of inhibition.

However, a unique effect of oxalomalate was observed for the flux of malate to pyruvate, catalyzed by malic enzyme (Fig. 2.11). Dose-dependent decrease of this flux was not reproduced by 2-methylisocitrate (Fig. 2.12). There has been no report of oxalomalate's direct inhibition of malic enzyme. The possibility that oxalomalate might indirectly affect the activity of malic enzyme by inhibition of $NADP^+ \leftrightarrow NADPH$ interconversion was excluded, because treatment with 2-methylisocitrate had very little effect on the 'malate → pyruvate' flux. This unique effect of oxalomalate might be associated with its decomposition into glyoxylate + oxaloacetate (15). Indeed, it was shown that glyoxylate is a potent inhibitor of $NADP^+$-dependent malic enzyme from *Pseudomonas putida* (3), although the mechanism of this inhibition is not clear.

Existence of the significant flux of malate to pyruvate was further verified by an independent experiment using [U-^{13}C] aspartate (Fig. 2.14). The labeled carbon from 3 mM aspartate was incorporated into malate only at 6.0 %, probably due to considerable net flux from oxaloacetate to aspartate (Appendix C) and dilution by large fluxes from unlabeled glucose and unlabeled glutamine. Considering also the large dilution from unlabeled glucose to pyruvate, significant portion (2.2%) of pyruvate was labeled at all three carbons with ^{13}C, which can be derived from [U-^{13}C] aspartate only through 'malate → pyruvate' flux. The ratio of M+3 isotopomer of pyruvate to M+4 isotopomer of malate (0.37) was larger than the calculated ratio of the 'malate → pyruvate' flux to the 'glucose → pyruvate' flux in WT cells under standard condition (0.15: Appendix C), consistent with heavier flux from malate to pyruvate due to addition of 3 mM aspartate.

95

In order for the proposed metabolic network to function with the strong flux of reductive carboxylation pathway, there should be a constant source of NADPH to be supplied for reductive carboxylation of α-ketoglutarate to isocitrate in mitochondria. We have taken three possibilities into consideration: mitochondrial malic enzyme, $NADP^+$-dependent glutamate dehydrogenase, and isocitrate/α-ketoglutarate cycle mediated by H^+-transhydrogenase (28). Malic enzyme's active production of NADPH in differentiating brown adipocytes (12,13,33) has been associated with its role in providing reducing equivalents for fatty acid synthesis, but it is unlikely to be an important source of NADPH because it has been reported that malic enzyme activity in brown adipocytes is largely limited to cytosol (30) and NADPH cannot cross the mitochondrial membrane. $NADP^+$-dependent glutamate dehydrogenase can generate NADPH from mitochondrial conversion of glutamate to α-ketoglutarate. Significant activity of $NADP^+$-dependent glutamate dehydrogenase in brown adipose tissue (17) suggests that this enzyme may participate in providing NADPH for reductive carboxylation by NADP-ICDH. With regard to the third possibility, Sazanov and Jackson (28) suggested that, in tissues with high demand for NADPH-requiring biosynthesis and low requirement of ATP synthesis, H^+-transhydrogenase might mediate the transfer of reducing equivalents in mitochondria from NADH to NADPH. NADPH would then be consumed by reductive carboxylation of NADP-ICDH and regenerated by cytosolic NADP-ICDH in the opposite reaction. In order to complete this process, export of isocitrate and import of α-ketoglutarate need to be facilitated by their corresponding transporters. Substantial activity of tricarboxylic acid transporter in brown adipocytes shown here by inhibition studies with BTC and the high

lipogenic capacity of brown adipocytes suggests that this process may play an important role in providing NADPH for reductive carboxylation by NADP-ICDH.

Taken together, it has been demonstrated that the major metabolic route of glutamine to fatty acid synthesis follows reductive carboxylation pathway, which can be modulated by specific inhibitors of NADP-ICDH. Integration of isotopomer distribution data of multiple metabolites into estimation of fluxes in the metabolic network has made it possible to construct a whole picture in terms of the quantitative mechanism of glutamine's utilization in fatty acid synthesis of brown adipocytes. Because glucose has been thought to be the only major metabolic fuel for lipogenesis, the enzymes that were considered for regulating lipogenic flux have been limited to those that are in the pathway of converting glucose to lipogenic carbon source (glucose transporter, glycolytic enzymes), fatty acid synthesis (fatty acid synthase, acetyl-CoA carboxylase) or those that are related to production of NADPH (malic enzyme). Quantitative understanding of glutamine's flux to fatty acid synthesis may provide insights on other means of regulation for fat synthesis in the whole body, which is closely related to obesity and Type 2 diabetes through release of free fatty acids (22,32). Considering the high sensitivity of brown adipocytes to insulin-signaling (31), comparative study of wild-type (WT) and IRS-1 knockout (IRS-1 KO) brown adipocytes might shed light on the relationship between insulin signaling and glutamine's lipogenic flux, which may also provide potential sites for intervention of type 2 diabetes.

References

1. Ardawi, M.S. and E.A. Newsholme. 1982. Maximum activities of some enzymes of glycolysis, the tricarboxylic acid cycle and ketone-body and glutamine utilization pathways in lymphocytes of the rat. *Biochem J* **208**: 743-8.

2. Brock, M., C. Maerker, A. Schutz, U. Volker, and W. Buckel. 2002. Oxidation of propionate to pyruvate in Escherichia coli. Involvement of methylcitrate dehydratase and aconitase. *Eur J Biochem* **269**: 6184-94.

3. Cazzulo, J.J. and E. Massarini. 1972. Inhibition of NADP-linked malic enzyme by glyoxylate. *FEBS Letters* **22**: 76-79.

4. Comte, B., G. Vincent, B. Bouchard, and C. Des Rosiers. 1997. Probing the origin of acetyl-CoA and oxaloacetate entering the citric acid cycle from the 13C labeling of citrate released by perfused rat hearts. *J Biol Chem* **272**: 26117-24.

5. D'Adamo, A.F., Jr. and D.E. Haft. 1965. An Alternate Pathway of Alpha-Ketoglutarate Catabolism in the Isolated, Perfused Rat Liver. I. Studies with Dl-Glutamate-2- and -5-14c. *J Biol Chem* **240**: 613-7.

6. Dalziel, K. and J.C. Londesborough. 1968. The mechanisms of reductive carboxylation reactions. Carbon dioxide or bicarbonate as substrate of nicotinamide-adenine dinucleotide phosphate-linked isocitrate dehydrogenase and malic enzyme. *Biochem J* **110**: 223-30.

7. de Almeida, A.F., R. Curi, P. Newsholme, and E.A. Newsholme. 1989. Maximal activities of key enzymes of glutaminolysis, glycolysis, Krebs cycle and pentose-phosphate pathway of several tissues in mature and aged rats. *Int J Biochem* **21**: 937-40.

8. Des Rosiers, C., C.A. Fernandez, F. David, and H. Brunengraber. 1994. Reversibility of the mitochondrial isocitrate dehydrogenase reaction in the perfused rat liver. Evidence from isotopomer analysis of citric acid cycle intermediates. *J Biol Chem* **269**: 27179-82.

9. Drahota, Z., H. Rauchova, M. Mikova, P. Kaul, and A. Bass. 1983. Phosphoenolpyruvate shuttle--transport of energy from mitochondria to cytosol. *FEBS Lett* **157**: 347-9.

10. Fiehn, O., J. Kopka, R.N. Trethewey, and L. Willmitzer. 2000. Identification of uncommon plant metabolites based on calculation of elemental compositions using gas chromatography and quadrupole mass spectrometry. *Anal Chem* **72**: 3573-80.

11. Gabriel, J.L., P.R. Zervos, and G.W. Plaut. 1986. Activity of purified NAD-specific isocitrate dehydrogenase at modulator and substrate concentrations approximating conditions in mitochondria. *Metabolism* **35**: 661-7.

12. Garcia-Jimenez, C., A. Hernandez, M.J. Obregon, and P. Santisteban. 1993. Malic enzyme gene expression in differentiating brown adipocytes: regulation by insulin and triiodothyronine. *Endocrinology* **132**: 1537-43.

13. Hernandez, A., C. Garcia-Jimenez, P. Santisteban, and M.J. Obregon. 1993. Regulation of malic-enzyme-gene expression by cAMP and retinoic acid in differentiating brown adipocytes. *Eur J Biochem* **215**: 285-90.

14. Holleran, A.L., D.A. Briscoe, G. Fiskum, and J.K. Kelleher. 1995. Glutamine metabolism in AS-30D hepatoma cells. Evidence for its conversion into lipids via reductive carboxylation. *Mol Cell Biochem* **152**: 95-101.

15. Johanson, R.A. and H.C. Reeves. 1977. Concerted inhibition of NADP+-specific isocitrate dehydrogenase by oxalacetate and glyoxylate. I. Oxalomalate formation and stability, and nature of the enzyme inhibition. *Biochim Biophys Acta* **483**: 24-34.

16. Kharroubi, A.T., T.M. Masterson, T.A. Aldaghlas, K.A. Kennedy, and J.K. Kelleher. 1992. Isotopomer spectral analysis of triglyceride fatty acid synthesis in 3T3-L1 cells. *Am J Physiol* **263**: E667-75.

17. Kochan, Z., G. Bukato, and J. Swierczynski. 1993. Inhibition of lipogenesis in rat brown adipose tissue by clofibrate. *Biochem Pharmacol* **46**: 1501-6.

18. Kowalchuk, J.M., R. Curi, and E.A. Newsholme. 1988. Glutamine metabolism in isolated incubated adipocytes of the rat. *Biochem J* **249**: 705-8.

19. Lenartowicz, E. and M.V. Savina. 1984. Intramitochondrial reductive carboxylation of 2-oxoglutarate in adipose tissue and its contribution to fatty acid synthesis. *Int J Biochem* **16**: 1223-9.

20. Madsen, J., A. S., and I. Chaikoff. 1964. Conversion of glutamate carbon to fatty acid carbon via citrate in rat epididymal fat pads. *J Lipid Res* **5**: 548-553.

21. McKeehan, W.L. 1982. Glycolysis, glutaminolysis and cell proliferation. *Cell Biol Int Rep* **6**: 635-50.

22. Montague, C.T. and S. O'Rahilly. 2000. The perils of portliness: causes and consequences of visceral adiposity. *Diabetes* **49**: 883-8.

23. Plaut, G.W., R.L. Beach, and T. Aogaichi. 1975. Alpha-methylisocitrate. A selective inhibitor of TPN-linked isocitrate dehydrogenase from bovine heart and rat liver. *J Biol Chem* **250**: 6351-4.

24. Reed, W.D., H.R. Zielke, P.J. Baab, and P.T. Ozand. 1981. Ketone bodies, glucose and glutamine as lipogenic precursors in human diploid fibroblasts. *Lipids* **16**: 677-84.

25. Reynolds, C.H., P.W. Kuchel, and K. Dalziel. 1978. Equilibrium binding of coenzymes and substrates to nicotinamide-adenine dinucleotide phosphate-linked isocitrate dehydrogenase from bovine heart mitochondria. *Biochem J* **171**: 733-42.

26. Ritchie, J.W.A., F.E. Baird, G.R. Christie, A. Stewart, S.Y. Low, H.S. Hundal, and P.M. Taylor. 2001. Mechanisms of glutamine transport in rat adipocytes and acute regulation by cell swelling. *Cellular Physiology and Biochemistry* **11**: 259-270.

27. Sabine, J.R., L. Kopelovich, S. Abraham, and H.P. Morris. 1973. Control of lipid metabolism in hepatomas: conversion of glutamate carbon to fatty acid carbon via citrate in several transplantable hepatomas. *Biochim Biophys Acta* **296**: 493-8.

28. Sazanov, L.A. and J.B. Jackson. 1994. Proton-translocating transhydrogenase and NAD- and NADP-linked isocitrate dehydrogenases operate in a substrate cycle which contributes to fine regulation of the tricarboxylic acid cycle activity in mitochondria. *FEBS Lett* **344**: 109-16.

29. Srere, P.A. 1959. The citrate cleavage enzyme. I. Distribution and purification. *J Biol Chem* **234**: 2544-7.

30. Swierczynski, J., P.W. Scislowski, Z. Aleksandrowicz, and M. Zydowo. 1981. Malic enzyme in brown adipose tissue--purification, some properties and possible physiological role. *Int J Biochem* **13**: 365-72.

31. Teruel, T., A.M. Valverde, M. Benito, and M. Lorenzo. 1996. Insulin-like growth factor I and insulin induce adipogenic-related gene expression in fetal brown adipocyte primary cultures. *Biochem J* **319** (**Pt 2**): 627-32.

32. Unger, R.H. and L. Orci. 2001. Diseases of liporegulation: new perspective on obesity and related disorders. *Faseb J* **15**: 312-21.

33. Valverde, A.M., M. Benito, and M. Lorenzo. 1992. Hormonal regulation of malic enzyme and glucose-6-phosphate-dehydrogenase expression in fetal brown-adipocyte primary cultures under non-proliferative conditions. *Eur J Biochem* **203**: 313-9.

34. Yoo, H., G. Stephanopoulos, and J.K. Kelleher. 2004. Quantifying carbon sources for de novo lipogenesis in wild-type and IRS-1 knockout brown adipocytes. *J Lipid Res* **45**: 1324-1332.

35. Groot, P.H., H.R. Scholte, and W.C. Hulsmann. 1974. Proceedings: The subcellular localization of acetyl- (EC 6.2.1.1), propionyl- and butyryl-CoA synthetase (EC 6.2.1.2) in rat and guinea-pig organs. *Hoppe Seylers Z Physiol Chem* **355**: 1199.

36. Matsunaga, T., F. Isohashi, Y. Nakanishi, and Y. Sakamoto. 1985. Physiological changes in the activities of extramitochondrial acetyl-CoA hydrolase in the liver of rats under various metabolic conditions. *Eur J Biochem* **152**: 331-6.

37. Prass, R.L., F. Isohashi, and M.F. Utter. 1980. Purification and characterization of an extramitochondrial acetyl coenzyme A hydrolase from rat liver. *J Biol Chem* **255**: 5215-23.

Chapter 3. Differential effects of insulin signaling on individual carbon fluxes for fatty acid synthesis in brown adipocytes

Introduction

Obesity and type 2 diabetes are among the most widespread and high-cost epidemics with rapid increase in the incidents for the last decade. There have been evidences that excessive fat synthesis in obesity may give rise to elevated free fatty acids, which in turn could lead to hepatic insulin resistance, one of the major early events of type 2 diabetes (5). Therefore, understanding the detailed mechanism of regulation for fat synthesis and its relationship with insulin signaling may provide insights into the pathogenesis of the two diseases and help preventing them.

Insulin signaling has long been associated with elevating overall lipogenic activity through increased activity of lipogenic enzymes (6). Evidences have been accumulated that many of these enzymes are stimulated directly by insulin signaling via insulin response element at their transcription level or indirectly by insulin signaling to transcription factors (7). However, studies on stimulation of lipogenic enzymes' activity by insulin signaling have been largely limited to the enzymes directly related to glucose's metabolic route to fatty acid synthesis, namely glucose transporter, glucokinase, glyceraldehyde-3-phosphate dehydrogenase, ATP-citrate lyase, acetyl-CoA carboxylase, fatty acid synthase, and malic enzyme (as supplier of NADPH for fatty acid synthesis). The effect of insulin on enzymes for lipogenic utilization of other carbon sources has been neglected because their contribution was thought to be minimal. Moreover, analysis of the lipogenic fluxes from glucose to fatty acid synthesis has been qualitative, examining only the overall lipogenic activity and not the individual fluxes.

Among alternative carbon sources for lipogenesis, glutamine has attracted some attention because its substantial contribution to lipogenesis in many mammalian tissues was shown by significant incorporation of ^{14}C-label from ^{14}C-glutamine into triglyceride (3,4,8). In wild-type (WT) brown adipocytes, glutamine's contribution to *de novo* synthesis of fatty acids has been shown to be higher than that of glucose in a previous report (11; see also Chapter 1). This report also showed that in insulin receptor substrate-1 knockout (IRS-1 KO) brown adipocytes glutamine's fractional contribution to fatty acid synthesis was much lower than that of glucose. It has been demonstrated that phosphatidylinositol 3-kinase (PI3K)-mediated insulin-signaling pathway was greatly impaired in IRS-1 KO brown adipocytes (1,10). Thus, utilization of glutamine as lipogenic carbon source may be regulated by insulin signaling to a stronger extent than that of glucose in brown adipocytes.

In this chapter, I have quantitatively analyzed the individual fluxes that make up the lipogenic routes from glucose and glutamine as two major carbon sources in IRS-1 KO brown adipocytes. Comparison of individual fluxes in WT cells (from Chapter 2) and IRS-1 KO cells incubated with ^{13}C-labeled glutamine confirmed the importance of glutamine as lipogenic carbon source in brown adipocytes. Moreover, the potential sites for regulating glutamine's lipogenic flux by insulin signaling were identified.

Experimental Procedures

Materials

Biochemicals were obtained from Sigma Chemical Co., St. Louis, MO. ^{13}C-labeled chemicals were obtained from Cambridge Isotope Laboratories, Inc., Andover, MA. Tissue culture media were obtained from Invitrogen, Co., Carlsbad, CA.

Cell culture and adipocyte differentiation

Brown adipocyte cells were cultured with the same procedure as in Yoo *et al.* (11). Briefly, IRS-1 KO brown preadipocytes were grown in 6-well plates (surface area = 10 cm^2) to confluence in differentiation media containing 25 mM glucose, 4 mM glutamine, 20 nM insulin, 1 nM T3, and 10 % fetal bovine serum as well as 44 mM $NaHCO_3$ (day 0). The media were then replaced with fresh induction media, which was differentiation media plus 0.125 mM indomethacin, 0.25 mM IBMX, and 5 μM dexamethasone. On day 2 and day 4, the media were replaced with fresh differentiation media to reach day 6. In [5-^{13}C] glutamine experiment, the media from day 2 to day 6 contained 4 mM [5-^{13}C] glutamine and 25 mM unlabeled glucose. In studies for the determination of carbon flux from glucose or glutamine to fatty acid synthesis through tricarboxylic acid (TCA) cycle, on day 4 the media were changed to differentiation media without glucose or glutamine at 42 hrs after day 2. The differentiation media were incubated at 37°C for 10 min, followed by addition of glucose and glutamine with specified ^{13}C-labeling. After 6-hr incubation at 37°C, the media were removed and cells were extracted for organic/amino acids or lipids.

Isolation and derivatization of organic/amino acids and lipids

For isolation of organic/amino acids, the procedure described in Fiehn *et al.* (2) was modified as follows. 0.7 mL methanol and 25 μL water was added to each well of 6-well plate immediately after removal of the media. In 15 min after incubation at room temperature, methanol extract was mixed with 0.7 mL water and 0.37 mL chloroform in 15 mL tube. Vigorous vortexing was followed by centrifugation at 3000 x *g* for 3 min. The chloroform layer was carefully removed and the methanol/water layer was centrifuged again at 3000 x *g* for 3 min. Clear solution of methanol/water layer (separated from white precipitate) was then transferred to glass vial and evaporated. The residue was dissolved in 70 μL of methoxyamine hydrochloride (20 mg/mL in pyridine) and vortexed. After 90 min incubation at 37°C, organic/amino acids were derivatized with 70 μL of N-methyl-N-*tert*-butyldimethylsilyltrifluoroacetamide (MTBSTFA) at 70°C for 30 min. The reaction mixture was then directly injected into GC/MS instrument for analysis of the isotopomer distribution of organic/amino acids.

Isolation of lipids and derivatization of palmitate moiety into methyl ester were performed as described previously (11).

GC/MS for isotopomer distribution measurement

Samples from [5-^{13}C] glutamine experiment were analyzed for palmitate isotopomer distribution with the same instrumental setup as previously reported (11). The samples from the rest of the experiments were analyzed with another GC/MS instrument described below. Isotopomer distributions of fatty acid methyl esters measured with the second

GC/MS instrument with scan mode were essentially identical to those measured with the first GC/MS with selected ion monitoring (SIM) mode.

Samples were injected into a Hewlett-Packard model 5890 series II Gas Chromatograph connected to HP5971 series Mass Selective Detector and equipped with DB-XLB (60 m x 0.25 mm id x 0.25 μm) capillary column (J&W Scientific, Folsom, CA). Helium flow with 10 psi inlet pressure was maintained by electronic control. The temperatures of the injector and the detector were kept at 230°C and 300°C, respectively. For isotopomer distribution analysis of methyl palmitate and its isotopomers (M+0 to M+16 (m/z=270 to 286)), GC column temperature was started at 100°C and held for 1 min. The temperature was then increased to 250°C at 10°C/min, and held for 5 min. It was increased to 300°C at 25°C/min and held for 2 min. Mass range of 100 to 350 was recorded at 2.7 scans per second. For isotopomer distribution analysis of acid derivatives, GC temperature was started at 100°C and held for 5 min. The temperature was then increased to 300°C at 10°C/min, and held for 5 min. Mass range of 50 to 550 was recorded at 1.5 scans per second. The most abundant fragments (M−57) of the following acid derivatives (*tert*-butyldimethylsilyl; TBDMS) were analyzed for their isotopomer distributions: pyruvate (m/z=174-178), lactate (m/z=261-265), fumarate (m/z=287-293), α-ketoglutarate (m/z=346-354), malate (m/z=419-423), aspartate (m/z=418-424), glutamate (m/z=432-440), and citrate (m/z=459-468).

Measurement of uptake fluxes for glucose and glutamine

Uptake fluxes for glucose and glutamine into IRS-1 KO cells were calculated from the rates of consumption of glucose and glutamine from medium as reported previously (11).

Data analysis

The methods for data analysis are essentially identical to those described in "Data analysis" section of Chapter 2. Fractional contribution of ^{13}C-labeled carbon sources to fatty acid synthesis (D value) and fractional new synthesis of fatty acids during time t (g(t) value) were estimated with the isotopomer distribution measurements of palmitate based on the model of isotopomer spectral analysis (ISA) as reported previously (34). For estimation of fluxes in the metabolic network model (Fig. 2.9) by integrating the isotopomer distributions of palmitate, pyruvate, lactate, fumarate, α-ketoglutarate, malate, aspartate, glutamate, and citrate, a MATLAB program was used. Given a metabolic network consisting of a set of reactions with specific atomic transitions between defined metabolites, mass balance, metabolic/isotopic steady state, and unknown fluxes, the program can set up equations for all possible isotopomers for all metabolites. The exhaustive technique like this makes the equations non-linear so that the solution can be best derived computationally by least-square fit method. The program can then estimate fluxes for reactions in the metabolic network model that fit the inputs of the metabolic network and measurements of isotopomer distributions of some metabolites. Using measurement errors for the isotopomer distribution data, the program can also calculate how good the fit for each metabolite's measurement is and the uncertainty of each estimated flux.

Glucose and glutamine taken up from medium and preexisting palmitate were defined as substrates, and production of lactate (exported into medium), palmitate, and protein synthesis from aspartate were treated as sink. The rest of the metabolites were regarded as balanced except for CO_2, which was allowed to be unbalanced.

The equations for the whole metabolic network were set up with 32 variables (fluxes). The number of independent measurements for solving the equations was 50, the sum of "the number of isotopomers – 1" for nine metabolites. Each measurement of isotopomer distribution was corrected for natural abundance by the program before estimating fluxes.

For each set of flux estimation results, statistical evaluation of how good the fit was for each metabolite's isotopomer distribution was calculated in terms of sum of square residuals (SSRES) based on measurement errors. SSRES was defined as Σ (difference between data and fit / measurement error)^2. Overall goodness of fit was calculated by summing up SSRES values for all nine metabolites, which was compared with the range of SSRES values for 95% confidence calculated by the program.

Results

[5-^{13}C] glutamine's contribution to palmitate synthesis in IRS-1 KO brown adipocytes

In order to assess the significance of reductive carboxylation pathway in glutamine's

contribution to palmitate synthesis in IRS-1 KO brown adipocytes (11), incorporation of

^{13}C from [5-^{13}C] glutamine into palmitate synthesis was examined after 4-day incubation of

IRS-1 KO cells with 25 mM unlabeled glucose and 4 mM [5-^{13}C] glutamine from day 2 to

day 6. Substantial incorporation of ^{13}C from C-5 of glutamine into palmitate was also

analyzed for fractional contribution of [5-^{13}C] glutamine to lipogenic acetyl-CoA according

to ISA model, yielding D value of 0.185 ± 0.001 (Fig. 3.1).

Isotopomer distribution of nine metabolites related to fatty acid synthesis

Nine metabolites that are directly related to glutamine's metabolic routes to fatty acid

synthesis (glutamate, α-ketoglutarate, citrate, fumarate, malate, aspartate, pyruvate, and

lactate, as well as palmitate) were detected by MeOH extraction, TBDMS derivatization,

and GC/MS in IRS-1 KO cells on day 4. After 6-hr incubation in 25 mM unlabeled

glucose and 4 mM [U-^{13}C] glutamine, isotopomer distribution of the metabolites were

measured and compared with those of WT cells from Chapter 2 (Figs. 3.2-3.10).

Isotopomer distributions of glutamate, α-ketoglutarate and citrate in IRS-1 KO cells were

most distinct from those of WT cells in the fractional abundance of M+5 isotopomer (Figs.

3.2-3.4). M+4 isotopomers of fumarate, malate, and aspartate of IRS-1 KO cells were

remarkably higher in fractional abundance than those of WT cells (Figs. 3.5-3.7). In

contrast, lactate and pyruvate of IRS-1 KO cells were not much different from those of WT

cells in their isotopomer distributions, except for slightly higher M+1 isotopomer of
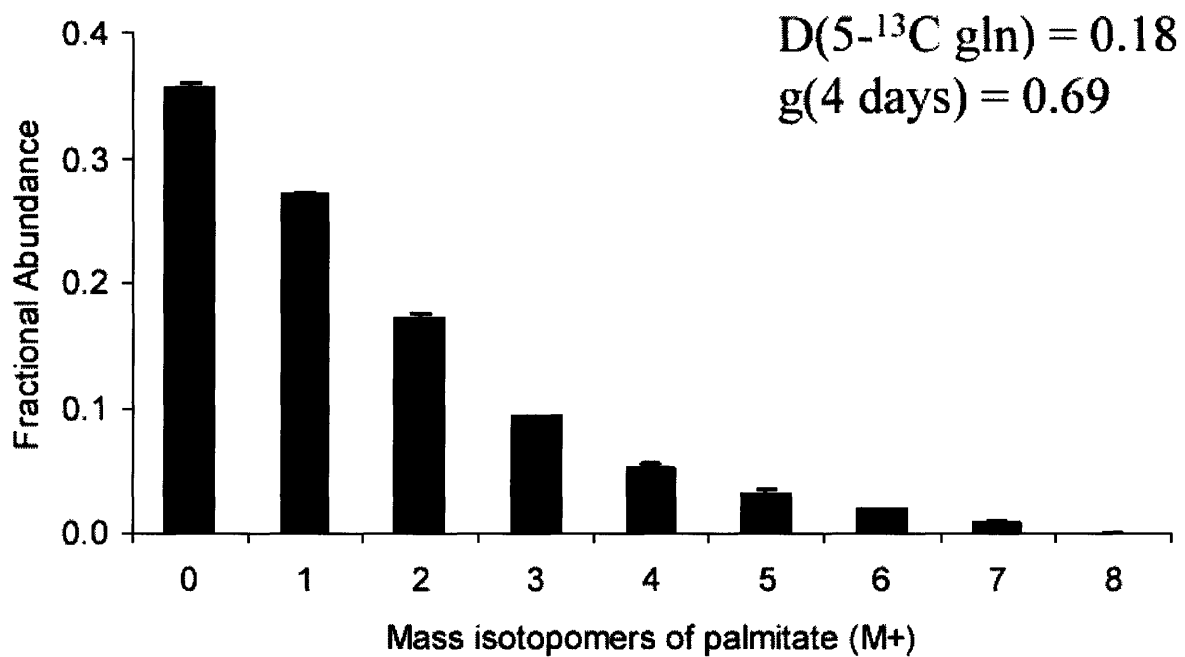
Fig. 3.1. Contribution of [5-^{13}C] glutamine to palmitate synthesis in IRS-1 KO brown adipocytes.

Isotopomer distribution of palmitate isolated from IRS-1 KO brown adipocytes under incubation in media containing 4 mM [5-^{13}C] glutamine from day 2 to day 6. Data shown are mean ± SEM (n = 3).

pyruvate in IRS-1 KO cells (Figs. 3.8 and 3.9). Extent of ^{13}C-labeling of palmitate from [U-^{13}C] glutamine in IRS-1 KO cells was significantly lower than in WT cells (Fig. 3.10), as reported previously (11; see also Chapter 1).

Assessment of goodness of fit and flux estimation

A metabolic network identical to that described in Chapter 2 (Fig. 2.9) was used for integration of the isotopomer distribution data of nine metabolites from IRS-1 KO cells into flux estimation. Overall goodness of fit in this flux estimation was calculated in terms of sum of square residuals (SSRES) as described previously (Chapter 2). SSRES value of 60.294 was well within 95% confidence range of 27.575 – 64.201.

Uptake rate for glutamine and glucose into IRS-1 KO cells were measured and the relative uptake fluxes were set to be 100 for glutamine and 1100 for glucose. When the absolute rates of glutamine uptake from IRS-1 KO cells and WT cells were compared, the ratio was 40 to 100. Estimated fluxes for all reactions in the metabolic network for IRS-1 KO cells are summarized in Table 2, as compared with those for WT cells under the same experimental condition (Chapter 2).

Compared to the positive net flux of reductive carboxylation in WT cells, the opposite net carbon flux (from citrate to α-ketoglutarate) was determined as 128 ± 4 in IRS-1 KO cells, which was also added to make the flux of α-ketoglutarate to succinate 6-fold higher in IRS-1 KO cells than in WT cells. Glycolytic fluxes were comparable between WT and IRS-1 KO cells until pyruvate was divided into dehydrogenation (AcCoA) or carboxylation (OAA). Pyruvate flux was heavily geared towards synthesis of acetyl-CoA in IRS-1 KO cells while it was more invested into carboxylation to oxaloacetate in WT cells.

Fig. 3.2. Isotopomer distribution of glutamate from WT and IRS-1 KO cells upon incubation with [U-^{13}C] glutamine.

Isotopomer distribution of glutamate from WT and IRS-1 brown adipocytes on day 4 under 6-hr incubation in media containing 25 mM unlabeled glucose and 4 mM [U-^{13}C] glutamine.

Fig. 3.3. Isotopomer distribution of α-ketoglutarate from WT and IRS-1 KO cells upon incubation with [U-^{13}C] glutamine.

Isotopomer distribution of α-ketoglutarate from WT and IRS-1 brown adipocytes on day 4 under 6-hr incubation in media containing 25 mM unlabeled glucose and 4 mM [U-^{13}C] glutamine.

112

Fig. 3.4. Isotopomer distribution of citrate from WT and IRS-1 KO cells upon incubation with [U-^{13}C] glutamine.

Isotopomer distribution of citrate from WT and IRS-1 brown adipocytes on day 4 under 6-hr incubation in media containing 25 mM unlabeled glucose and 4 mM [U-^{13}C] glutamine.
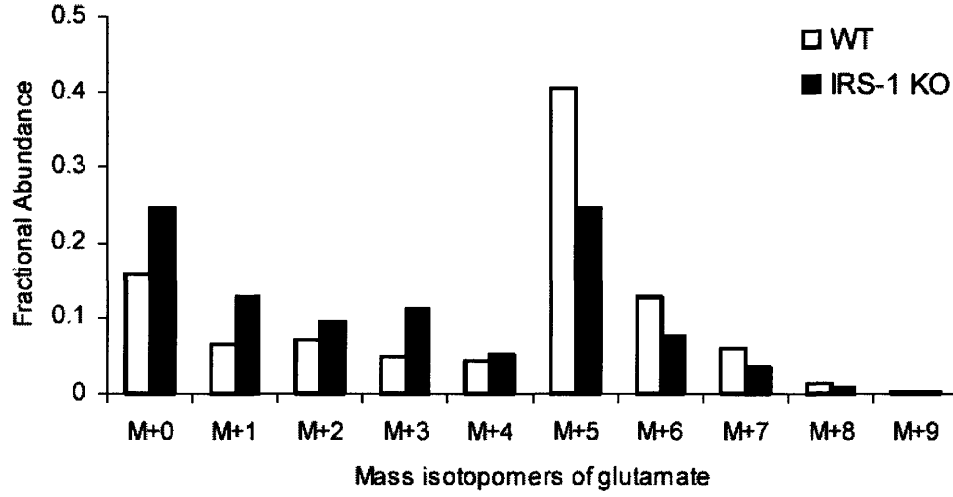

Fig. 3.5. Isotopomer distribution of fumarate from WT and IRS-1 KO cells upon incubation with [U-^{13}C] glutamine.

Isotopomer distribution of fumarate from WT and IRS-1 brown adipocytes on day 4 under 6-hr incubation in media containing 25 mM unlabeled glucose and 4 mM [U-^{13}C] glutamine.

113
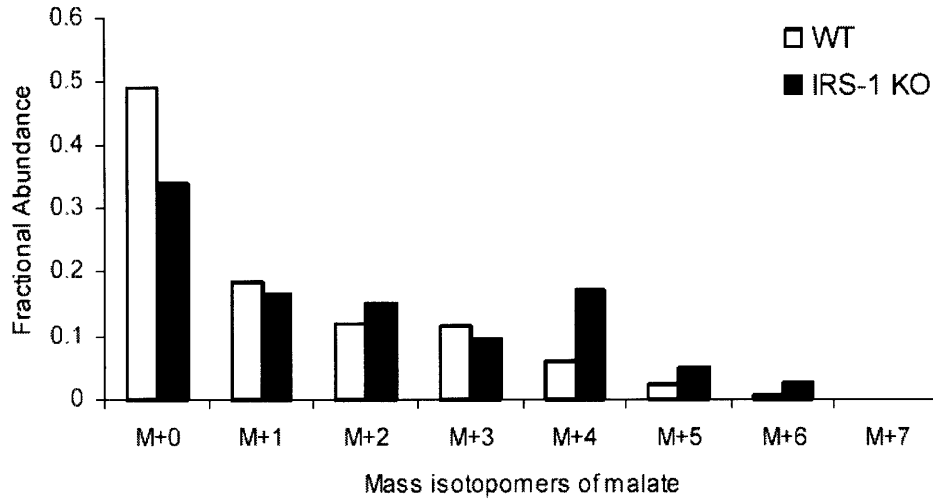
Fig. 3.6. Isotopomer distribution of malate from WT and IRS-1 KO cells upon incubation with [U-^{13}C] glutamine.

Isotopomer distribution of malate from WT and IRS-1 brown adipocytes on day 4 under 6-hr incubation in media containing 25 mM unlabeled glucose and 4 mM [U-^{13}C] glutamine.
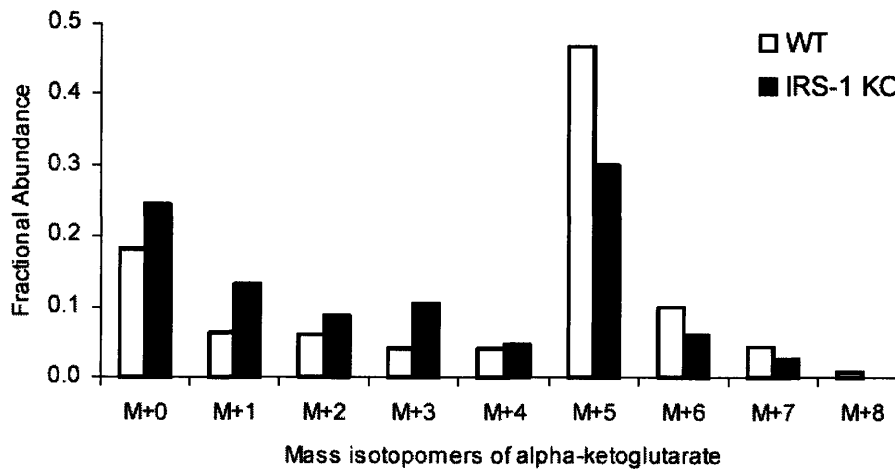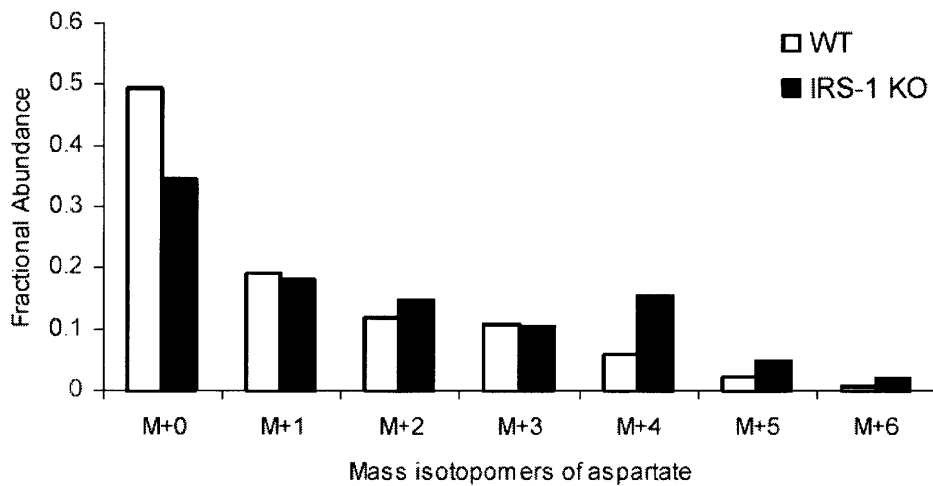

Fig. 3.7. Isotopomer distribution of aspartate from WT and IRS-1 KO cells upon incubation with [U-^{13}C] glutamine.

Isotopomer distribution of aspartate from WT and IRS-1 brown adipocytes on day 4 under 6-hr incubation in media containing 25 mM unlabeled glucose and 4 mM [U-^{13}C] glutamine.

114
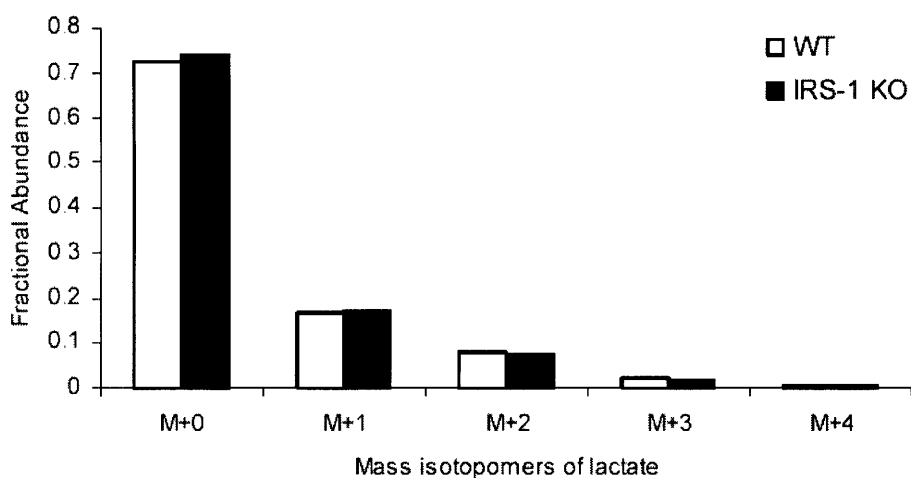
Fig. 3.8. Isotopomer distribution of lactate from WT and IRS-1 KO cells upon incubation with [U-^{13}C] glutamine.

Isotopomer distribution of lactate from WT and IRS-1 brown adipocytes on day 4 under 6-hr incubation in media containing 25 mM unlabeled glucose and 4 mM [U-^{13}C] glutamine.
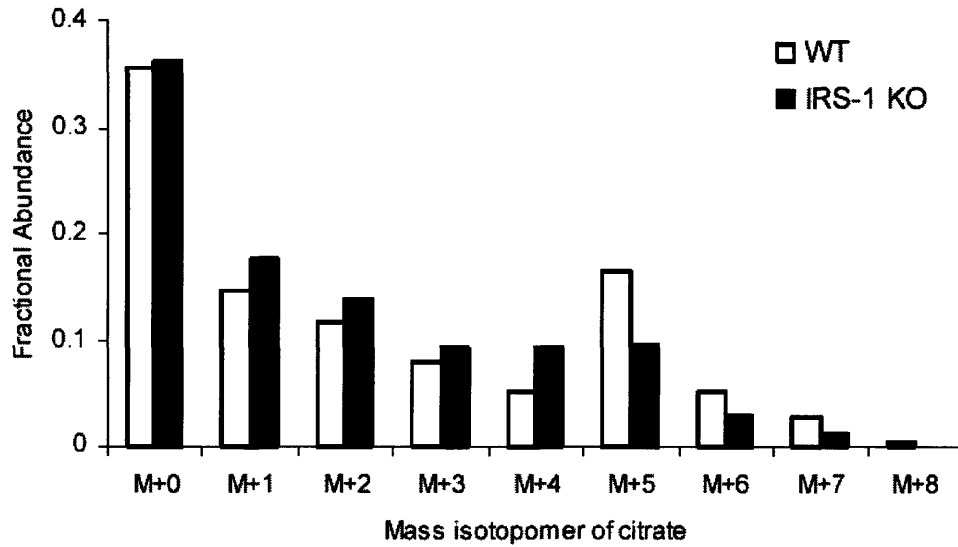

Fig. 3.9. Isotopomer distribution of pyruvate from WT and IRS-1 KO cells upon incubation with [U-^{13}C] glutamine.

Isotopomer distribution of pyruvate from WT and IRS-1 brown adipocytes on day 4 under 6-hr incubation in media containing 25 mM unlabeled glucose and 4 mM [U-^{13}C] glutamine.
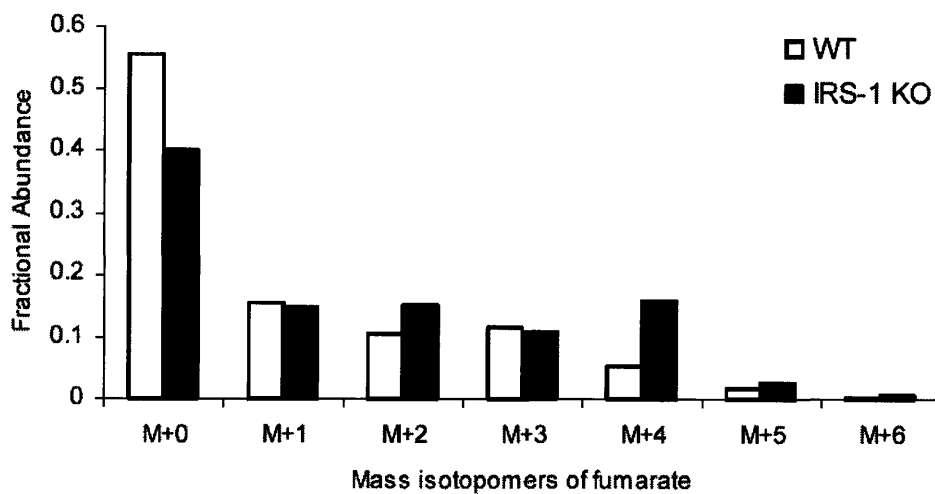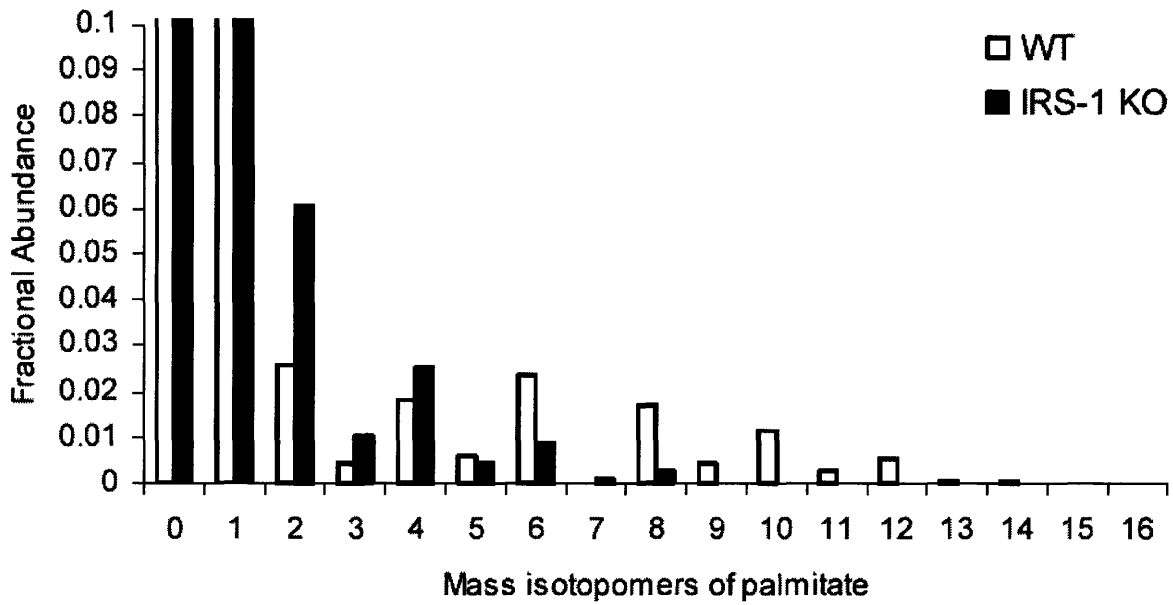
Fig. 3.10. Isotopomer distribution of palmitate from WT and IRS-1 KO cells upon incubation with [U-^{13}C] glutamine.

Isotopomer distribution of palmitate from WT and IRS-1 brown adipocytes on day 4 under 6-hr incubation in media containing 25 mM unlabeled glucose and 4 mM [U-^{13}C] glutamine.
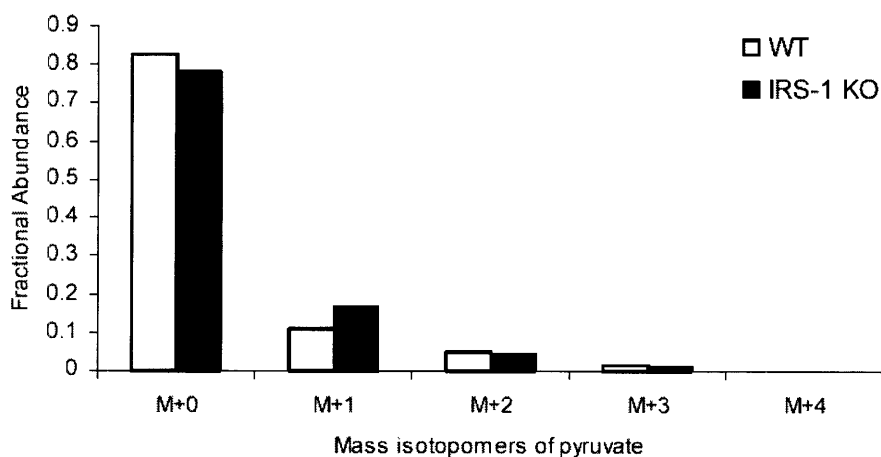
116

Table 2. Estimated fluxes for WT and IRS-1 KO brown adipocytes

The fluxes estimated based on the metabolic network model (Fig. 2.9) for WT and IRS-1 KO brown adipocytes under 6-hr incubation with 25 mM glucose and 4 mM [U-^{13}C] glutamine are compared. WT data was from Chapter 2. Rate of glutamine uptake in IRS-1 KO cells were set to be the same as in WT cells for the purpose of comparison, although the absolute rate is 40 for IRS-1 KO cells when it is 100 for WT cells.
Abbreviations used are: Gln – glutamine, Glu – glutamate, aKG – α-ketoglutarate, Cit – citrate, Suc – succinate, Fum – fumarate, Mal – malate, Glc – glucose, Pyr – pyruvate, Lac – lactate, OAA – oxaloacetate, AcCoA – acetyl-CoA, Ac – acetate, Pal – palmitate, Asp – aspartate, (ext) – external, (Cyt) – cytosolic, (pre) – preexisting.

reactions	estimated fluxes		standard error	
	WT	IRS-1 KO	WT	IRS-1 KO
Gln(ext) -> Gln -> Glu -> aKG	100	100	0	0
aKG + CO$_2$ -> Cit	64	-130	1	5
aKG -> Suc + CO$_2$, Suc->Fum->Mal	36	230	1	5
Glc (ext) -> Glc -> Pyr + Pyr	1547	1150	50	50
Pyr -> Lac -> Lac (ext)	2895	1936	118	104
Pyr + CO$_2$ -> OAA	519	129	13	5
Pyr -> AcCoA + CO$_2$	156	286	9	18
Mal -> Pyr + CO$_2$	477	51	31	7
OAA + AcCoA -> Cit	266	324	29	34
Cit -> AcCoA (Cyt) + OAA	330	194	29	35
AcCoA(Cyt) -> Ac -> AcCoA	110	39	30	35
8 AcCoA -> Pal	27	19	1	2
Pal (pre) -> Pal	273	119	21	14
OAA -> Asp -> sink	143	178	29	8

The flux of acetyl-CoA to palmitate synthesis relative to glutamine uptake rate was comparable between WT cells and IRS-1 KO cells, indicating relatively high activity of fatty acid synthase in IRS-1 KO cells. On the other hand, the flux of malate to pyruvate (catalyzed by malic enzyme) was 9-fold higher in WT cells than in IRS-1 KO cells.

Flux from malate to pyruvate verified by ^{13}C-aspartate experiment

The flux from malate to pyruvate in IRS-1 KO cells (Table 2), approximately 10-fold smaller than in WT cells, was verified by an independent experiment with 3 mM [U-^{13}C] aspartate, just as in Chapter 2. IRS-1 KO cells were incubated in medium containing 4 mM unlabeled glutamine, 25 mM unlabeled glucose and 3 mM [U-^{13}C] aspartate for 6 hrs on day 4. Then, the isotopomer distributions of malate and pyruvate in IRS-1 KO cells were measured and compared with those in WT cells (Fig. 3.11). M+4 isotopomer of malate in IRS-1 KO cells, derived from [U-^{13}C] aspartate via exchange reactions of aspartate ↔ oxaloacetate ↔ malate, was approximately twice higher than that in WT cells. On the other hand, M+3 isotopomer of pyruvate in IRS-1 KO cells, indicative of the flux from malate to pyruvate, was slightly lower than in WT cells.
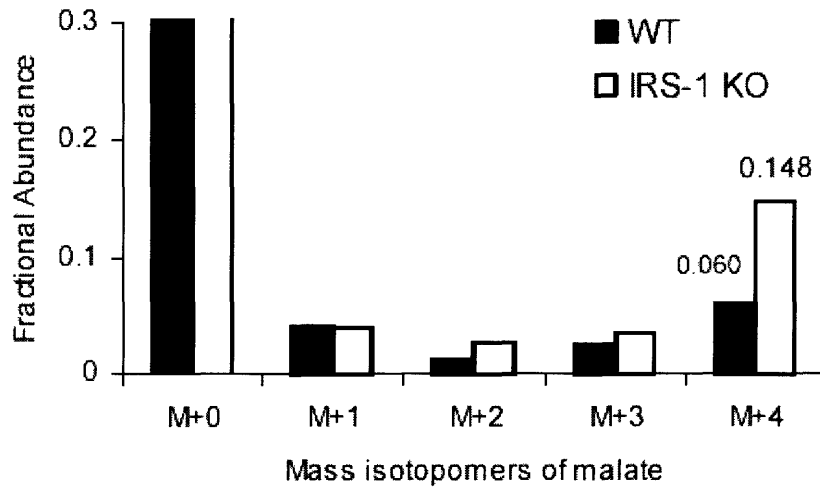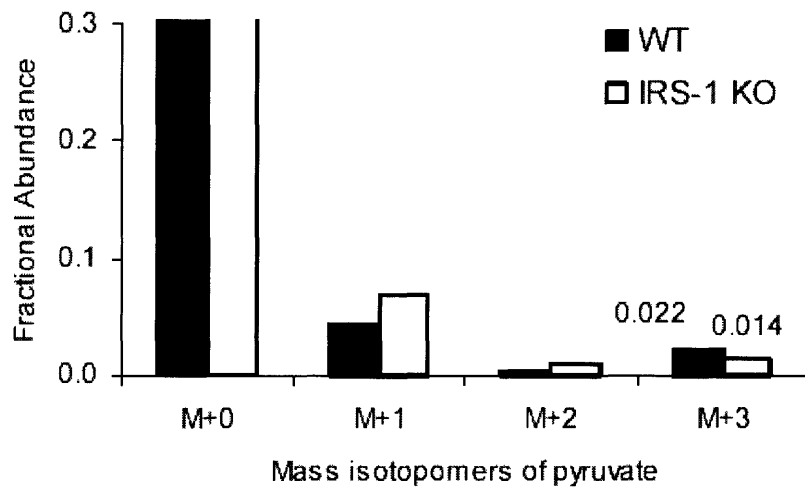
Fig. 3.11. Flux from malate to pyruvate in IRS-1 KO cells verified by ^{13}C-aspartate experiment.

Isotopomer distributions of malate (A) and pyruvate (B) from IRS-1 KO brown adipocytes on day 4 under 6-hr incubation in media containing 25 mM unlabeled glucose, 4 mM unlabeled glutamine and 3 mM [U-^{13}C] aspartate were measured (white bars) and compared with those of malate and pyruvate from WT cells under the same condition (solid bars), which was taken from Figure 2.14. The isotopomer distributions presented here have been corrected for natural abundance.

Discussion

In order to investigate in detail the effect of insulin signaling on the lipogenic activity

specifically involving glutamine's metabolic route to fatty acid synthesis, the fluxes of

individual reactions related to the route were estimated through integration of isotopomer

distribution data of nine metabolites from WT and IRS-1 KO brown adipocytes incubated

with [U-^{13}C] glutamine. Since WT cells were shown to considerably employ reductive

carboxylation pathway in their utilization of glutamine for fatty acid synthesis (11; see also

Chapter 1), the existence of the same pathway was first tested by measuring the

incorporation of ^{13}C-label from [5-^{13}C] glutamine into palmitate synthesis (Fig. 3.1).

Although ^{13}C-labeling of palmitate in IRS-1 KO cells was not as large as in WT cells (Fig.

2.3), significant amount of ^{13}C in palmitate from [5-^{13}C] glutamine indicated that reductive

carboxylation pathway should be included in the metabolic network of IRS-1 KO cells.

When isotopomer distribution data for nine lipogenesis-related metabolites were

compared between WT cells and IRS-1 KO cells under 6-hr incubation with 4 mM [U-^{13}C]

glutamine, the general similarity of isotopomer patterns also suggested that WT and IRS-1

KO cells have the same metabolic network with different profile of individual fluxes (Figs.

3.2-3.10). M+5 isotopomers of glutamate, α-ketoglutarate, and citrate were distinctively

smaller in IRS-1 KO cells than in WT cells (Figs. 3.2-3.4). Because this isotopomer can

originate from [U-^{13}C] glutamine only through reductive carboxylation pathway, the

smaller peaks of M+5 isotopomer strongly indicate that IRS-1 KO cells have relatively less

activity of reductive carboxylation. On the other hand, a common feature of the isotopomer

distributions of fumarate, malate, and aspartate from IRS-1 KO cells was greater abundance

of M+4 isotopomer than in WT cells (Figs. 3.5-3.7). M+4 isotopomer can be derived from

[U-^{13}C] glutamine via direct conversion of α-ketoglutarate to succinate, fumarate, malate, and oxaloacetate along the conventional direction of TCA cycle. Thus, greater abundance of M+4 isotopomers in fumarate, malate, and aspartate shows that IRS-1 KO cells have larger fluxes from α-ketoglutarate to the direction of succinate than WT cells.

In order to integrate the isotopomer distribution of the metabolites (including palmitate) into flux estimation, the same metabolic network as in WT cells were used. Overall goodness of fit for the flux estimation in terms of SSRES value fell within 95% confidence range of SSRES values, suggesting that this flux estimation is as close to reality as in WT cells. For the purpose of comparison between corresponding fluxes of WT and IRS-1 KO cells, uptake fluxes of glutamine and glucose in IRS-1 KO cells were set to be 100 and 1150 based on the measurement of consumption rate, although the absolute rate of glutamine uptake in IRS-1 KO cells was only 40% (40 and 460 for uptake fluxes of glutamine and glucose, respectively) of that in WT cells. Among all the estimated fluxes of WT and IRS-1 KO cells under standard condition, five fluxes were considered to be most meaningful for elucidating the fundamental difference in individual lipogenic fluxes (Fig. 3.12). Most distinctive was the net flux of α-ketoglutarate to citrate, which was a large negative flux as opposed to the positive net flux in WT cells. The limited contribution of reductive carboxylation pathway in IRS-1 KO cells as shown by [5-^{13}C] glutamine experiment (Fig. 3.1) was overcome by large flux of TCA cycle in the conventional direction, which was also demonstrated by 6-fold higher flux of α-ketoglutarate to succinate in IRS-1 KO cells. This result and the low D(Gln) (fractional contribution of glutamine to lipogenic acetyl-CoA) of IRS-1 KO cells in Chapter 1 indicate that the extent

of glutamine's contribution to fatty acid synthesis depends more on the flux through

reductive carboxylation pathway than the flux of conventional glutaminolysis
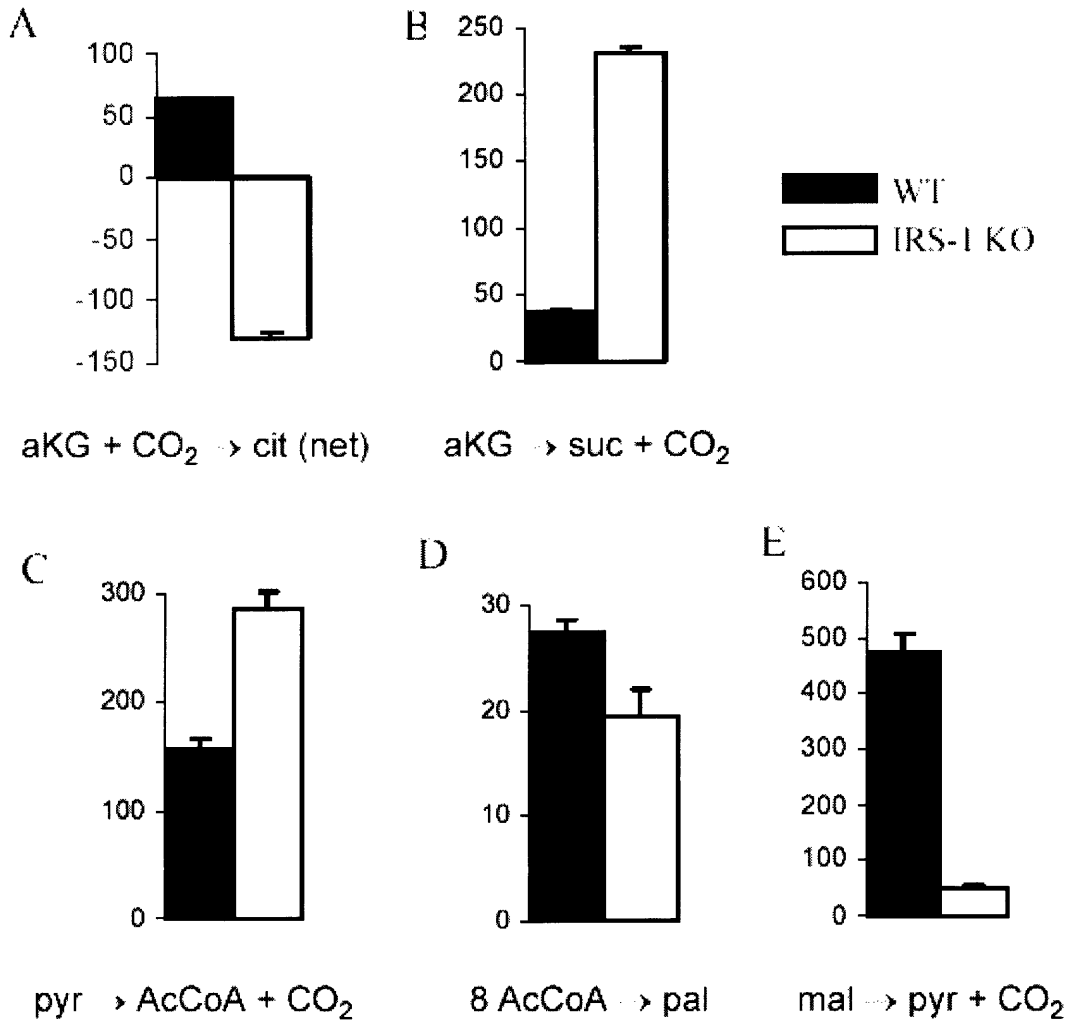
Fig. 3.12. Estimated fluxes for selected metabolic reactions in WT and IRS-1 KO brown adipocytes.

Estimated fluxes for α-ketoglutarate to citrate (A: represented in net flux), α-ketoglutarate to succinate (B), pyruvate to acetyl-CoA (C), acetyl-CoA to palmitate (D), and malate to pyruvate (E) in WT (solid bars) and IRS-1 KO (white bars) brown adipocytes under incubation with 25 mM unlabeled glucose and 4 mM [U-^{13}C] glutamine were taken from Table 2. Data shown are mean $\pm$ SEM (n = 3).

pathway.

Relatively larger flux of pyruvate to acetyl-CoA in IRS-1 KO cells than in WT cells is consistent with D(Glc) (fractional contribution of glucose to lipogenic acetyl-CoA) in WT cells being significantly lower than that of IRS-1 KO cells (Chapter 1) because conversion of pyruvate to acetyl-CoA is the first committed step for glucose flux to lipogenic acetyl-CoA pool. On the other hand, the extent of decrease in the flux of acetyl-CoA to palmitate (catalyzed by fatty acid synthase) due to the absence of insulin signaling was not as significant despite the 9-fold smaller flux of malate to pyruvate via malic enzyme, which has been believed to heavily contribute to the supply of NADPH for fatty acid synthesis in brown adipose tissue (9).

The relatively small flux from malate to pyruvate in IRS-1 KO cells was further verified by an independent experiment with [U-^{13}C] aspartate in comparison with that in WT cells (Fig. 3.11). Higher fractional abundance of M+4 isotopomer of malate in IRS-1 KO cells than in WT cells is consistent with lower diluting fluxes from unlabeled glucose and glutamine (the absolute rates of glucose uptake (460) and glutamine uptake (40) in IRS-1 KO cells are much lower than those in WT cells (1540 for glucose and 100 for glutamine)). Low fractional abundance of M+3 isotopomer of pyruvate in IRS-1 KO cells as compared to that of M+4 isotopomer of malate (0.014 to 0.148) is consistent with low level of malate-to-pyruvate flux (Table 2 and Fig. 3.12). The ratio between these two fractional abundances (0.097) was considerably higher than the ratio of the 'malate → pyruvate' flux to the 'glucose → pyruvate' flux in IRS-1 KO cells (0.022: from Table 2), just as in WT cells (Chapter 2), which can be explained by large additional flux from malate to pyruvate due to added aspartate.

124

Taken together, the low lipogenic activity in IRS-1 KO cells as shown by limited fat accumulation (1,11) was deconvoluted into differential contribution of individual fluxes related to the metabolic routes of glucose and glutamine to fatty acid synthesis. At least in brown adipocytes, lack of insulin signaling affected the lipogenic fluxes from glutamine to fatty acids to a greater degree than those from glucose to fatty acids. Decreased contribution of glutamine to fatty acid synthesis was mainly due to reduced flux of reductive carboxylation from α-ketoglutarate to citrate. Thus, together with the results from Chapter 2, it was revealed that reductive carboxylation through NADP-dependent isocitrate dehydrogenase can be a critical site of regulation for glutamine utilization in fatty acid synthesis of adipose cells and its activity can be manipulated either by hormone (insulin) or exogenous chemicals (specific inhibitors of NADP-ICDH).

References

1. Fasshauer, M., J. Klein, K.M. Kriauciunas, K. Ueki, M. Benito, and C.R. Kahn. 2001. Essential role of insulin receptor substrate 1 in differentiation of brown adipocytes. *Mol Cell Biol* **21**: 319-29.

2. Fiehn, O., J. Kopka, R.N. Trethewey, and L. Willmitzer. 2000. Identification of uncommon plant metabolites based on calculation of elemental compositions using gas chromatography and quadrupole mass spectrometry. *Anal Chem* **72**: 3573-80.

3. Holleran, A.L., D.A. Briscoe, G. Fiskum, and J.K. Kelleher. 1995. Glutamine metabolism in AS-30D hepatoma cells. Evidence for its conversion into lipids via reductive carboxylation. *Mol Cell Biochem* **152**: 95-101.

4. Kowalchuk, J.M., R. Curi, and E.A. Newsholme. 1988. Glutamine metabolism in isolated incubated adipocytes of the rat. *Biochem J* **249**: 705-8.

5. Montague, C.T. and S. O'Rahilly. 2000. The perils of portliness: causes and consequences of visceral adiposity. *Diabetes* **49**: 883-8.

6. Nepokroeff, C.M., M.R. Lakshmanan, G.C. Ness, R.A. Muesing, D.A. Kleinsek, and J.W. Porter. 1974. Coordinate control of rat liver lipogenic enzymes by insulin. *Arch Biochem Biophys* **162**: 340-4.

7. O'Brien, R.M. and D.K. Granner. 1996. Regulation of gene expression by insulin. *Physiol Rev* **76**: 1109-61.

8. Reed, W.D., H.R. Zielke, P.J. Baab, and P.T. Ozand. 1981. Ketone bodies, glucose and glutamine as lipogenic precursors in human diploid fibroblasts. *Lipids* **16**: 677-84.

9. Swierczynski, J., P.W. Scislowski, Z. Aleksandrowicz, and M. Zydowo. 1981. Malic enzyme in brown adipose tissue--purification, some properties and possible physiological role. *Int J Biochem* **13**: 365-72.

10. Valverde, A.M., M. Lorenzo, P. Navarro, and M. Benito. 1997. Phosphatidylinositol 3-kinase is a requirement for insulin-like growth factor I-induced differentiation, but not for mitogenesis, in fetal brown adipocytes. *Mol Endocrinol* **11**: 595-607.

11. Yoo, H., G. Stephanopoulos, and J.K. Kelleher. 2004. Quantifying carbon sources for de novo lipogenesis in wild-type and IRS-1 knockout brown adipocytes. *J Lipid Res* **45**: 1324-1332.

Chapter 4. Restoration of fat synthesis in IRS-1 KO cells by metabolite supplementation

Introduction

Regulation of fat synthesis in adipocytes by insulin signaling has been established by a series of studies by Kahn and coworkers, which has also supported the role of adipocytes in the development of obesity and type 2 diabetes (1). The multi-faceted effects of insulin signaling on fat synthesis include stimulation of glucose uptake by activation of glucose transporter-4 (GLUT4) and upregulation of fatty acid synthase expression through upregulation of transcription factors, C/EBPβ and PPARγ, by mediation of insulin receptor substrate-1 (IRS-1) and phosphatidylinositol 3-kinase (PI3K) (2, 3). Thus, IRS-1 KO brown adipocytes were shown to have limited capability of fat synthesis due to lack of insulin-signaling, which led to inactivation of glucose uptake and fatty acid synthase expression (3).

While a lot of emphasis has been put on the dominating roles of insulin signaling in fat synthesis system of adipocytes, some researchers have paid more attention to the complementary roles of metabolites in regulation of lipogenic enzymes' activity. Ferre and coworkers have published a series of reports on the role of glucose in the expression of fatty acid synthase in liver and adipose tissue ((4) and references therein). Hexosamine biosynthesis pathway has been identified as the mediating factor for glucose-induced desensitization of glucose transport and insulin resistance (5). More recently, it was shown that glucosamine can upregulate the expression of fatty acid synthase mRNA in a dose-dependent manner in primary adipocytes (6). Based on these reports, we have postulated that it might be possible to replace insulin signaling with supplementation of metabolites in

the medium of cultured adipocytes for regulation of fat synthesis. If these modified

conditions can stimulate fat synthesis of adipocytes together with enhanced glucose uptake

in insulin-resistant cells, they may give us insights on alternative approach to the

therapeutics of diabetes. IRS-1 KO brown adipocyte was selected as a model system for

this endeavor, and attempts were made to find a set of conditions with supplementation of

metabolites that may help restoring the level of fat synthesis in IRS-1 KO cells.

Experimental Procedures

Materials

Biochemicals were obtained from Sigma Chemical Co., St. Louis, MO. Tissue culture media were obtained from Invitrogen, Co., Carlsbad, CA.

Cell culture and adipocyte differentiation

See "Experimental Procedures" in Chapter 1 for details.

Oil Red O staining

Staining of cells for quick screening of triglyceride content was done by Oil Red O (Fig. 4.1), following the procedure in Fasshauer, *et al.* (3). On day 6 of differentiation procedure, medium was removed and cells were rinsed with phosphate-buffered saline (PBS). Then, cells were fixed by covering with 1 mL buffered formalin per well. Oil Red O working solution was prepared by adding 6 mL stock solution (0.5 g Oil Red O in 100 mL isopropanol) to 4 mL distilled water and filtering the well-mixed solution through Whatman #1 filter paper). After 1 hr of fixation at room temperature, fixation agent was removed and 1 mL of the Oil Red O working solution was added per well of 6-well plate (10 cm^2). After 2 hrs or longer at room temperature, staining solution was removed and the cells were carefully rinsed several times with distilled water to remove excess stain and any precipitate that forms. The cells in 6-well plates were digitally scanned for recording their redness, which is indicative of the amount of triglyceride in the cells.
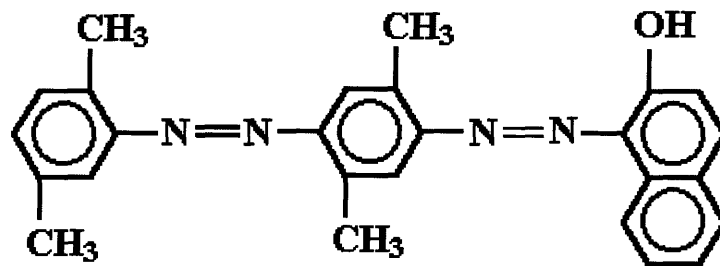
Fig. 4.1. Chemical structure of Oil Red O.

Oil Red O is a lysochrome (fat soluble dye) predominantly used for demonstrating triglycerides in frozen sections, which may also stain some protein bound lipids in paraffin sections (7).

Measurement of amounts of total fatty acids

See "Experimental Procedures" in Chapter 1 for details.

Glucose uptake assay

The rate of glucose uptake was assayed essentially as described in Fasshauer *et al.* (3).

On day 6 of differentiation procedure, the medium was removed from a well of 6-well plate,

and cells were washed twice with 1 mL of DMEM medium. Cells were then incubated

with 4 mL of DMEM high medium at 37°C for 16 hrs for serum deprivation. Cells were

then washed three times with KRP buffer (136 mM NaCl / 4.7 mM KCl / 1.25 mM $CaCl_2$ /

1.25 mM $MgSO_4$ / 10 mM NaH_2PO_4 / pH 7.4) and incubated in 0.9 mL of KRP buffer at

37°C for 30 min. In the beginning of this incubation, 100 nM insulin was added alone or

together with 10 μM of cytochalasin (as control for non-specific uptake of 2-deoxyglucose).

After the 30-min incubation, 50 μM (0.5 μCi/mL) of 2-^{3}H-deoxyglucose (DOG) was added

and the plate was swirled. After 5-min incubation at 37°C, the medium was removed and

the cells were washed three times with 0.5 mL cold PBS buffer. Cells were then

solubilized with 0.7 mL of 1 % Triton X-100 for 20 min at 37°C, which was centrifuged at

14000 rpm for 2 min. The supernatant was used for radioactivity measurement using liquid

scintillation counting by Tri-carb 1500 Liquid Scintillation Analyzer from Packard. Part of

the supernatant was also used for determination of protein amount by Lowry assay.

Results and Discussion

Results of screening for increased fat production in IRS-1 KO brown adipocytes

In order to test the effects of metabolites and other hormones for bypassing insulin signaling, the cell differentiation protocol was first examined for perturbation. When various combinations of the three compounds for induction during the first two days were tried, the Oil Red O staining experiments on day 6 led to interesting results: among the seven combinations with partial combination of the three compounds, only those without dexamethasone resulted in noticeably higher level of fat than the standard condition (Fig. 4.2). Also, in order to test various metabolites for replacing glucose as lipogenic precursor, WT cells were deprived of glucose and supplemented with glycerol, lactate, and acetoacetate. Glycerol was tested for providing alternative carbon source for glycerol backbone of triglyceride while lactate and acetoacetate were tested for precursors of lipogenic acetyl-CoA. Interestingly, acetoacetate was effective in increasing the impaired fat synthesis in glucose-deprived WT cells (Fig. 4.3).

Dexamethasone is a synthetic glucocorticoid to substitute for the effects of natural hormone cortisol and corticosterone. Brown adipose tissue has been shown to contain high level of glucocorticoid receptors (8), but little is known about the significance of the receptor for the function of the tissue. Dexamethasone has been studied for its differential effect on two kinds of glucose transporters, GLUT1 and GLUT4 in brown adipocytes (9, 10). Within the gene family of facilitative glucose transporters, GLUT1 is an insulin-independent glucose transporter while GLUT4 is responsible for insulin-induced glucose uptake in muscle and adipose tissues (11). Thus, dexamethasone was shown to increase the expression of GLUT4 and decrease that of GLUT1 in a dose-dependent manner (9).

	A.	B.	C.	D.
Induction chemicals	Dex	+	+	−	−
	Indo	+	−	−	±
	IBMX	+	+	−	−

	E.	F.	G.	H.
*WT				
Dex	−	+	−	−
Indo	−	−	−	−
IBMX	+	−	−	−

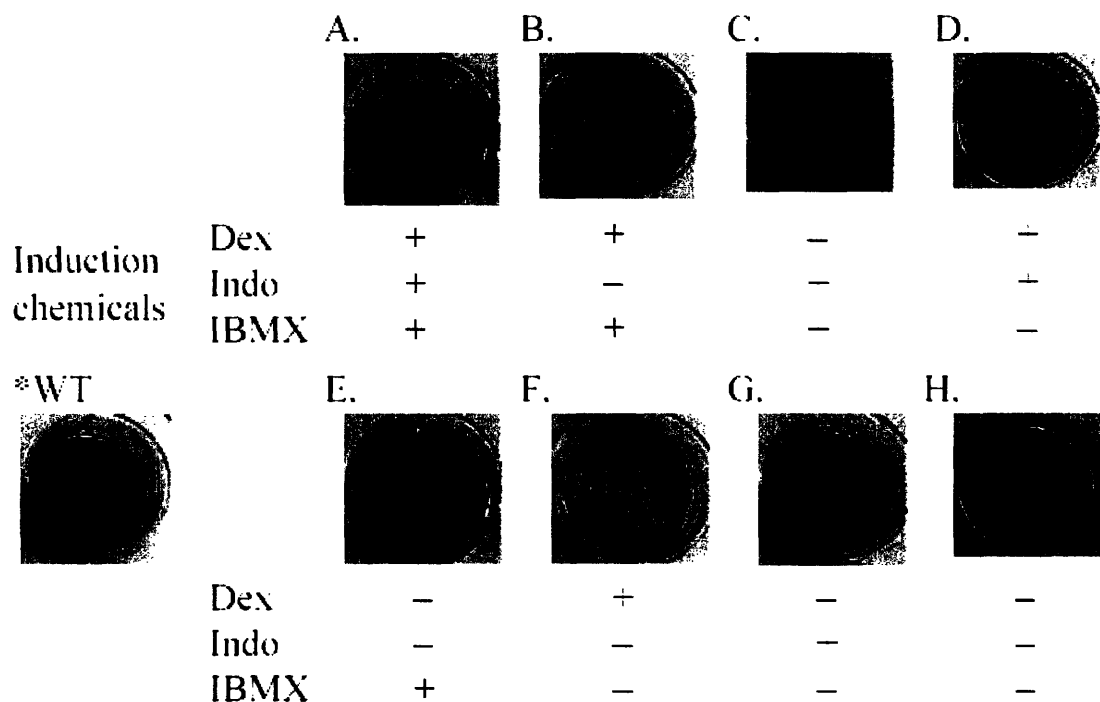Fig. 4.2. Effect of combinations of induction chemicals on fat synthesis of IRS-1 KO brown adipocytes.

Results of triglyceride staining by Oil Red O for IRS-1 KO brown adipocytes on day 6 from 2-day incubation (day 0 – day 2) with eight different combinations (A ~ H) of three induction chemicals: dexamethasone (5 μM), indomethacin (0.125 mM), IBMX (0.25 mM). (*WT: WT brown adipocytes grown under standard condition shown as control)
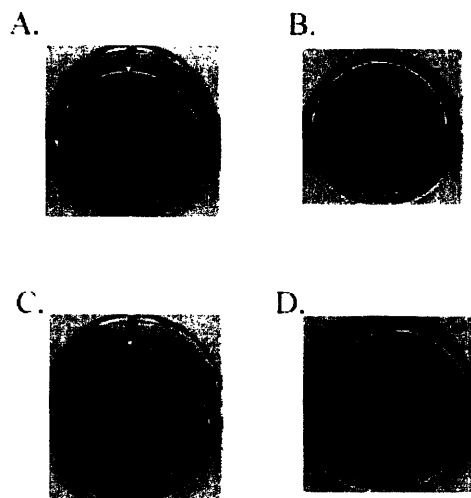
Fig. 4.3. Screening for additive metabolites to substitute for glucose as lipogenic carbon source.

Results of triglyceride staining by Oil Red O for WT brown adipocytes on day 6 grown in the absence of glucose from day 0 to day 6 and added lactate (10 mM, B), glycerol (5 mM, C), or acetoacetate (10 mM, D). A:WT cells grown under standard condition.

134

Therefore, it was hypothesized that absence of dexamethasone in the medium of IRS-1 KO cells during induction period may help the cells maintain the activity of GLUT1 so as to increase glucose uptake relative to the standard condition.

In a preliminary experiment, the rates of glucose uptake were measured for WT and IRS-1 KO cells on day 6 to test this hypothesis (Fig. 4.4). In accordance with the hypothesis, insulin-stimulated glucose uptake was repressed in WT cells grown in the absence of dexamethasone (WT_std vs. WT_Dex-, change from –ins to +ins) while the rate of glucose uptake in the absence of insulin was increased (KO std vs. KO Dex-, –ins) with little effect on insulin-stimulated glucose uptake in IRS-1 KO cells grown in the absence of dexamethasone (KO_std vs. KO_Dex-, change from –ins to +ins). However, this effect did not lead to the increase in D(Glc) value of IRS-1 KO cells under Dex- condition (Fig. 1.6A), and the amount of total fatty acids in IRS-1 KO cells under Dex- condition was marginally increased relative to that under standard condition (Fig. 1.3).

The hypothesis that acetoacetate may be able to replace glucose as precursor for lipogenic acetyl-CoA was supported by ^{13}C-labeling of acetoacetate followed by ISA (Fig. 1.6A). However, inability of acetoacetate or glutamine to provide carbon source for glycerol backbone of triglyceride (Fig. 1.10B) limited the extent to which WT cells could use acetoacetate to increase fat synthesis in the absence of glucose (Fig. 1.9B). Therefore, addition of acetoacetate in the medium for IRS-1 KO cells during 4-day differentiation period did not help noticeably increasing the amount of fat synthesis in IRS-1 KO cells (Fig. 1.3). In another preliminary experiment, when Dex- and AcAc+ conditions were combined (removal of dexamethasone from day 0 to day 2 and addition of acetoacetate from day 2 to
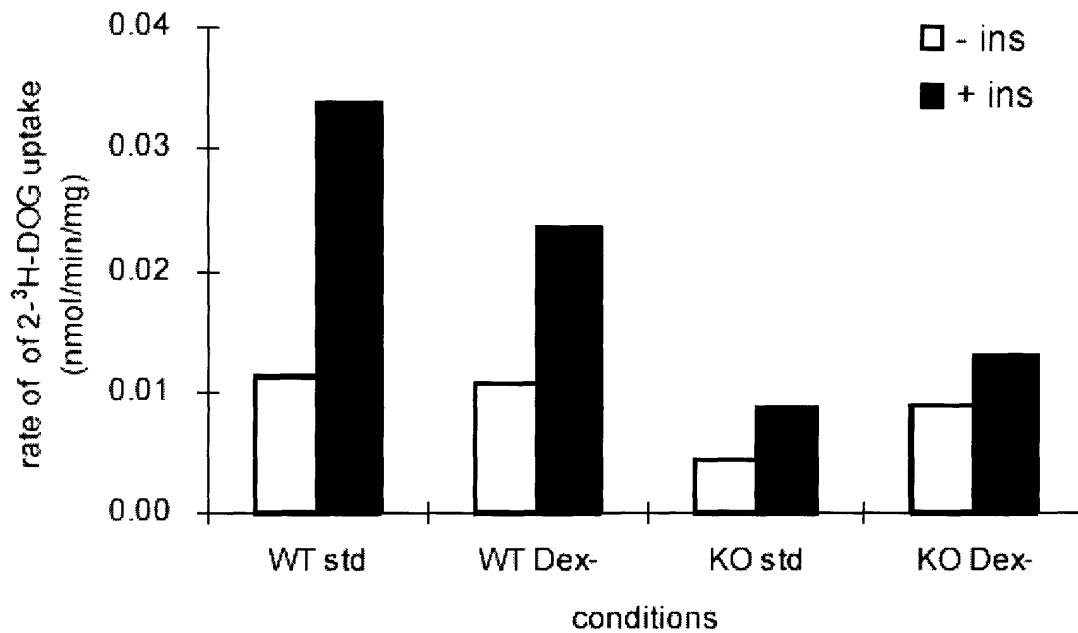
Fig. 4.4. Glucose uptake assay for WT and IRS-1 KO brown adipocytes under standard or Dex- condition.

Rate of $[2-^3H]$-deoxyglucose uptake was measured on day 6 for WT and IRS-1 KO brown adipocytes grown under standard condition (std) or without dexamethasone from day 0 to day 2 (Dex-). See "Experimental Procedures" for experimental details.

day 6), IRS-1 KO cells produced 30% more total fatty acids per protein mass than under standard condition.

Supplementation of metabolites for alternative carbon source of glycerol backbone of triglyceride

Although AcAc+ condition did not result in considerable enhancement of fat synthesis in IRS-1 KO cells, the fact that addition of acetoacetate led to approximately 50% increase in the amount of total fatty acids in WT cells under glucose-deprived condition (Fig. 1.9B) was considered very promising. Therefore, in an attempt to find the metabolites that could alternatively provide precursors for glycerol backbone of triglyceride, the metabolites with such capacity were tested. Since such metabolites as glycerol, lactate, and pyruvate have been reported to show this capacity (12, 13), these metabolites were added to WT cells under the AcAc+/Glc- condition and the amount of total fatty acids were measured (Fig. 4.5: WT(Glc-)). Addition of lactate and pyruvate in a 10:1 ratio ("lac/pyr"), in order to maintain the physiological reduction potential, was most effective (~ 30%) in increasing fat synthesis of WT cells under glucose-deprived AcAc+ condition. When the same metabolites were tested in IRS-1 KO cells under AcAc+ condition, addition of lactate and pyruvate (10:1) was also most effective to a similar extent (~ 30%) (Fig. 4.5: KO).

In an attempt to further increase the amount of fat synthesis in IRS-1 KO cell by metabolite supplementation, the concentration of lactate/pyruvate (10:1) was varied from 5 mM to 25 mM and the amount of total fatty acids was compared with that in IRS-1 KO cells under standard condition (Fig. 4.6). Contrary to the expectation, increasing amounts of lactate and pyruvate (10:1) from 5 mM to 25 mM in addition to 10 mM acetoacetate
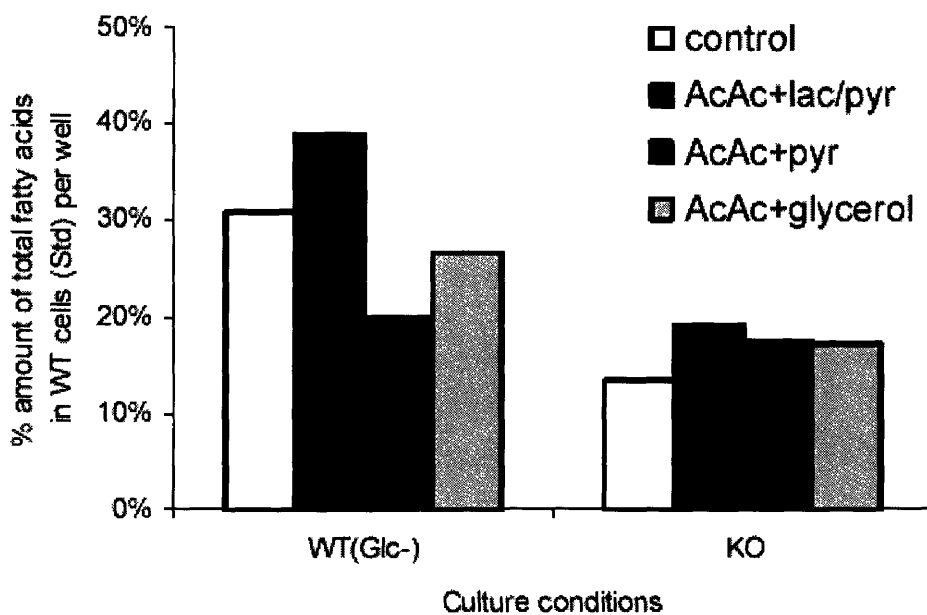
Fig. 4.5. Screening for additive metabolites to substitute for glucose as precursor of glycerol backbone of triglyceride.

WT brown adipocytes grown without glucose and added 10 mM acetoacetate (control, left) or IRS-1 KO cells grown with 25 mM glucose and added 10 mM acetoacetate (control, right) were supplemented with 5 mM lactate/0.5 mM pyruvate (lac/pyr), 5 mM pyruvate (pyr), or 5 mM glycerol (glycerol) from day 2 to day 6 and the respective amount of total fatty acids per well was measured as percentage of that amount in WT cells under standard condition on day 6.

repressed fat synthesis in IRS-1 KO cells.

Supplementation with glucosamine and its combination with Dex- / AcAc+ conditions

Among the limiting factors in lipogenesis system of IRS-1 KO cells, low expression of

fatty acid synthase (FAS) would be difficult to overcome by supplementation of

metabolites or hormones. Recently, glucosamine has been shown to induce upregulation of

the mRNA expression of FAS in adipocytes, possibly via activating hexosamine

biosynthesis pathway (6). In preliminary experiments with addition of 2 mM glucosamine

from day 2 to day 6 in medium for IRS-1 KO cells, the amounts of total fatty acids per well

was increased only by 5%. In order to provide more lipogenic precursors together with

increased expression of FAS, the Dex- condition and Dex- / AcAc+ conditions were

combined with glucosamine+ condition. Combination of Dex- condition and glucosamine+

condition (removal of dexamethasone from day 0 to day 2, and addition of glucosamine

from day 2 to day 6) led to 25% increase in amounts of total fatty acids. Considering the

possibility that addition of glucosamine from day 0 instead of day 2 might be better in

increasing the expression of FAS, another preliminary experiment was performed with

removal of dexamethasone from day 0 to day 2 and addition of glucosamine and

acetoacetate from day 0 to day 6. Contrary to expectations, the amount of total fatty acids

was increased only by 10%, even less than the amount of total fatty acids under Dex- /

AcAc+ condition (30% increase, see above).

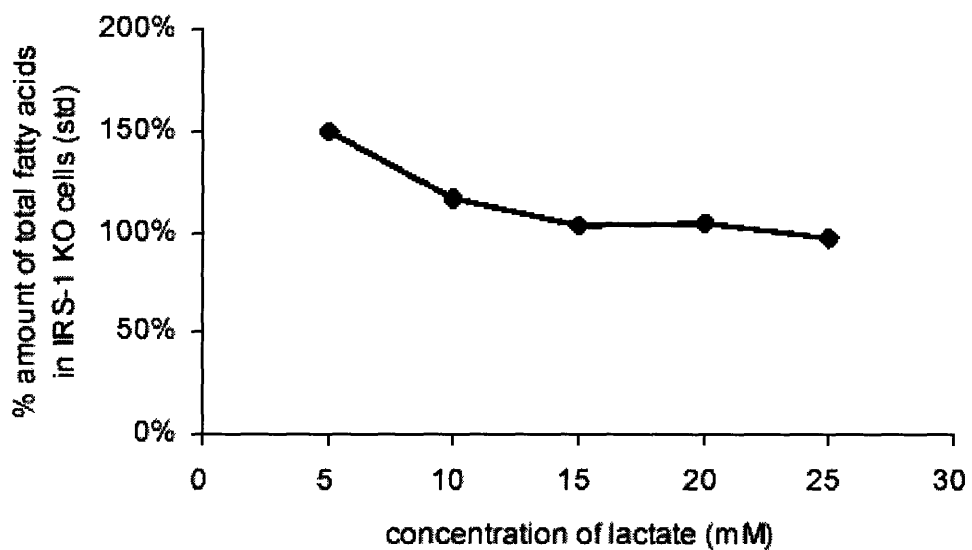Fig. 4.6. Effect of increasing amount of lactate/pyruvate (10:1) on fat synthesis in IRS-1 KO brown adipocytes grown in the presence of 10 mM acetoacetate.

IRS-1 KO brown adipocytes were grown in the presence of 10 mM acetoacetate and 5 to 25 mM lactate/pyruvate (10:1) from day 2 to day 6 and the amount of total fatty acids were measured as percentage of the amount in IRS-1 KO cells under standard condition.

Conclusion

Among the discussed conditions, 10 mM AcAc / 5 mM lactate / 0.5 mM pyruvate condition was most effective in increasing the level of fat synthesis in IRS-1 KO cells, but the extent of increase was not more than 50%. In IRS-1 KO cells, absence of dexamethasone was helpful in increasing the insulin-independent glucose uptake and addition of acetoacetate, lactate, and pyruvate provided further increase in the level of fat synthesis probably by providing alternative carbon source for lipogenesis. However, addition of glucosamine, which was hypothesized to stimulate the expression of fatty acid synthase, was not helpful in increasing the level of fat synthesis when combined with other perturbed conditions. Although it is deemed still possible that further combination of these perturbed conditions could lead to more impressive results, the repressed fat synthesis in IRS-1 KO cells seems to involve more extensive defects in lipogenesis system than lack of lipogenic precursors or low expression of FAS. As discussed in Chapters 2 and 3, WT cells utilizes glutamine to a larger degree than glucose and IRS-1 KO cells have much lower capacity for this utilization. It is plausible that enhancement of the system for converting glutamine (as well as glucose) to lipogenic acetyl-CoA may be crucial in improving fat synthesis in IRS-1 KO cells.

References

1. Klein, J., M. Fasshauer, H.H. Klein, M. Benito, and C.R. Kahn. 2002. Novel adipocyte lines from brown fat: a model system for the study of differentiation, energy metabolism, and insulin action. Bioessays 24: 382-8.

2. Valverde, A.M., M. Lorenzo, P. Navarro, and M. Benito. 1997. Phosphatidylinositol 3-kinase is a requirement for insulin-like growth factor I-induced differentiation, but not for mitogenesis, in fetal brown adipocytes. Mol Endocrinol 11: 595-607.

3. Fasshauer, M., J. Klein, K.M. Kriauciunas, K. Ueki, M. Benito, and C.R. Kahn. 2001. Essential role of insulin receptor substrate 1 in differentiation of brown adipocytes. Mol Cell Biol 21: 319-29.

4. Ferre, P. 1999. Regulation of gene expression by glucose. Proc Nutr Soc 58: 621-3.

5. Marshall, S., V. Bacote, and R.R. Traxinger. 1991. Discovery of a metabolic pathway mediating glucose-induced desensitization of the glucose transport system. Role of hexosamine biosynthesis in the induction of insulin resistance. J Biol Chem 266: 4706-12.

6. Rumberger, J.M., T. Wu, M.A. Hering, and S. Marshall. 2003. Role of hexosamine biosynthesis in glucose-mediated up-regulation of lipogenic enzyme mRNA levels: Effects of glucose, glutamine and glucosamine on glycerophosphate dehydrogenase, fatty acid synthase, and acetyl-CoA carboxylase mRNA levels. J Biol Chem.

7. Lillie, R.D. and L.L. Ashburn. 1943. Supersaturated solutions of fat stains in dilute isopropanol for demonstration of acute fatty degeneration not shown by Herxheimer's technique. Arch. Pathol. 36: 432-440.

8. Feldman, D. and D. Loose. 1977. Glucocorticoid receptors in adipose tissue. Endocrinology 100: 398-405.

9. Shima, A., Y. Shinohara, K. Doi, and H. Terada. 1994. Normal differentiation of rat brown adipocytes in primary culture judged by their expressions of uncoupling protein and the physiological isoform of glucose transporter. Biochim Biophys Acta 1223: 1-8.

10. Shimizu, Y., D. Kielar, H. Masuno, Y. Minokoshi, and T. Shimazu. 1994. Dexamethasone induces the GLUT4 glucose transporter, and responses of glucose transport to norepinephrine and insulin in primary cultures of brown adipocytes. J Biochem (Tokyo) 115: 1069-74.

11. Olson, A.L. and J.E. Pessin. 1996. Structure, function, and regulation of the mammalian facilitative glucose transporter gene family. Annu Rev Nutr 16: 235-56.

12. Festuccia, W.T., N.H. Kawashita, M.A. Garofalo, M.A. Moura, S.R. Brito, I.C. Kettelhut, and R.H. Migliorini. 2003. Control of glyceroneogenic activity in rat brown adipose tissue. Am J Physiol Regul Integr Comp Physiol 285: R177-82.

13. Declercq, P.E., L.J. Debeer, and G.P. Mannaerts. 1982. Glucagon inhibits triacylglycerol synthesis in isolated hepatocytes by lowering their glycerol 3-phosphate content. Biochem J 202: 803-6.

Chapter 5. Conclusion and Future experiments

Conclusion

The whole research in this thesis has started with a hypothesis that addition of a set of metabolites to cell culture medium carefully selected to compensate for lack of insulin signaling might be able to stimulate the defective lipogenesis system of adipocyte cell line where insulin signaling pathway has been impaired by knockout of an important mediator, insulin receptor substrate-1 (IRS-1). The endeavor to find those metabolites led to discovery of the combination of metabolites where acetoacetate, lactate, and pyruvate can substitute for glucose as lipogenic precursors of fatty acids and glycerol backbone of triglyceride (Chapter 4). Under this condition, fat synthesis in IRS-1 KO brown adipocytes (which can produce only one third of total fatty acids per protein mass in WT brown adipocytes by day 6 of standard differentiation procedure) was increased by less than 50%. However, with quantitative examination of individual carbon fluxes for fat biosynthesis in WT and IRS-1 KO brown adipocytes using ^{13}C-labeling, GC/MS analysis, and flux estimation, detailed knowledge of the flow of carbon sources to fat synthesis has been gained. While no other carbon sources than glucose were able to supply carbon sources for glycerol backbone of triglyceride, glutamine and acetoacetate were utilized more actively than glucose in fatty acid synthesis of WT brown adipocytes (Chapter 1). Unlike the well-known pathways for utilization of glucose and acetoacetate for fatty acid synthesis, there has been a controversy on the metabolic routes of glutamine to fatty acid synthesis between glutaminolysis pathway (via the conventional pathway of tricarboxylic acid (TCA) cycle) and reductive carboxylation pathway (via the novel pathway of reductive carboxylation of α-ketoglutarate to isocitrate/citrate). In Chapter 2, these two pathways were integrated into

a metabolic network model together with glucose utilization pathway for quantitative estimation of lipogenic fluxes based on isotopomer patterns of the component metabolites following incubation of the cells in [U-^{13}C] glutamine containing media. Unexpectedly, the contribution of reductive carboxylation pathway was so significant that the net carbon flux from α-ketoglutarate to isocitrate/citrate was observed in WT cells under standard condition. This net carbon flux was further supported by dose-dependent repression of this flux upon treatment with specific inhibitors of NADP-ICDH, the enzyme responsible for reductive carboxylation. In Chapter 3, the significance of reductive carboxylation pathway for utilization of glutamine as lipogenic carbon source was associated with the metabolic effect of insulin signaling, by showing dramatically repressed carbon flux through reductive carboxylation in IRS-1 KO cells as compared with that in WT cells, which is also consistent with reduced capacity of IRS-1 KO cells to utilize glutamine as precursor for fatty acid synthesis (Chapter 1). Thus, quantitative understanding of the individual carbon fluxes for fat synthesis by stable-isotope labeling and flux estimation was crucial in revealing the importance of other carbon sources such as glutamine in fat synthesis and the means by which the contribution of these carbon sources to fat synthesis can be manipulated. Moreover, detailed information of individual carbon fluxes in connection with the global influence of insulin signaling on the use of the carbon sources in lipogenesis provided a unique perspective as to the end-point results of presence or absence of insulin signaling in the lipogenic process, so that an in-depth understanding of the effects of insulin signaling on lipid metabolism was obtained. This understanding in metabolite level will complement the studies focused on the hormonal effects in terms of the changes in mRNA

and protein levels of lipogenic genes, leading to comprehensive grasp of the lipogenic system.

Future experiments

The flux estimation in Chapters 2 and 3 was based on a relatively simple model of metabolic network (Fig. 2.9), which only contained those metabolic reactions that are immediately related to fatty acid synthesis. It was surprising that the data set of isotopomer distribution for as many as nine metabolites could fit this model with 95% statistical confidence. Considering that the flux estimation was based on the ^{13}C-labeling of only glutamine as a carbon source, the validity of this model can be further examined in two ways: 1) to use another ^{13}C-labeled carbon source and see how close the flux estimation gets to the previous estimation; 2) to extend the range of metabolites and see how good the fit becomes for the more complicated network. In the present study, attempts were made to use [U-^{13}C] glucose for fitting the model with measurements from ^{13}C-labeled metabolites. Unfortunately, the isotopomer patterns of all nine metabolites did not reach steady-state within 6 hours, making it impossible to use those data for flux estimation because all the equations and their solutions for the estimation were based on steady-state assumption. It seems most likely that the steady state was not reached within 6 hours because of slow labeling of the large intracellular pool of lactate by ^{13}C-glucose. Thus, longer incubation of the cells with ^{13}C-glucose may lead to steady state by metabolites of interest, when the metabolic network model can be cross-examined by flux estimation results from two independent labeling schemes with ^{13}C-glucose and ^{13}C-glutamine. As a second way to examine the validity of the model, a set of amino acids can be included in the extended

146

model because the reactions between many amino acids and the TCA cycle intermediates are well established. Besides those amino acids that were included in the present model (glutamate and glutamine, and aspartate), alanine can be derived from pyruvate, asparagine from aspartate, and proline from glutamate. Also, aspartate can generate lysine, threonine, and methionine while pyruvate carbon can be incorporated into valine, leucine, and isoleucine. Thus, extensive measurement of isotopomer distribution of these amino acids and careful examination of the reactions between them and the pre-existing metabolites can make the model more compelling with additional flux estimation results.

In addition, isotopomer distribution of other fragments of the nine metabolites can be considered in the flux estimation to verify the present model. The present study examined only the main fragments (M – *tert*-butyl: *tert*-butyl from derivatizing agent, MTBSTFA) that contain all of the original carbons of the metabolites in order to gather the most information out of GC/MS measurement. Although m/z values from other fragments may not necessarily distinguish between loss of one carbon versus the other, which would make it difficult to assign the GC/MS data to a specific subset of the original carbons of the metabolite, there may be some cases where loss of a certain carbon is much more favored than any other during ionization for GC/MS measurement. This relationship can be established by careful preliminary experiments of GC/MS with standard metabolites labeled at specific position(s). Then, careful inspection of the current GC/MS data will lead to obtaining additional information to validate the flux estimation and the metabolic network model.

Although the results of flux estimation in Chapter 2 and Chapter 3 were shown to be reliable within 95% confidence range by statistical examination, the metabolic network

model used in the flux estimation (Fig. 2.9) did not distinguish between mitochondrial and cytosolic activities of NADP-ICDH in terms of the flux from glutamine to fatty acid synthesis via reductive carboxylation. This issue could not be resolved by specific inhibition of NADP-ICDH with oxalomalate or 2-methyisocitrate because these inhibitors are supposed to be effective for both mitochondrial and cytosolic activities of NADP-ICDH. Results from inhibition of tricarboxylic acid transport across mitochondrial membrane (using benzenetricarboxylate (BTC): Chapter 2) were consistent with the reductive carboxylation flux within mitochondria in that fractional contribution of $[U-^{13}C]$ glutamine to palmitate synthesis (D(Gln)) was 20% reduced. However, concurrent 50% decrease in fractional new synthesis of palmitate (g(6hr)) suggests that the process of fatty acid synthesis was also affected by the inhibition, which leaves the possibility that reduced cytosolic flux of reductive carboxylation could have lowered the amount of lipogenic acetyl-CoA and decreased fractional new synthesis of palmitate while the small decrease in D value could have been due to nonspecific or indirect effect of the BTC inhibition on the cytosolic flux. The limitation of this experiment can be overcome by another set of experiment where g(t) value is maintained by providing sufficient amount of alternative source for lipogenic acetyl-CoA. As shown in Chapter 1, acetoacetate can be used as the major lipogenic carbon source at 10 mM concentration in the presence of 25 mM glucose and 4 mM glutamine. Therefore, the BTC inhibition experiment can be performed for ^{13}C-glutamine in the presence of unlabeled glucose and acetoacetate, where decreased D(Gln) value with constant g(t) value would strongly indicate the involvement of mitochondrial reductive carboxylation in fatty acid synthesis. As a control, the same experiment can be repeated for ^{13}C-glucose in the presence of unlabeled glutamine and acetoacetate. D(Glc) is

expected to decrease because it is well known that glucose's route to fatty acid synthesis has to go through mitochondrial citrate and its transport to cytosol. If glutamine also has to go through mitochondrial citrate in its route to fatty acid synthesis, the inhibition by BTC should affect D(Glc) and D(Gln) to the same extent. One thing to be seriously considered in design of this experiment is that in the presence of 10 mM acetoacetate neither D(Glc) nor D(Gln) was larger than 0.2 (Fig. 1.6), which may be too small for reliable estimation of D values in the inhibition studies. Thus, the appropriate concentration of acetoacetate should be carefully examined and selected as well as the appropriate time span of the labeling, in order to detect distinct changes in D values while maintaining constant $g(t)$ values.

A more compelling evidence for reductive carboxylation flux in mitochondria can be obtained if the mitochondrial and cytosolic activities of NADP-ICDH can be differentially modulated. Protein sequences for mitochondrial (ID: AAC52473) and cytosolic (ID: AAD02919) enzymes of murine NADP-ICDH have only 68% sequence identity (by LALIGN) while protein sequences for mitochondrial (or cytosolic) NADP-ICDH are well reserved across mammals (e.g. human – pig – mouse) with ~95% sequence identity. Therefore, it is conceivable that mammalian application of the RNA interference technology (1) can be employed to specifically knockdown the expression of mitochondrial NADP-ICDH (idh2) and maintain the expression level of cytosolic NADP-ICDH (idh1). Considering that murine idh2 gene sequence (ID: U51167, 1.8 kb) has 75% sequence identity with the corresponding idh1 gene sequence (ID: AF020039), one or more sequences of small interfering RNA (siRNA) with 21-22 nucleotides may be found. Good candidate sequences of siRNA can be designed either manually by using the empirical

criteria (2) or from commercial sources such as Ambion, Inc. Through careful consideration of synthesis and degradation of idh2 gene in both mRNA and protein levels as well as the effective range of dose for the designed siRNA molecule based on a set of preliminary experiments (3), it may be possible to perform the inhibition experiments comparable to those performed in Chapter 2 with oxalomalate or 2-methylisocitrate for 6-hr inhibition of NADP-ICDH activity. If the activity of mitochondrial NADP-ICDH can be readily controlled by combination of the parameters of siRNA experiment as demonstrated with mouse hepa1-6 cells (3), appropriate timeframes for the incubation of cells with ^{13}C-labeled glutamine and for the transfection of cells with idh2-specific siRNA can be used to test whether repression of mitochondrial NADP-ICDH would give rise to corresponding reduction in estimated flux of reductive carboxylation from α-ketoglutarate to isocitrate/citrate. Results of the experiments with idh2-specific siRNA or idh1-specific siRNA would provide definitive evidences for the question of whether the reductive carboxylation happens in mitochondria or cytosol of mouse brown adipocytes. Moreover, the outcome of these experiments would make it possible to develop methods for precise manipulation of the glutamine's flux to fatty acid synthesis, as compared to the selective control by NADP-ICDH inhibitors (Chapter 2) or the global regulation of this flux by insulin as proposed in Chapter 3. In this regard, it is interesting to note that an *in vitro* evidence was recently put forth to suggest that cytosolic NADP-ICDH is more involved in regulation of fatty acid biosynthesis than its mitochondrial counterpart (4). This hypothesis was supported later by an *in vivo* study where overexpression of the cytosolic enzyme stimulated overall fat synthesis in transgenic mice (5). Although both studies associated these results with the lipogenic role of NADP-ICDH to supply NADPH by catalyzing

oxidative decarboxylation, these studies may as well be interpreted in terms of its direct role for lipogenesis through reductive carboxylation, especially because the level of NADPH did not change significantly in liver and adipose following overexpression of cytosolic NADP-ICDH (5).

The abolition of net flux through reductive carboxylation in IRS-1 KO brown adipocytes, as demonstrated in Chapter 3, could be caused by either low expression of NADP-ICDH or lack of NADPH in the compartment where the reductive carboxylation happens. In order to examine the first possibility, mRNA and protein expression levels of mitochondrial and cytosolic NADP-ICDH can be measured and compared with the corresponding levels of other lipogenic enzymes such as fatty acid synthase with normalization by β-actin. The same set of experiments have been recently reported for rat brain cells using RT-PCR analysis and western blotting with minimal cross-activities of antibodies for cytosolic and mitochondrial isozymes (6). This experiment can be complemented by examining the effect of overexpressing mitochondrial or cytosolic NADP-ICDH in IRS-1 KO cells, as recently performed using retroviral transfection of cytosolic NADP-ICDH into NIH3T3 white adipocytes (7). Measurement of the *in vivo* level of NADPH is generally performed by using indicator metabolites with the provision that the reaction catalyzed by the relevant enzyme can be shown to be at equilibrium (8). This measurement has been more difficult to do for mitochondrial matrix because substantial fraction of mitochondrial nucleotides are bound to proteins. Thus, gathering evidence for lack of NADPH causing abolition of net flux of reductive carboxylation will be less straightforward.

References

1. Hannon, G.J. and J.J. Rossi. 2004. Unlocking the potential of the human genome with RNA interference. *Nature* **431**: 371-8.

2. Mittal, V. 2004. Improving the efficiency of RNA interference in mammals. *Nat Rev Genet* **5**: 355-65.

3. Raab, R.M. and G. Stephanopoulos. 2004. Dynamics of gene silencing by RNA interference. *Biotechnol Bioeng* **88**: 121-32.

4. Shechter, I., P. Dai, L. Huo, and G. Guan. 2003. IDH1 gene transcription is sterol regulated and activated by SREBP-1a and SREBP-2 in human hepatoma HepG2 cells: evidence that IDH1 may regulate lipogenesis in hepatic cells. *J. Lipid Res.* **44**: 2169-2180.

5. Koh, H.-J., S.-M. Lee, B.-G. Son, S.-H. Lee, Z.Y. Ryoo, K.-T. Chang, J.-W. Park, D.-C. Park, B.J. Song, R.L. Veech, H. Song, and T.-L. Huh. 2004. Cytosolic NADP+-dependent Isocitrate Dehydrogenase Plays a Key Role in Lipid Metabolism. *J. Biol. Chem.* **279**: 39968-39974.

6. Minich, T., S. Yokota, and R. Dringen. 2003. Cytosolic and mitochondrial isoforms of NADP+-dependent isocitrate dehydrogenases are expressed in cultured rat neurons, astrocytes, oligodendrocytes and microglial cells. *J Neurochem* **86**: 605-14.

7. Lee, S.M., H.-J. Koh, D.-C. Park, B.J. Song, T.-L. Huh, and J.-W. Park. 2002. Cytosolic NADP+-dependent isocitrate dehydrogenase status modulates oxidative damage to cells. *Free Radical Biology and Medicine* **32**: 1185-1196.

8. Veech, R.L. 1987. In *Coenzymes and Cofactors* (ed. D. Dolphin, R. Poulson, and O. Avramovic) Vol IIB, pp. 79-104. J. Wiley and Sons, New York.

Appendices

Appendix A. Effect of increasing inhibition of NADP-ICDH by oxalomalate on isotopomer distribution of fumarate, malate, aspartate, pyruvate, and lactate.

Isotopomer distribution of fumarate (a), malate (b), aspartate (c), pyruvate (d), and lactate (e) from WT brown adipocytes on day 4 under 6-hr incubation in media containing 4 mM [U-^{13}C] glutamine and 0, 5, or 10 mM oxalomalate (OM). Data shown are mean ± SEM (n = 3).
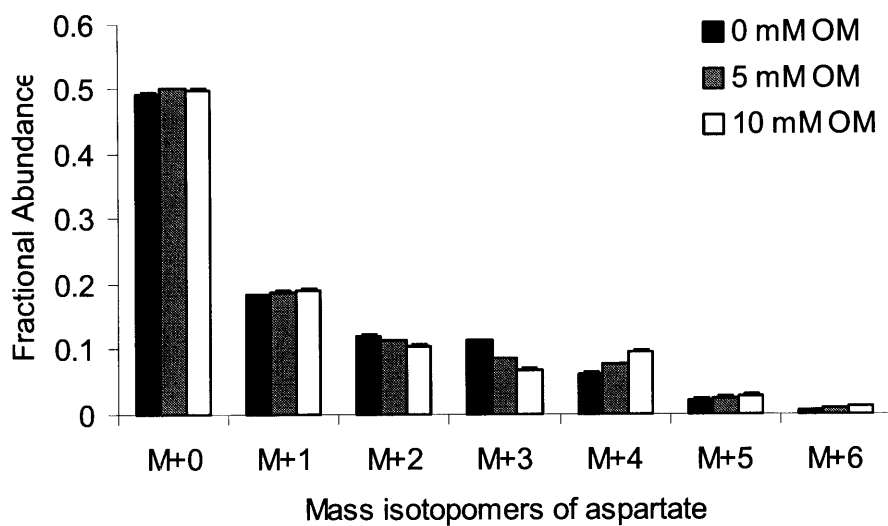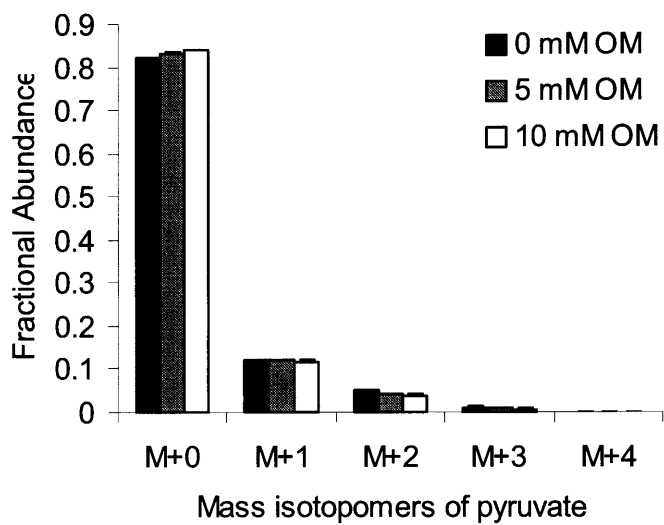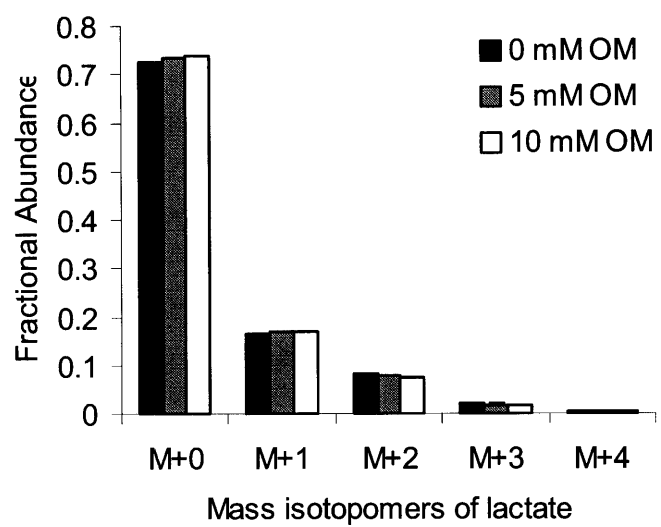
a.

b.

c.

Mass isotopomers of aspartate

d.

Mass isotopomers of pyruvate

154

e.
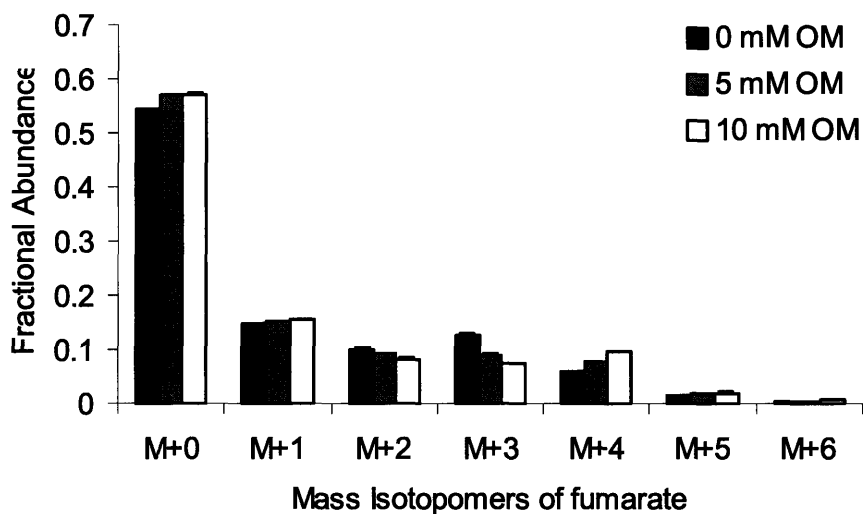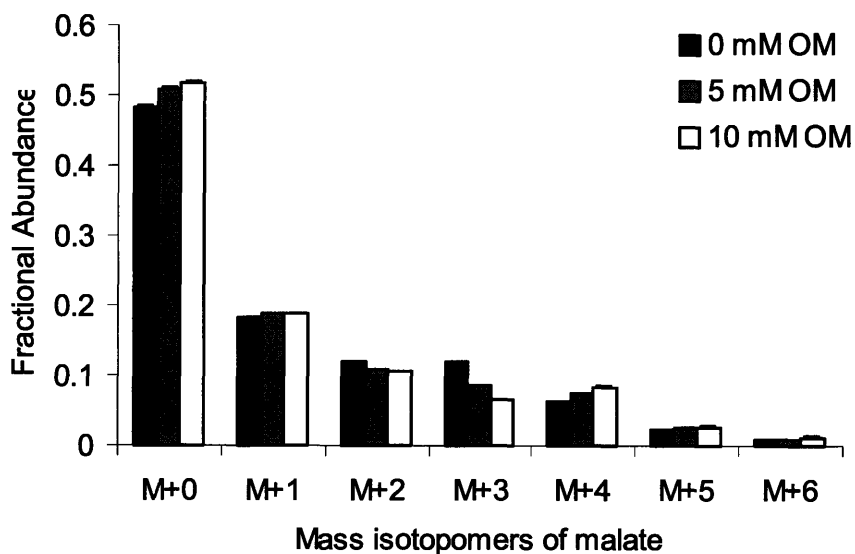
Mass isotopomers of lactate

Appendix B. Confirmation of steady-state assumption by time-course ^{13}C-labeling experiment.

Isotopomer distribution of glutamate (a), α-ketoglutarate (b), fumarate (c), aspartate (d), pyruvate (e), and lactate (f) from WT brown adipocytes measured at 2 hr, 4 hr, and 6 hr after incubation with 4 mM [U-^{13}C] glutamine on day 4.
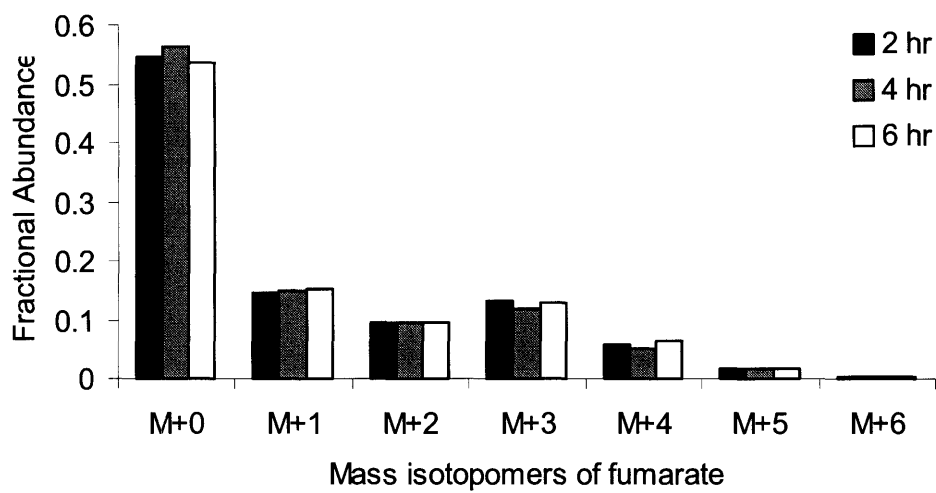
a.

b.

c.

d.

e.
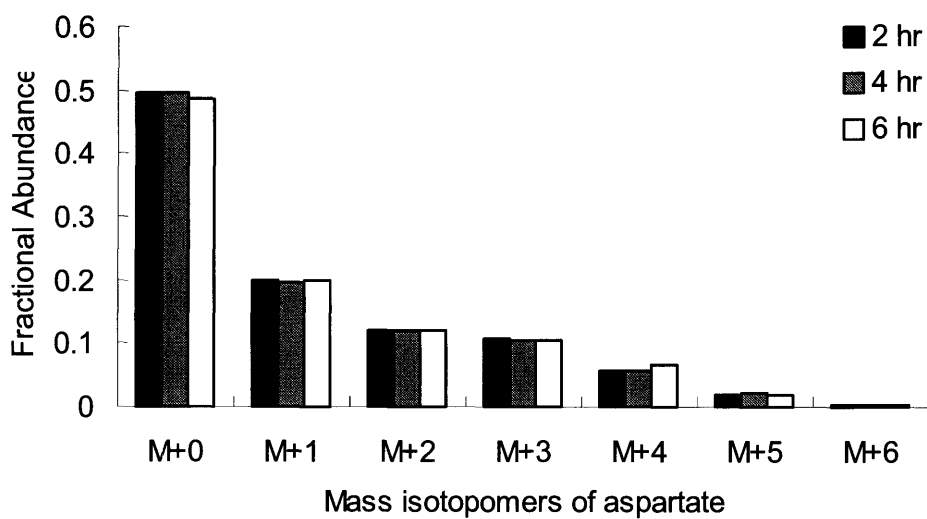
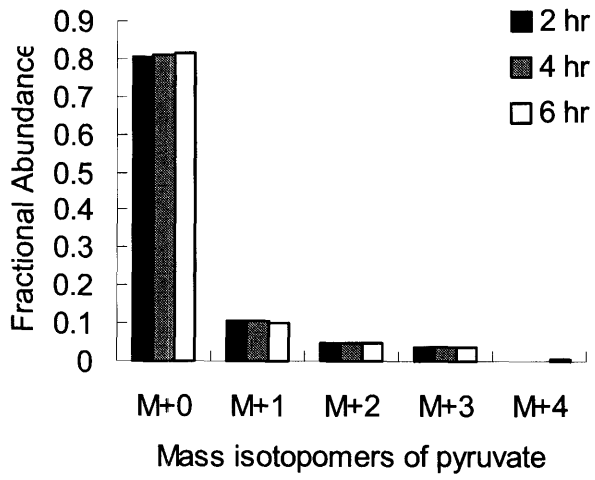

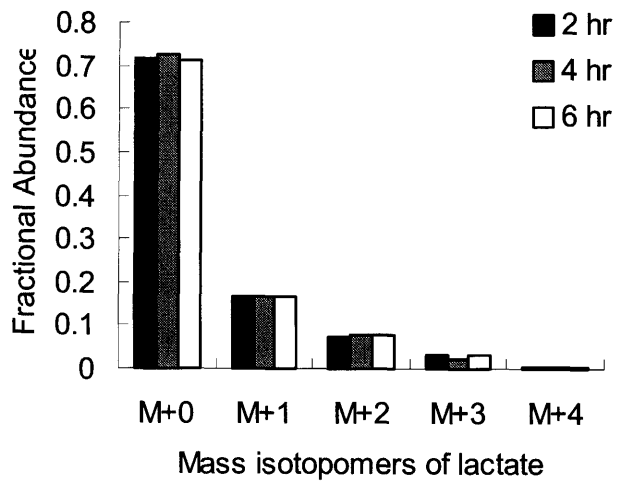Mass isotopomers of pyruvate

f.

Mass isotopomers of lactate
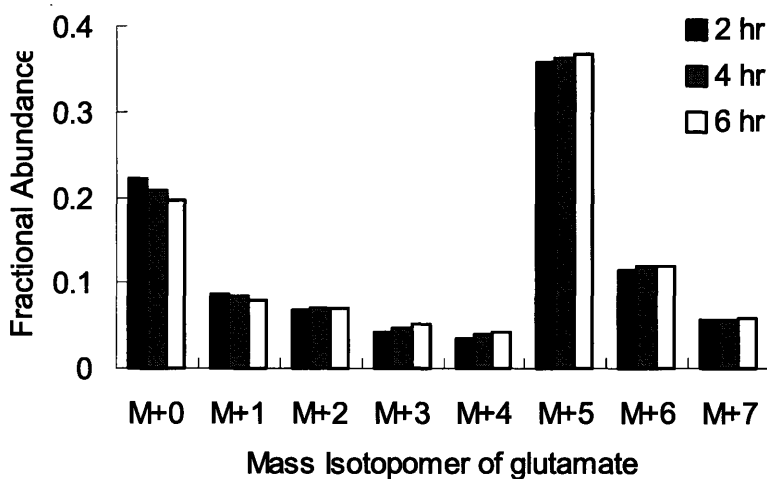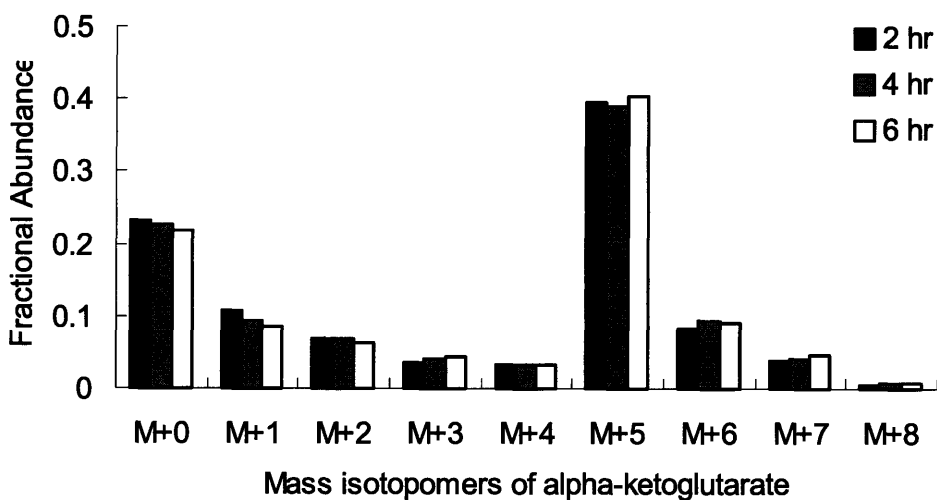
Appendix C. Estimated fluxes for WT brown adipocytes upon specific inhibition of NADP-ICDH.

The fluxes estimated based on the metabolic network model (Fig. 2.9) for WT brown adipocytes under 6-hr incubation with 25 mM glucose and 4 mM [U-^{13}C] glutamine in the presence of 0, 5, 10 mM oxalomalate (a) or 0, 2, 4 mM 2-methylisocitrate (b) are compared. Abbreviations used are: Gln – glutamine, Glu – glutamate, aKG – α-ketoglutarate, Cit – citrate, Suc – succinate, Fum – fumarate, Mal – malate, Glc – glucose, Pyr – pyruvate, Lac – lactate, OAA – oxaloacetate, AcCoA – acetyl-CoA, Ac – acetate, Pal – palmitate, Asp – aspartate, (ext) – external, (Cyt) – cytosolic, (pre) – preexisting.

a.

reactions	estimated fluxes			standard error		
	oxalomalate conc. (mM)			oxalomalate conc. (mM)		
	0	5	10	0	5	10
Gln(ext) -> Gln -> Glu -> aKG	100	100	100	0	0	0
aKG + CO₂ -> Cit	63	32	5	1	2	2
aKG -> Suc + CO₂, Suc->Fum->Mal	37	68	95	1	2	2
Glc (ext) -> Glc -> Pyr + Pyr	1540	1552	1550	50	50	50
Pyr -> Lac -> Lac (ext)	2905	2648	2583	116	113	109
Pyr + CO₂ -> OAA	460	513	497	11	13	12
Pyr -> AcCoA + CO₂	153	244	215	8	15	19
Mal -> Pyr + CO₂	438	303	195	27	27	21
OAA + AcCoA -> Cit	236	357	305	23	27	38
Cit -> AcCoA (Cyt) + OAA	299	389	310	23	27	38
AcCoA(Cyt) -> Ac -> AcCoA	83	113	90	24	16	23
8 AcCoA -> Pal	27	35	28	1	2	3
Pal (pre) -> Pal	181	340	234	10	26	20
g(6hr): Fractional Synthesis of Palmitate	0.13	0.09	0.11	0.009	0.009	0.013
OAA -> Asp -> sink	122	310	401	25	25	21

b.

reactions	estimated fluxes			standard error		
	2-MIC conc. (mM)			2-MIC conc. (mM)		
	0	2	4	0	2	4
Gln(ext) -> Gln -> Glu -> aKG	100	100	100	0	0	0
aKG + CO_2 -> Cit	64	34	9	1	2	2
aKG -> Suc + CO_2, Suc->Fum->Mal	36	66	91	1	2	2
Glc (ext) -> Glc -> Pyr + Pyr	1547	1550	1559	50	50	50
Pyr -> Lac -> Lac (ext)	2895	2789	2729	118	121	121
Pyr + CO_2 -> OAA	519	543	607	13	14	18
Pyr -> AcCoA + CO_2	156	231	238	9	28	29
Mal -> Pyr + CO_2	477	463	455	31	33	35
OAA + AcCoA -> Cit	266	270	311	29	16	41
Cit -> AcCoA (Cyt) + OAA	330	303	320	29	17	41
AcCoA(Cyt) -> Ac -> AcCoA	110	39	73	30	32	49
8 AcCoA -> Pal	27	33	31	1	4	4
Pal (pre) -> Pal	273	315	411	21	39	50
g(6hr): Fractional Synthesis of Palmitate	0.09	0.09	0.07	0.008	0.016	0.012
OAA -> Asp -> sink	143	180	251	29	30	31

160

Hyuntae Yoo

Education   1999 – 2005   Massachusetts Institute of Technology   Cambridge, MA
Ph.D. in (Biological) Chemistry
- Thesis title: Quantitative Analysis of Carbon Fluxes for Fat Biosynthesis in Wild-type and IRS-1 Knockout Brown adipocytes
- Advisor: Professor Gregory Stephanopoulos

1992 – 1998   Seoul National University   Seoul, Korea
B.S. in Chemistry
- Summa Cum Laude

Research
Experience   2001 – present   Massachusetts Institute of Technology   Cambridge, MA
Research Assistant – Metabolic Engineering and Bioinformatics Laboratory
(Principal Investigator: Professor Gregory Stephanopoulos)

2000 – 2001   Massachusetts Institute of Technology   Cambridge, MA
Research Assistant – Stubbe Research Group (P.I.: Professor JoAnne Stubbe)

1998 – 1999   Seoul National University   Seoul, Korea
Postundergraduate Research Assistant – Synthetic and Medicinal Chemistry Lab.
(P.I.: Professor B. Moon Kim)

Skills and
Techniques   Mammalian cell culture; GC/MS; NMR; HPLC; Protein purification and assay;
Western blotting; Organic Synthesis; Radioactive assay

Publications   **Hyuntae Yoo,** Maciek Antoniewicz, Joanne K. Kelleher and Gregory Stephanopoulos (2005) Quantitative analysis of individual carbon fluxes from glutamine to fatty acid synthesis in wild-type brown adipocytes. In preparation.

Maciek Antoniewicz, **Hyuntae Yoo,** Joanne K. Kelleher and Gregory Stephanopoulos (2005) Comprehensive analysis of metabolic networks for flux determination using stable-isotope labeling data. In preparation.

Hyuntae Yoo, Gregory Stephanopoulos and Joanne K. Kelleher (2004) Quantifying carbon sources for de novo lipogenesis in wild-type and IRS-1 knockout brown adipocytes. J. Lipid Res., Vol. 45, pp. 1324-1332.

B. Moon Kim, Sung Jin Bae, Soon Mog So, **Hyun Tae Yoo,** Sun Ki Chang, Jung Hwan Lee, and JaeSung Kang (2001) Synthesis of a Chiral Aziridine Derivative as a Versatile Intermediate for HIV Protease Inhibitors. Organic Letters, Vol. 3(15), 2001; pp. 2349-2351.

Awards received   Merck Poster Award, Metabolic Engineering IV Conference (2002)